Application of Cone Beam Computed Tomography in Facial Imaging Science

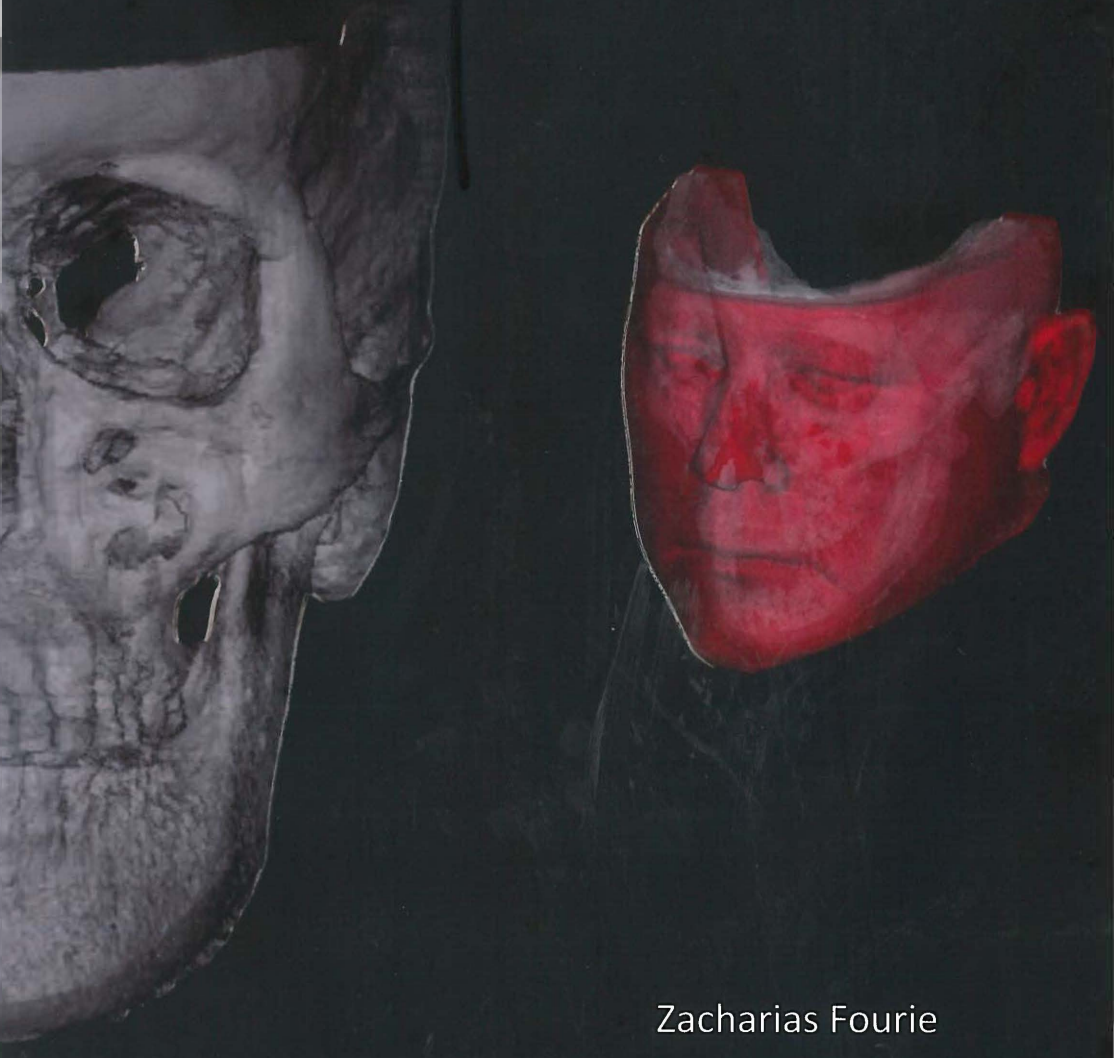

Zacharias Fourie

Application of Cone Beam Computed Tomography in Facial Imaging Science

Zacharias Fourie

STELLINGEN

behorende bij het Proefschrift:

APPLICA ION OF CONE BEAM COMPUTED TOMOGRAPHY IN FACIAL IMAGING SCIENCE

Zacharias Fourie
Groningen, 26 september 2011

1. Producing 3D surface models from Cone beam computerized tomography (CBCT) datasets is still less accurate than the reality when using threshold based methods. Differences in the segmentation process resulted in significant clinical differences between the measurements.*(This thesis)*

2. The commercially segmented surface models were more accurate than the experienced clinician's segmented surface models. However, equal quality may also be reached by a clinician if sufficient training and time is taken to segment a CBCT surface model. *(This thesis)*

3. Because CBCT images are often used for pre-surgical planning, the accuracy is of utmost importance. *(This thesis)*

4. There are clear potential benefits of using 3D measurements appose to direct measurements in the assessment of facial deformities. Measurements recorded by 3D systems appeared to be both sufficiently accurate and reliable enough for research and clinical use. *(This thesis)*

5. The soft tissue measurements on surface models derived from CBCT are reliable and accurate. Existing CBCT images can be used to derive accurate measurements for establishing soft tissue thickness databases of different populations. *(This thesis)*

6. All children are artists. The problem is how to remain an artist once he grows up. *(Pablo Picasso)*

7. A person who won't read has no advantage over one who can't read. *(Mark Twain)*

8. A man is but the product of his thoughts. What he thinks, he becomes. *(Mohandas Gandhi)*

9. A successful man is one who makes more money than his wife can spend. A successful woman is one who can find such a man. *(Lana Turner)*

10. Education without values, as useful as it is, seems rather to make man a more clever devil. *(C.S. Lewis)*

11. Work as if you were to live a hundred years. Pray as if you were to die tomorrow. *(Benjamin Franklin)*

12. The more I practice, the luckier I get. *(Gary Player)*

The research described in this thesis was carried out and supported by:

University Medical Center Groningen (UMCG), Faculty of Medical Sciences, University of Groningen, Department of Orthodontics, Groningen, the Netherlands

Publication of this thesis was supported by:

Prof.K.G.Bijlstra stichting
Department of Orthodontics (UMCG)
University of Groningen
Vereniging van Orthodontisten (VvO)
Ortholab B.V.
Dentsply Lomberg B.V.
Fa-med B.V.
Netpoint B.V.
Orthoproof B.V.
Straumann B.V.
Utrecht dental B.V.
Noord Negentig accountants en belastingadviseurs
Kema financieel adviseurs
Ormco Europe B.V.

cmb.

RIJKSUNIVERSITEIT GRONINGEN

Application of Cone Beam Computed Tomography in Facial Imaging Science

Proefschrift

ter verkrijging van het doctoraat in de
Medische Wetenschappen
aan de Rijksuniversiteit Groningen
op gezag van de
Rector Magnificus, dr. E. Sterken,
in het openbaar te verdedigen op
maandag 26 september 2011
om 16:15 uur

door

Zacharias Fourie

geboren op 12 juli 1976
te Heidelberg, Zuid-Afrika

Promotor:	Prof. dr. Y. Ren
Beoordelingscommissie:	Prof. dr. R.R.M. Bos Prof. dr. A.M. Kuijpers-Jagtman Prof. dr. P.E. Rossouw

Paranimfen: Drs. Katrina Finnema
Drs. Alianne Renkema

ISBN: 978-90-77724-15-6
NUR: 888

Lay-out & Cover: J Damstra

Printed by: Drukkerij G van Ark

Table of contents

Chapter 1	**Introduction and aims of the study**	**11**
Chapter 2	**Segmentation Process Significantly Influences the Accuracy of 3D Surface Models Derived from Cone Beam Computed Tomography** (Eur J Radiol 2011; Accepted)	**35**
Chapter 3	**The Influence of the Segmentation Process on the Linear and Angular Accuracy of 3D Surface Models Derived from Cone Beam Computed Tomography** (Clin Oral Invest 2011; Accepted)	**53**
Chapter 4	**Reliability and the smallest detectable difference of three-dimensional cephalometric measurements** (Am J Orthod Dentofacial Orthop 2011; Accepted)	**71**
Chapter 5	**Linear accuracy and repeatability of anthropometric facial measurements using cone-beam computed tomography.** (Cleft-Palate Craniofac J 2010; doi: 10.1597/10-076)	**89**
Chapter 6	**Evaluation of anthropometric accuracy and reliability using different three-dimensional scanning systems.** (Forensic Sci Int 2011; 207:127-134.)	**109**
Chapter 7	**Accuracy and reliability of facial soft tissue thickness measurements of cone beam CT scans.** (Forensic Sci Int 2010; 199: 9-14.)	**131**
Chapter 8	**General discussion**	**147**
Chapter 9	**Summaries**	**163**
9.1	Summary (English)	165
9.2	Samevatting (Dutch)	170

9.3 Opsomming (Afrikaans) 175

Appendices **I. List of publications** **183**
II. Acknowledgements **185**
III. Curriculum Vitae **187**

Chapter 1

Introduction and aims of the study

This chapter is based on the following publication:

Fourie Z, Damstra J, Ren Y. Application of cone beam computed tomography in facial imaging science. Shanghai J Stomatol 2011; Accepted

1.1 Introduction

Facial imaging is used to study the facial shape and its developmental changes over time. This is important to diagnose acquired malformations, to study normal and abnormal growth and to differentiate between the results of treatment and normal growth, and to validate facial recognition. The two main methods to study and record facial imaging are by means of cephalometry and anthropometry.[1] Cephalometrics is the scientific study of the measurements of the head's size and proportion while facial anthropometrics is the physical measurement of the human face and its parts. While the term anthropometry covers measurement of any aspect of the human form, the term surface anthropometry is used in this thesis to refer to the measurement of surface features. Cephalometry refers to the analysis of craniofacial features from X-ray images of the head, or cephalograms.[1] Cephalometry does not replace but complements anthropometry, because the facial form cannot be evaluated through analysis of hard tissue (bone and teeth) only.

Anthropometric and cephalometric studies are based on biological homology, i.e. spatial correspondence between definable points on structures in individuals, and geometric variation in the relative location or pattern of these points or landmarks. [2] Craniofacial form is defined by size and shape. Quantitatively determining the extent of deviation of an individual's facial pattern from the norm requires the collection of data from a large number of individuals in order to establish numerical descriptions of normal measurement ranges. Syndrome diagnosis requires the definition of characteristic abnormal patterns associated with a given syndrome.[3] Growth studies require facial pattern changes to be monitored over time.[1] Surgical planning requires three-dimensional (3D) visualization and quantification of dysmorphic features and the ability to model the changes that surgery is expected to bring about. Most people think that it has been only until recently that 3D imaging became available for the study of facial form and development but it has existed for much longer.

1.2 History of the development of facial imaging

Artists have long been interested in the direct anatomical relationship between the skull and facial appearance. Gaetano Guilio Zumbo (1656-1701), became famous for his macabre scenes depicting various stages of decomposition of the human body.[4] One of his most famous pieces is the head of a dead man, with facial muscles recreated in wax over a real skull. This is the earliest surviving anatomical wax model created for didactic purposes and exhibits extraordinary anatomical precision alongside an artistic sense of horror and decay. Zumbo pioneered the development of scientific art and this work ranks as one of the finest examples of 3D facial

reconstruction.[4] The search for an ideal flourished though the magnificent and prolific contributions of da Vinci and particularly the famous *Books of Proportions* by Dürer (1603).[5] In the eighteen century, Camper (1791) distilled one aspect from Dürer namely that the difference between two individuals could be defined by a change in the angulation of the vertical to the horizontal axes of a coordinate system. For Camper, that angle became the key to characterizing differences in facial profile.[6]

Later, George Northcroft, who was interested in the development of the face, took plaster casts of his son's face and dentition to record the 3D changes from 6 to 21 years of age. Further, records were also taken of his son at 75, 82, and 88 years of age. These records illustrated the changes in the soft tissues and the dentition over that period of time. [7] The advent of X-ray machines in the early 1900s brought about understandable excitement in the medical community, and cephalometrics quickly became a main clinical and research tool in craniofacial studies. In 1915 J.A. van Loon took it a step further by introducing his *Cubus craniophor,* a method that in which the dentition and face could be studied separately and in relation to reach other. [8] This enabled him to do comparative studies between different patients and pre- and post-treatment models of the same patients as the plaster facial cast and models were placed at the same position in the metal frame. Because it was such a time-consuming procedure to make this model, it was not really used in clinical practice.[8] Simon (1922), developed this method further by eliminating the Cubus craniophorus and used a facebow with calibrate rods to register the patient in natural head position and mounted a trimmed dental cast in the right relation to the Frankfurt horizontal. [9]

Broadbent (1931) made an attempt to record the 3D nature of the head by using a combination of lateral and antero-posterior radiographs and introduced a standard way of taking cephalometric radiographs. [10] After the invention of the cephalometric radiograph, de Coster (1939) was the first to publish an analysis based on proportional relationships of the face conforming to principles used in antiquity and portray differences in the location of landmarks in comparison to a norm. [11] However, this was 2D of nature. An avalanche of 3D methods followed in rapid succession to overcome the limitations of 2D. [12] The first 3D laser scanning technology was created in the 1960's. Due to limitations of this equipment it often took a lot of time and effort to scan objects accurately. Stereophotogrammetry has also become available for craniofacial imaging around the same time. [13] One of the earliest methods using the 'structured light' technique utilized 'Moiré' fringe patterns and was first described in 1970. [14] Computed Tomography (CT) imaging was invented in 1972 by British engineer Godfrey Hounsfield of EMI Laboraties, England

and by South African-born physicist Allan Cormack of Tulfts University, Massachusetts. Hounsfield and Cormack were later awarded the Nobel prize for their contribution to medicine and science. [15] The first clinical CT scanners were initiated between 1974 and 1976. But CT became widely available in early 1980s. [15] Around the same time facial detection became available. This was done using a camera that detect only facial features and ignores all the structures around that are not relevant, such as buildings, trees and bodies. This was regularly used in forensic science. In the 1980's, 3D images of the maxillofacial region started to develop rapidly. With the improvement of the digital photography and computer applications, stereo-photogrammetry became very popular. [16] The use of dedicated Cone beam computerized tomography (CBCT) scanners for the oral and maxillofacial (OMF) region was pioneered in the late 1990's independently by Arai et al. [17] in Japan and Mozzo et al. [18] in Italy. CBCT is a medical imaging acquisition technique based on a cone–shaped X-ray beam centered a two-dimensional detector. Since then there has been an explosion of interest in this new imaging technique in the OMF region by different research groups. [19]

1.3 2D facial imaging

1.3.1 Types of 2D imaging

Today, several competing methods are available for capturing and quantifying craniofacial surface morphology.[1,19] These include traditional methods, such as direct anthropometry, 2D photogrammetry and 2D cephalometry.[20] It was readily adopted by the medical community to enhance the patient's records. Lateral cephalograms were and are still part of the standard clinical orthodontic examination procedure. In special cases of craniofacial asymmetry and other disorders, additional posterior-anterior cephalograms are often needed. Cephalometry is widely used to study the bony structure of the face for diagnosis, treatment planning, evaluation of treatment outcome and growth prediction and monitoring. Relying on cephalometric dentoskeletal analysis for treatment planning can sometimes lead to aesthetic problems, especially when the orthodontist tries to predict soft tissue outcome using only hard tissue norm values.[20] The soft tissue covering the teeth and bones can vary so greatly that the dentoskeletal pattern may be an inadequate guide in evaluating facial disharmony.[20]

Direct facial anthropometric measurements, has been limited to measurements using traditional manual instruments (e.g. slicing and spreading calipers) during an examination. Surface anthropometry for the assessment of facial features in

dysmorphic patients was first used for facial clefts. It provides a quantitative basis for pattern recognition and syndrome diagnosis, additionally the range of variability of expression of any given syndrome can be established.[20,21]

Facial measurements using 2D images, such as photogrammetry and lateral cephalometry, would seem to hold obvious appeal over direct measurement of a moving subject.[22] The advantages of 2D images are rapid acquisition, archival capabilities, simplicity, low cost, and non-invasiveness.[23] With only 2D projection images, it is difficult to understand the precise anatomy or the morphology of an area under examination.[24] One of the primary goals of any craniofacial treatment is to attain and preserve optimal facial attractiveness. To accomplish this, it is important to conduct a thorough facial examination to make sure that the normal facial traits are maintained.[23]

The rapid evolution of digital radiographic systems and digital tracing software has had an impact on cephalometrics, slowly replacing traditional hand-tracing methods on hard copies of radiographic films.[25] Digital imaging offers several advantages over conventional film-based radiography: faster data processing, elimination of chemicals and associated environmental hazards, and the ability to alter and improve the image and correct for exposure errors, thus virtually eliminating the need for a second exposure.[25-27] Individualization of landmarks is facilitated by image improving features in software programs, and most final tracing is quickly completed by the software after landmark identification.

1.3.2 Limitations of 2D facial imaging

There are several limitations in the use of direct anthropometry. Although the direct anthropometric technique is non-invasive, displays technological simplicity, and is a low-cost approach, it is time-consuming to perform multiple direct measurements during an examination, requires adequate training of the examiner and proper instrumentation, and depends on patient cooperation for reliable results; as a result, this method may be impractical in the clinical setting.[24] Moreover, the direct technique does not provide a permanent record other than a list of numbers at the end of data collection. There is no opportunity to archive craniofacial surface morphology. Serial measurements are sometimes needed because 3D abnormalities in craniofacial disorders may undergo substantial changes in time.[24,28-29]

Cephalometry has inherent limitations as a result of distortion and differential magnification of the craniofacial complex. This may lead to errors in landmarks identification and reduce measurement accuracy.[30] Hand-traced cephalometry depends on correct head posture, proper exposure settings and developing

techniques, and the accuracy of the tracing. A radiograph with exposure errors is difficult to interpret, and the reduction of a 3D structure to a 2D image adds to the difficulty. This means that a second radiograph might be needed to get the information required. The hand-tracing process is also time-consuming and requires a skilled operator and a properly darkened room. [25]

In the attempt to minimize registration problems Dvortsin et al[31] presented a new method to reorient radiographs via standardized photographs made at the natural head position (NHP) according to the Nose-Best-Fit-Line in obtaining the NHP for radiographs. The proposed method has proved to be simple and highly reliable to obtain standardized radiographs at the NHP for orthodontic diagnosis, treatment planning and evaluation of treatment results. [31] Several variables can cause disparity when comparing 2 apparently similar photographs: distance between camera and subject, camera angle, head position (roll-pitch-jaw orientation), and photography protocol inconsistencies. These problems are further compounded when combining a patient's lateral photograph with a lateral cephalometric image for analysis. Achieving a repeatable and reliable registration between 2 images is unlikely, considering all of the variables involved. [32] The ability to obtain reliable and accurate measurement data is perhaps the most important criterion upon which to evaluate any measurement technique. [33] Because anthropometric data acquired with invalidated technology could potentially contain unacceptably high levels of measurement error, results based on such data must be interpreted with extreme caution. [34]

A substitute for the original cephalogram has been attempted by conducting cephalometric measurements on 2D facial photographs. It was concluded that facial photography is at least as reliable as cephalometrics to study facial morphology. Yet, lateral head-films are still necessary for good diagnostic purposes, since not all soft-tissue points are in close relationship to the hard-tissue location. In 2003, Nagasaki et al. [35] developed a non-radiographic cephalometric system, in which landmark identification and measurements were made directly on the patient's face with a 3D digitizer. The software program then constructed a 3D coordinate system with all required points in it. However in this system, it is not possible to add other landmarks later. A similar coordinate system can be added to 3D photographs. Moreover, the clinician can add more digital landmarks at libery; with is a distinctive edvantage. [36]

A combination of lateral and frontal cephalograms has been proposed to generate a 3D image of the head, but these approaches are not true 3D. They rely on identifying the same point on both radiographs and use geometry to calculate the 3D

position. The main limitations of such methods are obvious: accuracy depends on a correct correspondence between the landmark locations on the 2 radiographs. [12]

1.4 3D facial imaging

1.4.1 Types of 3D imaging

3D imaging is an innovative approach in the field of facial imaging that in a very short time has found a considerable number of applications throughout the medical, dental and forensic sciences. 3D reconstructed images can provide precise and detailed information for the diagnosis of craniofacial structural problems, enhancing the specialist's perception thereof and facilitating a more efficient treatment planning, thus making them preferable to the conventional 2D modalities. They are expected to help a specialist to select the most appropriate treatment intervention while offering the possibility of preoperative treatment simulation, especially in cases of craniofacial anomalies, head and neck abnormalities, craniofacial trauma surgery, cranial bone defects, and malocclusion problems. [25] Furthermore, the communication between specialists is made easier and more direct, and consultation with the patient becomes more interactive.

Many techniques for taking 3D measurements of soft tissues are available in facial imaging, including stereo-photogrammetry, [37-38] morphanalysis, laser scanning, [39-41] 3D digitization, Moiré scanning, [42-43] and ultrasonography. [42] The techniques able to scan both soft-tissue and skeletal structures are: Computed Tomography (CT), CBCT and the Magnetic Resonance Imaging (MRI). [44] These methods are non-invasive, allow images to be archived, and avoid measurement errors that occur with 2D representations of 3D surfaces. The advances in computer and imaging technologies have made possible the generation and handling of precise 3D reconstructed images for routine clinical use.

The laser surface scanner is the most common type of surface data acquisition device in use by craniofacial investigators today. [39] Laser surface scanning is reliable and accurate for identifying craniofacial surface landmarks. It is common in industry and medicine as a non-invasive method for generating a 3D computerized image. Despite its ability to scan only visible surfaces, its advantages in ease of use, self-calibration, and auto image distortion correction make generating 3D computerized images very convenient. [45] However, image capturing of this technique can be slow (up to 20 seconds) and may result in motion artifact in live subjects.

3D stereo-photogrammetry, a new method of craniofacial imaging, overcomes the limitations of laser scanning. With this technique, synchronized digital cameras obtain images from multiple angles and reconstruct a 3D image. The advantages are

near-instantaneous image capture (± 1.5ms) which minimizes motion artifact, provision of archived image for subsequent and repeated analyses, collection of data points in 3D coordinate format for subsequent morphometric studies, and high resolution colour representation. Furthermore, software tools are available that allow the user to manipulate the image to facilitate landmark identification and calculate anthropometric or volume measurements. [46-47] In recent years, a wide variety of commercially available digital 3D photogrammetric devices have become available, many of which differ considerably in terms of cost, imaging capturing method, hardware and software. [24,33] e.g., the C3D Imaging System (Ferranti, Birmingham, UK), Genex 3D Camera System (Genex 3D Technologies, Kensington, MD), DSP400 System (3dMD, Atlanta, GA), 3dMDface System (3dMD) [21,24,33] and recently the Di3D system (Di3D, Dimensional Imaging, Hillington Park, Glasgow, UK). [48] The Di3D system (Di3D, Dimensional Imaging, Hillington Park, Glasgow, UK) uses stereo-photogrammetry to produce fully textured surface contour maps of the head and face (180° ear to ear view). The system captures two stereo pairs of images (4 cameras in total) and specialist software is used to create a 3D surface using triangulation. [48] By using commercially available professional high-resolution colour digital cameras (4000 × 3500 pixels) it is possible to capture images that resolve local details of linear densities approaching 0.1 mm / pixel on human faces. At this resolution there is enough information about local texture to achieve reliable area-based stereo matching. Projection of texture is therefore no longer required to achieve a good 3D reconstruction of the human face and the capture time is shortened to 1 ms. [48-49]

With the introduction of digital dental models at the end of the 20th century, 3D digital data sets, combining the triad bone, soft tissues, and the dentition, have regained interest. Curry et al [50] developed a 3D data set, combining 3D facial photographs, digital dental casts, and antero-posterior and lateral headfilms. The only disadvantage of this method is that 2 X-ray radiographs must be taken, one of which is not routinely taken in orthodontic patients - the antero-posterior cephalogram. [36] More attempts are being made to integrate new 3D records that will lead to a virtual head of the patient.

Technologies such as 3D stereo-photogrammetry and laser scanning of the face have been used for 3D soft tissue superimposition. The major limitation is the inability to standardize image registration over time or to visualize the hard tissue structures. [51] In addition, current procedures to integrate 3D facial images have reported significant errors in head positioning and potential errors in facial expression. [52-53] The major advantage of a CBCT scan is that the relation between the hard and soft

tissue are visible and the superimposition can be done on a stable hard tissue structure like the cranial base. [51]

1.4.2 CBCT applications in Facial Evaluations

CBCT is a medical imaging acquisition technique based on a cone–shaped X-ray beam centered on a 2D detector. The source-detector system performs one rotation around the object producing a series of 2D images. The images are reconstructed in a 3D data set using a modification of the original cone-beam algorithm developed by Feldkamp et al. [54] in 1994. Since then there has been an explosion of interest in this new imaging technique in the OMF region. The main advantage of CBCT technology is the drastic reduction of radiation exposure to the patient compared to conventional CT. [39]

1.4.2.1 *CBCT for soft tissue evaluation*

For a maxillofacial surgeon it is important to know what the soft tissue movement will be after orthognathic surgery. Previous studies have reported that soft tissue chin tended to follow the hard tissue chin, but the lower lip movement is unpredictable.[51] Assessment of soft tissue movement requires a 3D analysis and superimposition because of its complexity. With CBCT scan the hard and soft tissue changes can very accurately be superimposed and the changes can easily be visualized and measured. [51]

One of the disadvantages of the CBCT is the lack of texture information of the soft tissue surface model. 2D photographs of the patients can then be mapped or laid over the skin surface with the help of proper software to improve the surface structure and therefore make the 3D image more realistic. With surface registration methods it is now possible to superimpose 3D textured surface data on reconstructed 3D skin models. [55]This gives a realistic image of the skin surface and the right relationship to the hard tissue. From 3D data, it has been showed [56] that matching 3D textured surfaces with untextured skin surfaces segmented is accurate and provides a photorealistic 3D model of a patient's face. It is of great importance that the CBCT image fusion of the 3D textured surface and segmented skin surface displays a high degree of accuracy (< 1 mm) [55] for preoperative planning of maxillofacial interventions [54,57-58]

Although various reconstructive and regenerative treatments have been developed, a facial prosthesis still is an effective rehabilitation for patients with congenital or acquired facial defects, including those resulting from trauma or surgical removal of neoplasms. Recently, a rapid-prototyping (RP) system was developed as a simpler method for fabricating facial prostheses without a facial

impression. [59-60] The facial data of patients can be acquired by CBCT, CT, MRI or surface scanning (photography, laser). [61] The problems of conventional facial impression techniques: it is uncomfortable for the patient; the weight of the impression material can deform the soft tissue; and sculpting the wax prototype is also time consuming, are avoided by the latter techniques. [62]

1.4.2.2 Other applications of CBCT

Due to their absolute accuracy, [12,18,30] CBCT images have become powerful tools for evaluation of craniofacial morphology and treatment outcome. In the maxillofacial region, CBCT is used for the evaluation of impacted teeth, implant treatment planning, diagnostics of the temporomandibular joint (TMJ), dental development, limits of tooth movement, airway assessment, craniofacial morphology and superimposition, simulations for orthodontic and surgical planning and planning.[63-67] In complex orthodontic cases (canine impactions and clefts), CBCT has become the method of choice. Furthermore, in cleft patients and those undergoing combined orthodontic and maxillofacial therapy, CBCT provided more information than conventional images. [68] Additional application for CBCT in other fields of dentistry includes identifying apical periodontitis, predictable endodontic planning, and periodontal bone levels. [69-72]

Many relationships of the craniofacial complex, such as the position of the mandibular condyles in the temporomandibular fossa with respect to the occlusal scheme and the association of airway abnormalities to craniofacial morphology, cannot be evaluated with conventional imaging approaches. [73] Common weaknesses of many outcomes studies are image fidelity and method errors in the superimposition process, leading to confounding and often conflicting results. The applications of CBCT in these fields have the potential to settle many controversies in orthodontics, such as the mechanism of functional appliances, non-extraction philosophies, molar distalization, temporomandibular effects and others. [73]

1.4.2.3 Factors influencing CBCT applications

The factors influencing the quality and accuracy of a 3D model derived from a CBCT can be divided into 3 main categories. The first are the CBCT system or scanner related factors such as different CBCT scanners, Field of View (FoV), artifacts and voxel size. The second are patient or subject related factors such as patient position and metal artifacts. The third are operator related factors, that includes segmentation process and the operator self.

(i) Scanner related factors

a. Different types of scanners

Various authors have looked at the effect of the scanner type on the quality of the 3D image.[74-76] The grey levels of the voxels of the same object imaged by two scanners are likely to differ, resulting in variation during the segmentation process and ultimately influence the image quality. The reason for this is because the voxel size and FoV of most of the scanners are limited. The difference in image quality from CBCT scanner, manufacturers and reconstruction parameters can results in variation of image quality and accuracy of the image as CBCT suffers from beam inhomogeneity. [74,76] Clinically significant differences excist between 3D models of the same skull from two different CBCT scanners, thus care should be taken when comparing measurements made on 3D models derived from different CBCT devices. [75]

b. Field of View (FoV)

One of the advantages of a CBCT is the flexibility of the FoV. FoV is an important factor as it can influence the size and quality of the 3D image. [77] To image the full height of a patient's skull, a CBCT device with a large field of view is required. Radiation doses of such a scan are 3 – 44 times greater than those of comparable panoramic examinations, depending on the CBCT device used. [78] FOV selection is specific to each system. In several systems, the scanning volume can be adapted according to the clinical demands (e.g. Scanora, NewTom 3G and i-CAT). In others, only a single FOV selection is available (e.g. Galileos). In general, it could be stated that small FOV and high-resolution scans are optimal for detailed diagnostic tasks (e.g. endodontics), while large volume scans are delivering better 3D models. [78]

c. Noise or artifacts

A small FOV selection with a thin slice setting does not necessarily directly translate to better image quality or higher spatial resolution because the noise level or specific artifacts can also be substantially increased. [79] Katsumata et al. [80] and Van Daatselaar et al. [81] reported specific artifacts due to data discontinuity using limited-volume CBCT systems. Hassan et al. [82] also reported more image artifacts associated with the smaller scan fields. This phenomenon was thought to be a CBCT artifact related to halation from the image intensifier (II). This artifact appeared only when the area to be imaged was positioned near the facial surface. In addition,

this artifact will not appear in CBCT systems using an image (II) which are designed to scan large FoV using larger II tubes. In limited volume CBCT imaging, the size of the FoV is small when compared to the entire head, and the intensity of transparent x-radiation fluctuates during the 360° scan. When an incident occurs in which some part of the x-ray beam reaches the fluorescent surface without passing through the patient's head, halation from the II is expected to occur. In practice possible solutions might be a lower voltage or current setting of the x-ray tube can reduce the influence of this artifact. It is clear that insufficient x-ray intensity leads to reduced image quality. [73]

d. Voxel size

The different scan fields have different voxel sizes, and various CBCT scanners also differ from each other in voxel size selections for each scan field. The importance of voxel size stems from a practical observation that very small voxels (e.g., 0.2 or 0.3 mm) result in an extremely large surface mesh model, which is difficult to process to create an accurate 3D surface model for treatment planning and simulation, although the image quality is higher. Large voxel resolution of 0.6, 0.9, or 1.2 mm significantly reduces the visibility of the occlusal surfaces of the teeth, interproximal space between the teeth, and alveolar bone. [76]

(ii) Operator related factors

a. Segmentation process

The 3D image is composed of voxels; each voxel has a grey-level value base in calculation of the amount of radiation absorbed. Visualization is based on a threshold filter. This filer assigns a binary value, either transparent or visible, to each voxel based on its grey-level value. The user defines the critical value that splits the voxels into viable and invisible. The result is a rendered image on the screen composed of all visible voxels. [83] Multiple threshold filters can be applied to the same image to distinguish between tissue different density – e.g. soft and hard tissue. [83] It is difficult to distinguish which voxel is air, soft tissue, bone, or something else. Unfortunately, the value (brightness) of a voxel is not a good indicator of the corresponding histological tissue. This is a classic problem in computer vision known as the segmentation problem. It arises because soft tissue tends to appear black or dark grey and bone tends to be white, hence, thin bones might have a lower density (brightness) than thick soft tissue, and the values of the soft and hard tissues thus merge in the middle greys. [12]

b. The operator

It is crucial to understand that the rendered image is the result of a user-entered threshold value. The visual perception of the operator defines what is bone and what is soft tissue. Many factors can affect this: contrast of the image, noise in the image, individual visual perception and prior knowledge of anatomy among others. [84] The same imply for the choice of voxel size, FoV, and positioning of the patient in the CBCT scanner which are all factors to be decided by the operator and will influence the quality of the CBCT image. [84]

(iii) Patient/subject related factors

a. Artifacts

The metal artifacts resulting from metal implants, dental filling and orthodontic fixed appliance on CBCT scan can influence the quality of the 3D soft tissue model. If metal is present in the FoV, X-ray imaging techniques are always prone to producing artifacts, as the X-ray beam cannot pass through the metal object and gives a distorted image of the area around it.[85] This "halo" effect made some metal markers appear almost 2 times larger than they actually were, and some appeared more elongated than perfectly round. [85] Gomi et al. [86] proposed an algorithm to reduce cone-beam artifacts by increasing the cone angle to achieve satisfactory image quality at the same radiation dose.

b. The position of the patient

As it takes a few seconds to make a CBCT scan, the head of the patient is often fixed to avoid distortion and movement artefacts during acquisition of the CBCT scan. As a lot of emphasis is placed on natural head position (NHP), one would think that it has an influence on the accuracy of the model. However, a variation in patient head position when a CBCT examination is performed does not affect the accuracy of 3D surface-rendered models.[87] In addition, the scan can later be adjusted to the proper position if need be.

1.5 Aims of this thesis

1. To evaluate if the segmentation process makes any difference on the quality of the 3D surface models produced from CBCT datasets using threshold based methods.

2. To investigate whether the measurement error of 3D measurements can be considered clinically relevant. A hight level of accuracy required is required for pre-surgical treatment planning and treatment outcome evaluation; moreover, it is essential to establish whether linear and angular 3D measurements can be used to detect true 3D treatment effects.
3. To determine if indirect anthropometric measurements made on 3D soft tissue surface models derived from different 3D scanning systems are accurate and reliable for research and clinical use.
4. To determine if the CBCT soft tissue images of the face is an accurate representation of the human face.

Chapter *1* *gives an overview including a short history of facial imaging.* The two main methods to study and record facial imaging are by means of cephalometry and anthropometry; this is discussed. The techniques used for facial imaging includes the traditional direct measurements, 2D photogrammetry and 2D cephalometry. More recently 3D techniques have been developed where 3D reconstructed images can provide precise and detailed information for the diagnosis of craniofacial structural problems, enhancing the specialist's perception and facilitating a more efficient treatment planning In Chapter 1 the factors influencing the quality and accuracy of a 3D model derived from a CBCT model are discussed.

In **Chapter 2** *we investigated the segmentation procedure as one of the possible factors that can influence the quality and accuracy of the 3D surface model derived from a CBCT.* This 3D technology displays a realistic representation of the human head and is used to create different 2D tomographic slices, projection images and 3D volume and surface reconstructions. Accuracy of these 3D surface models is of utmost importance. This study focused on the threshold based segmentation poses and the effect of different segmentation procedures on the quality of the 3D surface model.

In **Chapter 3** *the effect of two different CBCT segmentation protocols on the accuracy of linear measurements was determined.* Standard linear and angular measurements were made between different anatomic and cephalometric landmarks on 3D surface models derived from two different segmentation protocols using standard threshold based segmentation process.

Chapter 4 *investigated the measurement error in commonly used 3D cephalometric measurements.* Accuracy is of utmost importance because the data from CBCT images are used for pre-surgical planning; moreover, sufficiently accurate CBCT

information will prevent surgical inaccuracies. However, accurate CBCT images do not guarantee accurate measurements. As in traditional cephalometry, each 3D landmark has its own unique configuration and envelope of error which contributes to measurement error. In this chapter we looked at the measurement error in 3D cephalometry by means of the smallest detectable difference (SDD).

The study described in **Chapter 5** *focused on determining the accuracy of anthropometric measurements made in the soft tissue 3D models derived from the CBCT system. Is it accurate enough to do these measuremens or do you need additional surface information?* The purpose of this was to compare the repeatability and accuracy of linear measurements made on 3D soft tissue models generated with SimPlant® Ortho Pro software.

Chapter 6 *investigated the quality of the 3D soft tissue models derived from three different 3D systems.* Today, several competing methods are available for capturing and quantifying craniofacial surface morphology. We compared indirect standard anthropometric measurements on the 3D soft tissue models derived from the Di3D stereo-photogrammetry system, laser surface scanner and CBCT scanner with direct anthropometric measurement.

In **Chapter 7** *we investigated the quality and accuracy of the soft tissue 3D images derived from the CBCT.* CBCT images are mostly used for hard tissue diagnostic purposes. Traditionally, Laser surface scanning has been used to evaluate the surface characteristics of the face and MRI has been used for the deeper underlying soft tissue structures. Although it has a lack of textured information and detail in muscle information, the soft tissue images derived from the CBCT are often underestimated. The purpose of this study was to determine the reliability and accuracy of soft tissue thickness measurements using CBCT and the effects of slice thickness on the precision.

1.6 References

1. Douglas TS. Image processing for craniofacial landmark identification and measurement: a review of photogrammetry and cephalometry [J]. Comput Med Imag Graphics, 2004; 28 (7) :401-409
2. Thomas IT, Hintz RJ, Frias JL. New methods for quantitative and qualitative facial studies: an overview [J]. J Craniofacial Genet Dev Biol, 1989; 9(1)107-111
3. Bookstein FL. Size and shape spaces for landmark data in two dimensions [J]. Stat Sci 1986; 1(2):181–242

4. Olds C. Facial beauty in western art. In: McNamara J (ed.) Esthetics and the treatment of facial form [C]// Monograph No. 28, Craniofacial Growth Series [M]. Center for Craniofacial Growth and Development, University of Michgan, Ann Arbor, 1993: 7 – 25
5. Dürer A. Hjerinn sind begriffen vier Bücher von menschlicher Proportion, durch Alberechter Dürer von Nürmberg erfunden und beschrieben, zu nutz von alien denen, so zu dieser kunst bieb tragen [M].. Arnem: Beij Johan Janssen, Buchführer, 1603
6. Camper P. Dissertation physique sur les differences reelles qui presentent les traits du visage chez les hommes de differents pays et de differents ages. Sur le beau qui caracterise les statues antiques et les pierres gravees. Suivie de la proposition d'une Nouvelle Methode pour dessiner toutes sortes de têtes humaines avec la plus grande surete [M]. Utrecht: Wild B, Altheer j, 1791
7. Moss JP. Northcroft revisited [J]. British Journal of Orthodontics, 1989; 16(3) :155 – 167
8. van Loon JAW. A new method for indicating normal and abnormal relations of the teeth to the facial lines [J]. Dent Cosmos, 1915; 57: 973-83, 1093-1101, 1229-1235
9. Simon PM. Grundzuge einer systematischen Diagnostik der Gebissanomalien [M]. Berlin: Meusser, 1922
10. Broadbent BH. A new x-ray technique and its application to orthodontia [J]. Angle Orthod, 1931: 1(2); 45-66
11. deCoster L. The Network method of orthodontic diagnosis [J]. Angle Orthod, 1939; 9(1) : 3-14
12. Halazonetis DJ. From 2-dimensional cephalograms to 3-dimensional computed tomography scans [J]. Am J Orthod Dentofacial Orthop, 2005; 127(5): 627-637
13. Harrell WE, Jacobson RL, Hatcher DC, Mah J 2006 Cephalometric imaging in 3-D [C]// Jacobson A, Jacobson RL, eds: Radiographic cephalometry, From Basics to 3-D imaging [M]. Hanover Park, Quintessence Publishing Co, 1995: 233-247
14. Takasaki H. Moiré topography [J]. Appl Optics, 1970; 9(6): 1457-1472
15. Http://www.imaginis.com/ct-scan/brief history of CT
16. Papadopoulos MA, Christou KP, Athanasiou AE, Boettcher P, Zeilhofer HF, Sader HR, Papadopulos NA. Three-dimensional craniofacial reconstruction imaging [J]. Oral Surg Oral Med Oral Pathol Oral Radiol Endod, 2002; 93(4): 382-393
17. Arai Y, Tammisalo E, Iwai K, Hashimoto K, Shinoda K. Development of a compact computed tomographic apparatus for dental use [J]. Dentomaxillofac Radiol, 1999: 28(4): 245–248
18. Mozzo P, Procacci C, Tacconi A, Martini PT, Andreis IA. A new volumetric CT machine for dental imaging based on the cone-beam technique: preliminary results [J]. Eur Radiol, 1998: 8(9): 1558–1564

19. De Vos W, Casselman J, Swennen GR. Cone-beam computerized tomography (CBCT) imaging of the oral and maxillofacial region: a systematic review of the literature [J]. Int J Oral Maxillofac Surg, 2009 ; 38(6): 609-625
20. Bergman RT. Cephalometric soft tissue facial analysis [J]. Am J Orthod Dentofacial Orthop, 1999; 116(4) : 373-89
21. Farkas LG, Deutsch CK. Anthropometric determination of craniofacial morphology [J]. Am J Med Genet, 1996; 65(1): 1-4
22. Farkas LG. Anthropometry of the Head and Face [M]. New York: Raven Press, 1994.
23. Fanibunda K. Photoradiography of facial structures[J]. Br J Oral Surg 1983; 21(4): 246-58
24. Wong JY, Oh AK, Ohta E, Hunt AT, Rogers GF, Mulliken JB, Deutsch CK. Validity and reliability of 3D craniofacial anthropometric measurements [J]. Cleft Palate Craniofac J, 2008; 45(3): 232-239
25. Santoro M, Jarjoura K, Cangialosi TJ. Accuracy of digital and analogue cephalometric measurements assessed with the sandwich technique [J]. Am J Orthod Dentofacial Orthop, 2006; 129(3): 345-351
26. Quintero JC, Trosien A, Hatcher D, Kapila S. Craniofacial imaging in orthodontics: historical perspective, current status, and future developments [J]. Angle Orthod, 1999; 69(6): 491-506
27. Wenzel A, Gotfredsen E. Digital radiography for the orthodontist [J]. Am J Orthod Dentofacial Orthop, 2002; 121(2): 231-235
28. Deutsch CK, Mulliken JB. Discussion of surface anatomy of the face in Down's syndrome: anthropometric indices in the craniofacial regions. J Craniofac Surg, 2001; 12(3): 525–526
29. Mulliken JB, Burvin R, Farkas LG. Repair of bilateral complete cleft lip: intraoperative nasolabial anthropometry [J]. Plast Reconstr Surg, 2001; 107(2): 307–314
30. Kumar V, Ludlow J, Cevidanes LHS, Mol A. In Vivo Comparison of conventional and Cone beam CT synthesised cephalograms [J]. Angle Orthod, 2008; 78(5): 873-878
31. Dvortsin DP, Yeb Q, Pruim GJ, Dijkstra PU, Ren Y. Reliability of the integrated radiograph-photograph method to obtain natural head position in cephalometric diagnosis [J]. In press, Eur J Orthod, 2011
32. Lane C, Harrel W. Completing the 3-dimensional picture [J]. Am J Orthod Dentofacial Orthop, 2008; 133(4): 612-620
33. Weinberg SM, Naidoo S, Govier DP, Martin RA, Kane AA, Marazita ML. Anthropometric precision and accuracy of digital three-dimensional photogrammetry: comparing the Genex and 3dMD imaging systems with one another and with direct anthropometry [J]. J Craniofac Surg, 2006; 17(3): 477–483
34. Jamison PL, Ward RE. Brief communication: measurement size, precision, and reliability in craniofacial anthropometry: bigger is better [J]. Am J Phys Anthropol, 1993; 90(4): 495–500
35. Nagasaka S, Fujimura T, Segoshi K. Development of a nonradiographic cephalometric

system [J]. Eur J Orthod, 2003; 25(1): 77-85
36. Rangel FA, Maal TJJ, Bergé SJ, van Vlijmen OJC, Plooij JM, Schutyser F, Kuijpers-Jagtman AM. Integration of digital dental casts in 3-dimensional facial photographs [J]. Am J Orthod Dentofacial Orthop, 2008; 134(6): 820-826
37. Burke PH, Banks P, Beard LFH, Tee JE, Hughs C. Stereo-photography measurement of change in soft tissue following surgery [J]. Br J Oral Surg, 1983; 21(4): 237–245
38. Burke PH, Beard LFH. Stereo-photogrammetry of the face [J]. Am J Orthod, 1967; 53(10): 769–782
39. Kau CH, Richmond S, Incrapera A, English J, Xia JJ. Three-dimensional surface acquisition systems for the study of facial morphology and their application to maxillofacial surgery [J]. Int J Med Robotics Comput Assist Surg, 2007; 3(2): 97–110
40. Karas BV, Beaubien HF. Three-dimensional laser scanning of cultural heritage: the deer stones of Mongolia [J] Scanning, 2006; 28(3): 187–188
41. Park HK, Chung JW, Kho HS. Use of hand-held laser scanning in the assessment of craniometry [J] Forensic Sci Int, 2006; 160(2-3): 200–206
42. Kawai T, Natsume N, Shibata H, Yamamoto T. Three-dimensional analysis of facial morphology using moire´ stripes. Part I. Method [J]. Int J Oral Maxillofac Surg, 1990; 19(6): 356–358
43. Kawano Y. Three-dimensional analysis of the face in respect of zygomatic fractures and evaluation of the surgery with the aid of moire topography [J]. J Craniomaxillofac Surg, 1987; 15(2): 68–74
44. El-Mehallawi IH, Soliman EM. Ultrasonic assessment of facial soft tissue thicknesses in adult Egyptians [J] Forensic Sci Int, 2002; 117(1-2): 99–107
45. Kusnoto B, Evans CA. Reliability of a 3D surface laser scanner for orthodontic application [J]. Am J Orthod Dentofacial Orthop, 2002; 122(4): 342-348
46. Jacobs RA. Plastic Surgery Educational Foundation DATA Committee. Three-dimensional photography [J]. Plast Reconstr Surg, 2000; 107: 276-277
47. Weinberg SM, Kolar JC. Three-dimensional surface imaging: limitations and considerations from the anthropometric perspective [J]. J Craniofac Surg, 2005; 16(5): 847-851
48. Khambay B, Nairn N, Bell A, Miller J, Bowman A, Ayoub AF. Validation and reproducibility of a high-resolution tree-dimensional facial imaging system [J]. Br J Oral Maxillofac Surg, 2008; 46(1): 27-32
49. Winder RJ, Darvann TA, McKnight W, Magee JDM, Ramsay-Baggs P. Technical validation of the Di3D stereo-photogrammetry surface imaging system [J]. Br J Oral Maxillofac Surg, 2008; 46(1): 33-37
50. Curry S, Baumrind S, Carlson S, Beers A, Boyd RL. Integrated three-dimensional mapping at the Craniofacial Research Instrumentation Laboratory/University of the Pacific [J]. Semin Orthod, 2001; 7(2): 258-265
51. Almeida RC, Cevidanes LHS, Carvalho FAR, Motta AT, Almeida MAO, Styner M, Turvey T, Proffit WR, Phillips C. Soft tissue response to mandibular advancement

using 3D CBCT scanning [J]. Int J Oral Maxillofac Surg, 2011; 40(4): 353-359
52. Kau CH, Cronin AJ, Richmond S. A three-dimensional evaluation of post-operative swelling following orthognathic surgery at 6months [J]. Plast Reconstr Surg, 2007: 119(7): 2192–2199
53. Kau CH, Richmond S, Savio C, Mall-orie C. Measuring adult facial morphology in three-dimensions [J]. Angle Orthod, 2006: 76(5): 773–778
54. Feldkamp LA, Davis LC, Kress JW. Practical cone-beam algorithm [J]. J Opt Soc Am, 1994: 1(6): 612–619
55. Maal TJ, Plooij JM, Rangel FA, Mollemans W, Schutyser FAC, Berge SJ. The accuracy of matching three-dimensional photographs with skin surfaces derived from cone-beam computed tomography [J]. Int J Oral Maxillofac Surg, 2008: 37(7): 641–646
56. Groeve PD, Schutyser F, Cleynenbreugel JV, Suetens P. Registration of 3D photographs with spiral CT images for soft tissue simulation in maxillofacial surgery [J]. Med Image Comput Comput Assist Interv, 2001:(2208): 991–996
57. Ayoub AF, Wray D, Moos K, Siebert JP, Jin J, Niblett TB. Three-dimensional modeling for modern diagnosis and planning in maxillofacial surgery [J]. Int J Adult Orthodon Orthognath Surg, 1996: 113(3): 225–233
58. Ayoub AF, Xiao Y, Khambay B, Siebert JP, Hadley D. Towards building a photo-realistic virtual human face for craniomaxillofacial diagnosis and treatment planning [J]. Int J Oral Maxillofac Surg, 2007: 36(5): 423–428
59. Reitemeier B, Notni G, Heinze M, et al.: Optical modeling of extraoral defects [J]. J Prosthet Dent, 2004; 91(1): 80-84
60. Coward TJ, Scott BJJ, Watson RM, et al.: A comparison between computerized tomography, magnetic resonance imaging, and laser scanning for capturing 3-dimensional data from an object of standard form [J]. Int J Prosthodont, 2005; 18(5): 405-413
61. Verdonck HW, Poukens J, Overveld HV. Computer-assisted maxillofacial prosthodontics: a new treatment protocol [J]. Int J Prosthodont, 2003; 16(3): 326-328
62. Yoshioka F, Ozawa S, Okazaki S, Tanaka Y .Fabrication of an Orbital Prosthesis Using a Noncontact Three-Dimensional Digitizer and Rapid-Prototyping System [J]. J Prosthodont, 2010; 19(8): 598–600
63. Nakajima A, Sameshima GT, Arai Y, et al.. Two- and three-dimensional orthodontic imaging using limited cone beamcomputed tomography [J]. Angle Orthod, 2005; 75(6): 895–903
64. Madrigal C, Ortega R, Meniz C, et al. Study of available bone for interforaminal implant treatment using cone-beam computed [J]. Med Oral Patol Oral Cir Bucal, 2008; 1(13): E307–312
65. Honda K, Larheim TA, Maruhashi K, et al. Osseous abnormalities of the mandibular condyle: diagnostic reliability of cone beam computed tomography compared with helical computed tomography based on an autopsy material [J]. Dentomaxillofac

Radiol, 2006; 35(3): 152–157
66. Mah JK, Huang JC, Choo H. Practical applications of cone-beam computed tomography in orthodontics [J]. JADA, 2010; 141(suppl): 7S-13S
67. Maki K, Inou N, Takanishi A, et al. Computer-assisted simulations in orthodontic diagnosis and the application of a new cone beam X-ray computed tomography [J]. Orthod Craniofac Res, 2003; 6(suppl 1): 95–101; discussion 179–182
68. Korbmacher H, Kahl-Nieke B, Schollchen M, et al. Value of two cone-beam computed tomography systems from an orthodontic point of view [J]. J Orofac Orthop, 2007; 68(4): 278–289
69. Estrela C, Bueno MR, Leles CR, et al. Accuracy of cone beam computed tomography and panoramic and periapical radiography for detection of apical periodontitis [J]. J Endod, 2008; 34(3): 273–279
70. Estrela C, Bueno MR, Sousa-Neto MD, et al. Method for determination of root curvature radius using cone-beam computed tomography images [J]. Braz Dent J, 2008; 19(2): 114–118
71. Mol A, Balasundaram A. In vitro cone beam computed tomography imaging of periodontal bone [J]. Dentomaxillofac Radiol, 2008; 37(6): 319–324
72. Kau CH, Bozic M, English J, Lee R, Bussa H, Ellis RK. Cone-beam computed tomography of the maxillofacial region – an update [J]. Int J Med Robotics Comput Assist Surg, 2009; 5(4): 366–380
73. Liang X, Lambrichts I, Sun Y, Denis K, Hassan B, Li L, Pauwels R, Jacobs R. A comparative evaluation of Cone Beam Computed Tomography (CBCT) and Multi-Slice CT (MSCT). Part II: On 3D model accuracy [J]. Eur J Radiol, 2010; 75(2): 270–274
74. Loubele M, Maes F, Schutyser F, Marchal G, Jacobs R, Suetens P. Assessment of bone segmentation quality of cone-beam CT versus multislice spiral CT: a pilot study [J]. Oral Surg Oral Med Oral Pathol Oral Radiol Endod, 2006; 102(2): 225–234
75. Van Vlijmen OJ, Rangel FA, Berge SJ, Bronkhorst EM, Becking AC, Kuiper-Jagtman AM. Measurements on 3D models of human skulls derived from different cone beam scanners [J]. Clin Oral Investig, 2010: DOIL 10.1007/s00784-010-0440-8
76. Hassan B, Metska ME, Ozok AR, van der Stelt P, Wesselink PR. Comparison of Five Cone Beam Computed Tomography Systems for the Detection of vertical root fractures [J]. J Endod, 2010; 36(1): 126-129
77. Loubele M, Jacobs R, Maes F, Denis K, White S, Coudyser W et al. Image quality vs radiation dose of four cone-beam computerized scanners [J]. Dentomaxillofac Rad, 2008; 37(6); 309-319
78. Ludlow JB, Gubler M, Cevidanes LHS, Mol A. Precision of cephalometric landmark identification: cone-beam tomography vs. conventional cephalometric views [J]. Am J Orthod Dentofacial Orthop, 2009; 136(3): 312e1-10; discussion 312-313
79. Liang X, Lambrichts I, Sun Y, Denis K, Hassan B, Li L, Pauwels R, Jacobs R. A comparative evaluation of Cone Beam Computed Tomography (CBCT) and Multi-Slice CT (MSCT). Part I: On objective image quality [J]. Eur J Radiol; 2010; 75(2): 265–269

80. Katsumata A, Hirukawa A, Noujeim M, Okumura S, Naitoh M, Fujishita M, Ariji E, Langlais RP. Image artifact in dental cone-beam CT [J]. Oral Surg Oral Med Oral Pathol Oral Radiol Endod, 2006; 101(5): 652-657
81. Van Daatselaar AN, Dunn SM, Spoelder HJ, Germans DM, Renambot L, Bal HE. Feasibility of local CT of dental tissues [J]. Dentomaxillofac Radiol, 2003; 32(3): 173-180
82. Hassan B, Couto Souza PC, Jacobs R, de Azambuja Berti S, van der Stelt P. Influence of scanning and reconstruction parameters on quality of three-dimensional surface models of the dental arches from cone beam computed tomography. Clin Oral Investig, 2010; 14(3): 303-310
83. Halazonetis DJ. Morphometrics for cephalometric diagnosis [J]. Am J Orthod Dentofacial Orthop, 2004; 125(5): 571-581
84. Grauer D, LSH Cevidanes, Profitt WR. Working with DICOM craniofacial images [J]. Am J Orthod Dentofacial Orthop, 2009; 136(3): 460-470
85. Schuze RKW, Berndt D, d'Hoedt B. On cone-beam computed tomography artifacts induced by titanium implants [J]. Clin Oral Implants Res, 2010; 21(1): 100-107
86. Gomi T, Koshida K, Miyati T. Development of a cone angle weighted three-dimensional image reconstruction algorithm to reduce cone-beam artifacts [J]. Dentomaxillofac Rad, 2006; 35(6): 398-406
87. Hassan B, van der Stelt P, Sanderink G. Accuracy of three-dimensional measurements obtained from cone beam computed tomography surface-rendered images for cephalometric analysis: influence of patient scanning position [J]. Eur J Orthod, 2009; 31(2): 129-134

Chapter 2

Segmentation Process Significantly Influences the Accuracy of 3D Surface Models Derived from Cone Beam Computed Tomography

This chapter is based on the following publication:
Fourie Z, Damstra J, Schepers R, Gerrits PO, Ren Y. Segmentation Process Significantly Influences the Accuracy of 3D Surface Models Derived from Cone Beam Computed Tomography. Eur J Radiol, 2011; Accepted

Aims: To assess the accuracy of surface models derived from 3D Cone Beam Computed Tomography (CBCT) with two different segmentation protocols.
Materials and methods: Seven fresh-frozen cadaver heads were used. There was no conflict of interests in this study. CBCT scans were made of the heads and 3D surface models were created of the mandibles using two different segmentation protocols. The one series of 3D models was segmented by a commercial software company (CS), while the other series was done by an experienced 3D clinician (DS). The heads were then macerated following a standard process. A high resolution laser surface scanner (LSS) was used to make a 3D model of the macerated mandibles, which acted as the reference 3D model or "gold standard". The 3D models generated from the two rendering protocols were compared with the "gold standard" using a point-based rigid registration algorithm to superimpose the three 3D models. The linear difference at 25 anatomic and cephalometric landmarks between the laser surface scan and the 3D models generated from the two rendering protocols was measured repeatedly in two sessions with one week interval.
Results: The agreement between the repeated measurements was excellent (ICC = 0.923 – 1.000). The mean deviation from the gold standard by the 3D models generated from the CS group was 0.330 mm ± 0.427, while the mean deviation from the Clinician's rendering was 0.763 mm ± 0.392. The surface models segmented by both CS and DS protocols tend to be larger than those of the reference models. In the DS group, the biggest mean differences with the LSS models were found at the points ConLatR (CI: 0.83 – 1.23), ConMedR (CI: -3.16 – 2.25), CoLatL (CI: -0.68 – 2.23), Spine (CI: 1.19 – 2.28), ConAntL (CI: 0.84 – 1.69), ConSupR (CI: -1.12 –1.47) and RetMolR (CI: 0.84 – 1.80).
Conclusion: The Commercially segmented models resembled the reality more closely than the Doctor's segmented models. If 3D models are needed for surgical drilling guides or surgical planning which requires high precision, the additional cost of the commercial segmentation services seem to be justified to produce a more accurate surface model.

2.1 Introduction

Since Cone Beam Computed Tomography (CBCT) technology became available, its popularity has increased rapidly. This three dimensional (3D) technology displays a realistic representation of the human head[1] and is used to create different 2D tomographic slices, projection images and 3D volume and surface reconstructions. Images provided by CBCT are of diagnostic quality with relatively low radiation dose used.[2] Applications of 3D surface models derived from CBCT include pre-operative implant planning, evaluation of the jaws, assessment of the bone volume required for orthogenetic surgery,[3] and creating physical dental models of the jaws using stereo-lithography technology.[4] In addition, 3D surface models allow for actions such as indicating landmarks, performing measurements, moving bone fragments, pre-operative implant planning and performing virtual osteotomies. Recently, superimposition of 3D models has been used to evaluate the treatment outcomes of orthodontics and craniofacial surgery.[5] However, a high level of accuracy is required before 3D surface models can be applied in clinical settings.[6,7]

The 3D CBCT data are composed of voxels, each with its own gray level based on indirect calculation of the radiation absorbed. The voxel can be compared with the pixel of 2D images but with the added dimension of depth. The computer uses the voxel data to "draw" or reconstruct the 3D volume by means of algorithm, a process called "rendering". Following the volume rendering, 3D surface models of the bone and soft-tissues can be generated by a triangulated mesh covering the selected surface of interest by applying an algorithm.[8] The surface models constructed from voxel-based data require the input of a threshold value specifying what the structure of interest is.[8] The user determines the threshold value of visible and invisible voxels. Herein lays the major inherent problem associated with the segmentation process: The accuracy of segmentation relies on the gray-value and the threshold value entered by the operator.[8] In order to overcome this problem; Hassan et al. [7] and Loubele et al. [9] used a threshold automatically determined and operator independent. However, this process is complicated because CBCT imaging suffers from beam inhomogeneity which results in variation of image quality and accuracy among different manufactures and reconstruction parameters.[7,9] This means that the grey levels of the voxels of the same object imaged by different scanners are likely to differ, resulting in difference in the segmentation process.

In addition, the segmentation process could be very time consuming and arduous which may not be clinically viable. To overcome the segmentation problems regarding accuracy and time-management, companies specialized in 3D imaging technology now offer a commercial segmentation service, often costly, to clinicians. However, to justify the additional cost of this service, the perceived benefits e.g.,

time-saving and improved accuracy should be weighed. Therefore, the aims of this study are to assess the accuracy of the 3D CBCT derived surface models from different segmentation protocols. This will be achieved by comparing commercially segmented models and doctor's segmented models to 3D models derived from a laser surface scanner.[10] Uniquely we used cadaver heads with intact soft tissue covering to best simulate the clinical situation.

Table 1 Landmarks used in this study

Landmark and Abbreviation		Definition
Unilateral landmarks		
B-point	B	The deepest bony point of the contour of the mandible above pogonion
Pogonion	Pog	The most anterior midpoint of the chin on the outline of the mandibular symphysis
Gnathion	Gn	The midpoint between Pog and Me on the outline of the mandibular symphysis
Menton	Me	The most inferior midpoint of the chin on the outline of the mandibular symphysis
Inferior mental spine	Spine	The tip of the inferior mental spine at the lingual surface of the mandibular symphysis.
Bilateral landmarks		
Condylion laterale	CoLat	The most lateral point of each mandibular condyle in the coronal plane
Condylion	Co	The most superior point of each mandibular condyle in the sagittal plane
Condylion mediale	CoMed	The most medial point of each mandibular condyle in the coronal plane
Condylion Anterior	CoAnt	The most anterior point of each mandibular condyle in the sagittal plane
Condylion Posterior	CoPost	The most anterior point of each mandibular condyle in the sagittal plane
Gonion	Go	A point on the curvature of the angel of the mandible located by bisecting the angle from by lines tangent to the posterior ramus and the inferior border of the mandible
Coronoid proses	Cor	The most superior point on coronoid process
Mental foramen	Mentalis	The distal part of mental foramen
Lingula Mandibulae	LingMand	The tip of the lingula mandibulæ, a sharp spine superior presents in front a prominent ridge at the foramen mandibulae
Retromolar	RetMol	The point in the middle of alveolar ridge the retromolar area of mandible

2.2 Materials and Methods

Our study sample consisted of seven fresh cadaver heads supplied by the Department of Anatomy, University Medical Centre Groningen (UMCG), the Netherlands. Ethical approval was granted before starting with this project. In the present study only surface models of the mandible were used for comparison. A high resolution laser surface scanner was used to create the reference or gold standard 3D model.[10]

Figure 1: *Isometric view of the 3D surface models of the laser surface scan (LSS), Commercial segmentation (CS) and Doctor's segmentation (DS) separately before they were superimposed. This is to show the difference in surface quality.*

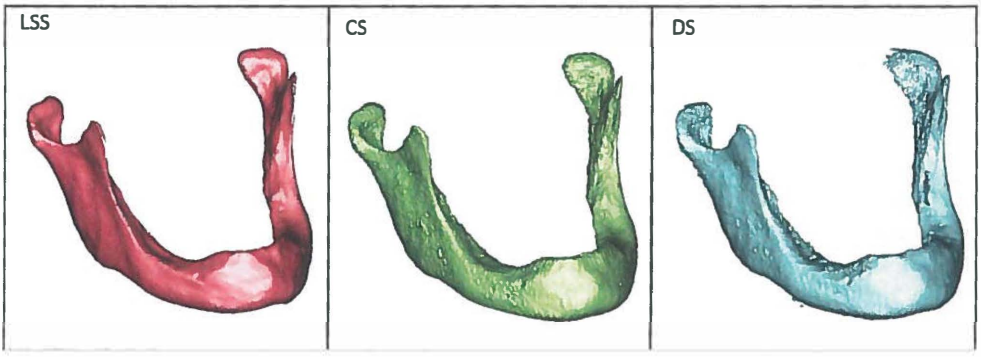

Cone beam computed tomography (CBCT) imaging and segmentation protocols

The cadaver heads were scanned with the KaVo 3D exam scanner (KaVo Dental GmbH, Bismarckring, Germany) according to the manufacturer's instructions. The head was positioned and fixated in the scanner with the head facing forward and Frankfurt horizontal plane parallel to the floor. The head was scanned with a 0.3 mm voxel size with a 17 mm field of view.[11,12] The acquired CBCT DICOM datasets were transferred to a personal laptop computer before performing the segmentations. Two segmentation protocols were followed. 1: the acquired CBCT DICOM files were sent to Materialise Dental, (Leuven, Belgium) for segmentation. The surface models were segmented by experienced 3D technicians and are referred to as the commercial segmentation (CS) group in this study; 2: CBCT images were exported in DICOM multi-file format and imported into SimPlant Ortho Pro® 2.1 (Materialise Dental, Leuven, Belgium) software on an Acer Aspire 7730G laptop (Acer, s'Hertogenbosch, the Netherlands) with a dedicated 512 mb video card (Nvidia® Geforce ® 9600M-GT, NVIDIA, Santa Clara, California, USA). The 3D surface models of

all CBCT images were generated by a clinician with 3 years' experience in 3D CBCT imaging (RS) using the same software. These segmentations are referred to as the doctor's segmentation (DS) group (Figure 1). To avoid any bias, the aims of this study were neither known to the commercial segmentation service nor to the clinician.

Laser surface scan procedure

The soft tissue was removed from all the cadaver heads by the Department of Anatomy. Thereafter, the cadaver heads were macerated following a standard protocol to remove the remaining soft tissue and to produce dry mandibles. The laser surface scan procedure was performed by a 3D scanning and 3D printing company (CNC consult, Den Bosch, The Netherlands). The dry mandibles were scanned individually using the Metris® ModelMarker D 100 with ESP2 laser surface scanner on a Metris®2400 M7 Measuring Coordinating Arm (Metris® HQ, Leuven, Belgium). The scanning was performed by an experienced 3D technician. The laser scanner allows obtaining surfaces in the form of a point cloud with an accuracy of 23 µm. The top and the bottom halves of the mandibles were scanned individually and then joined together using Geomagic® Studio 11 (Geomagic® International, NC, America) by the same technician. The resulting 3D surface models were extracted as an STL file. The laser surface scanning models were regarded as the reference or "gold standard" and are referred to as the laser surface scanning (LSS) group (Figure 1).

Measuring procedure

The CS and DS models of each mandible were superimposed with the LSS models. A large number of point clouds distributed along the surface models were compared and matched. The 3D models had valid geometric matching points ranging from 67838 – 87914. The registration process was fully automatic and performed using Mimics® Medical Image Processing Software (Materialise®, Leuven, Belgium).[10,13,22] This point-based registration method has been proven to be extremely accurate and reliable.[21] Firstly, the average differences of the whole surfaces of the 3D models superimposed were calculated by the computer (Table 1). Secondly, twenty five anatomical and cephalometric landmarks (10 bilateral and 5 unilateral) were identified and marked on the laser surface scan (Table I) to get a better indication of the distribution of the differences. These landmarks were chosen to represent the whole surface of the mandible, with the emphasis on those commonly used in cephalometry. At each landmark, the difference in millimetre (mm) was measured between the LSS and the CS and between the LSS and the DS using the measuring tool of the SimPlant Ortho Pro® 2.1 software under the maximum magnification

Figure 2: *Measurement "a" was made between the laser surface scan (pink) and the Commercial segmentation (green) while measurement "b" was made between the laser surface scan (pink) and the Doctor's segmentation (blue) 3D model of the mandible. A – Axial view of point Mentalis with measurement "a" and "b" made in the zoomed in view. B- Sagittal views of point Pog with measurement "a" and "b" made in the zoomed in view. C - Coronal view of point Cor with measurement "a" and "b" made in the zoomed in view.*

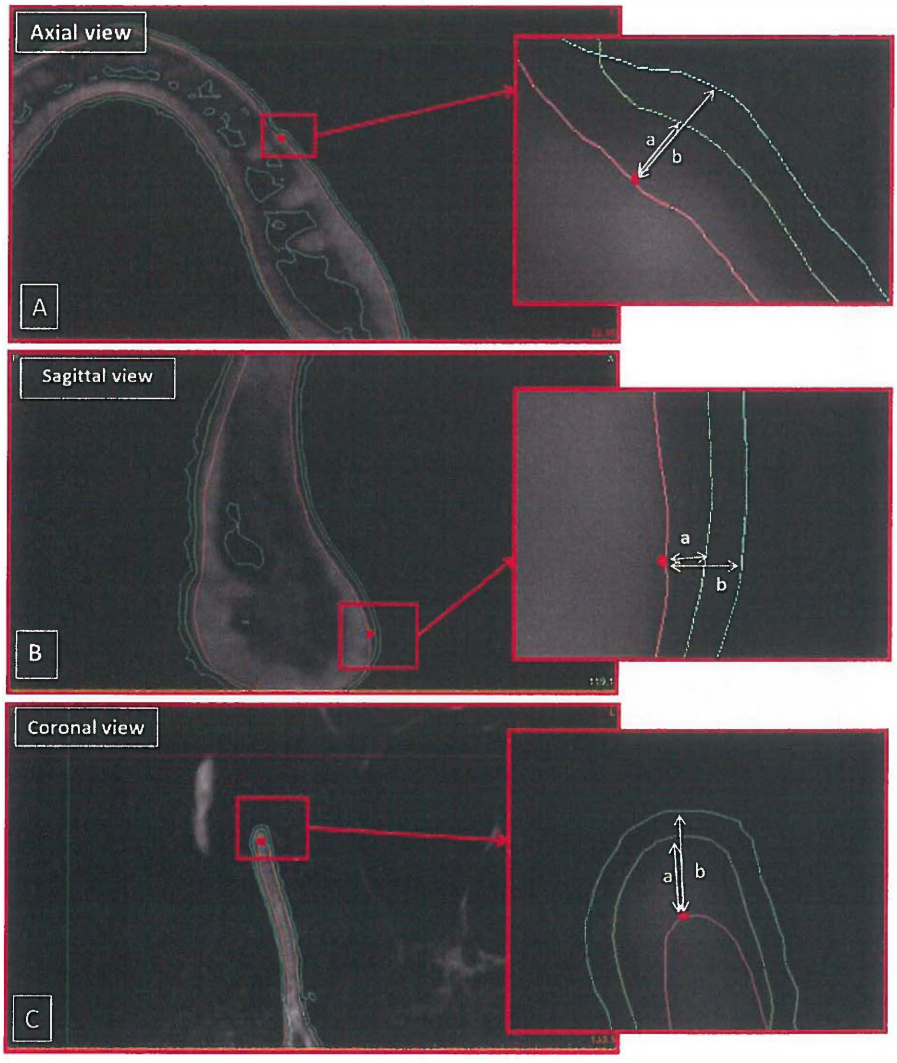

(Figure 3). Each measurement was made in the direction of interest of the specific landmark e.g., the axial view (ConLat, ConMed, Ment, LingMand), the sagittal view (B, Pog, Gn, Me, Spine, CoAnt, CoPost, Go) or the coronal views (ConSup, Cor, RetMol). These measurements were repeated by one operator (ZF) after one week.

Statistical analysis

All analyses were performed with a standard statistical software package (SPSS version 16, Chicago, IL). An error study was performed. The method of determining the differences between CS vs. LSS and DS vs. LSS was repeated (T1 and T2) by one observer with a week interval. The differences for each measurement were pooled and total of 700 measurements were repeated and compared. Agreement between measurements was evaluated by means of the intraclass correlation coefficient (ICC) for absolute agreement based on a 2-way random effects analysis of variance (ANOVA). The method error was determined with Dahlberg's formula: $S^2 = \sum d^2/2n$ (d = difference between the paired measurements, n = sample size).

Accuracy of the CS and DS models was determined by examining the difference between the landmark locations on the CS or DS to those on the LSS models upon superposition. Means, standard deviations and confidence intervals for the differences were calculated for the two segmentation protocols. Differences between the CS and DS groups were analysed with Wilcoxon ranked sum tests. Significance at $P < 0.05$

Table 2 Mean and standard deviation (SD) of the Doctor's segmentation and Commercial segmentation vs. the laser surface scan (gold standard) using the point based analysis

	vs. Laser surface scan			
	Commercial segmentation		Doctor's segmentation	
	Mean (mm)	SD (mm)	Mean (mm)	SD (mm)
Mandible 1	0.291	0.409	0.655	0.249
Mandible 2	0.251	0.391	0.654	0.318
Mandible 3	0.403	0.469	0.734	0.439
Mandible 4	0.420	0.423	0.706	0.365
Mandible 5	0.466	0.399	0.894	0.306
Mandible 6	0.208	0.524	0.727	0.372
Mandible 7	0.273	0.351	0.974	0.697
Average	**0.330**	**0.427**	**0.763**	**0.392**

2.3 Results

The mean deviations of the 3D surface models from the gold standard are summarized in Table 2. The CS group had a smaller mean deviation (0.330 mm ± 0.427) compared to the DS group (0.763 mm ± 0.392), in other words, the CS models resemble the LSS models more closely. To visualize the differences, the matching fit level of each model was marked with a colour bar (Figure 3).

The results of the error study are summarized in Table 3. The agreement between the repeated measurement was very high (ICC = 0.98). The average method error was very small mean = 0.05 (95% CI: 0.03 – 0.07) in both groups, confirming the high accuracy of the method used.

Means, standard deviations and confidence intervals for the differences of the CS and DS groups from the LSS are summarized in Table 4. The surfaces models from both CS and DS groups were generally larger than the LSS models. In the CS group 84% of all measurements were larger than the laser model. In the DS group 90% of all measurements were larger than the laser model. In addition, the magnitude of surface models from the DS group tended to be larger than for the CS group based on the absolute mean values (Table 4). In the DS group, the biggest mean differences with the LSS models were found at the points ConLatR (CI: 0.83 – 1.23), ConMedR (CI: -3.16 – 2.25), CoLatL (CI: -0.68 – 2.23), Spine (CI: 1.19 – 2.28), ConAntL (CI: 0.84 – 1.69), ConSupR (CI: -1.12 –1.47) and RetMolR (CI: 0.84 – 1.80). In general the smaller differences were found in the unilateral landmarks than in the bilateral landmarks.

2.4 Discussion

This study was performed to assess and compare the geometric accuracy of 3D surface models from different segmentation protocols. The results showed that a clear difference existed between the accuracy of the CS and DS models. Overall, the CS models resembled more closely the LSS models than the DS models. This was especially true for the measurement involving the condylar landmarks and those on the lingual side of the mandible. A general trend was found that the models from CS and DS groups were larger than the LSS. The findings of the present study are important for clinical procedures requiring high accuracy i.e. 3D planning of surgical drilling guides for implant placement, in which minimal transfer error from preoperative planning can result in significant errors to the surgical field.[13]

Table 3 Results of the error study. (T = measuring session, ICC = intercorrelation coefficient, ME = Method error)

		CS vs. LSS		DS vs. LSS	
Direction of interest		T1 - T2		T1 - T2	
		ICC	ME	ICC	ME
Axial					
1	ConLatR	0.99	0.02	0.99	0.03
2	ConLatL	1.00	0.12	1.00	0.03
3	ConMedR	1.00	0.02	1.00	0.02
4	ConMedL	1.00	0.17	1.00	0.03
5	LingMandR	1.00	0.01	0.96	0.11
6	LingMandL	0.99	0.01	0.99	0.02
7	MentalisR	0.85	0.12	0.91	0.12
8	MentalisL	0.99	0.03	0.98	0.03
Sagittal					
9	B	0.98	0.03	0.99	0.04
10	Pog	0.99	0.02	0.82	0.09
11	Gn	1.00	0.01	1.00	0.02
12	Me	0.99	0.02	0.98	0.02
13	Spine	1.00	0.03	1.00	0.04
14	Go	0.86	0.18	0.83	0.19
15	GoL	1.00	0.01	0.99	0.03
16	ConAntR	1.00	0.01	1.00	0.01
17	ConAntL	0.99	0.03	1.00	0.02
18	ConPostR	1.00	0.01	1.00	0.03
19	ConPostL	1.00	0.02	1.00	0.04
Coronal					
20	ConSupR	1.00	0.01	1.00	0.02
21	ConSupL	1.00	0.18	1.00	0.04
22	CorR	0.95	0.17	0.96	0.23
23	CorL	1.00	0.01	1.00	0.02
24	RetMolR	1.00	0.01	1.00	0.03
25	RetMolL	1.00	0.02	0.98	0.08
Average		**0.98**	**0.05**	**0.98**	**0.05**

We had the unique opportunity to first use fresh cadaver heads and then the skulls after maceration, so all data from the same head could be compared and no artificial media was needed to mimic soft tissues. In previous studies comparing surface models derived from CBCT scans, either only dry skulls were used or simulation of soft-tissue attenuation was added. The simulation methods include placing a latex balloon filled with water at the lingual area of the dry mandible,[14] or placing the dry skull in a water bath. The latter could be problematic during positioning in the CBCT scanner and might damage the dry skull.[15] Moreover, if only scanning the mandible, the missing cervical vertebra and skull base could influence the results[21]. For this reason, a full cadaver skull including both lower and upper jaws with soft tissue and

cervical vertebra was suggested[10]. In the present study a full fresh cadaver head with cervical vertebrae were used for the CBCT scans.

The factors with significant influence on the quality of the CBCT derived 3D segmented models are voxel size, patient scanning position, beam inhomogeneity of CBCT scanners etc.[14-16] Significant differences has been reported between 3D models of the same skull from different CBCT scanners.[17] In the present study, these factors were controlled by using the same CBCT scanner and scanning parameters. Our results suggest that the most significant factor determining the accuracy of surface models is likely to be the differences between threshold dependant methods. Although there is a standard pre-set threshold for bone, soft tissue and teeth specified by the software, the threshold can be adjusted by the operator to enhance the quality of a certain region of interest. This makes DS a very subjective method. In order to overcome this problem, Hassan et al.[7] and Loubele et al.[9] used a threshold automatically determined and observer independent and found that the threshold value was less in the mandible than in the maxilla. The explanation could be that cortical bone in the mandible is thick enough to keep the attenuation profile inform across the entire bone surface, while in the maxilla the varied thin cortical bone especially in the palate and tuberosity regions created significant bone dehiscence and fenestrations artefacts in the 3D model.[8] It is therefore almost impossible to apply a single threshold value for the whole bone tissue or even just a single jaw. When segmenting the mandible or maxilla, choosing a single threshold value (whether operator or automatically determined) is likely to be inaccurate since the density of the bone differs significantly within the structures itself.

Superimposition of 3D surface models is an effective method to evaluate growth, treatment outcome of orthodontic and craniofacial treatment and to determine differences between 3D models. After superimposition of pre- and post-treatment 3D models, change can be quantified by means of colour maps.[5] In the present study an automated surface matching algorithm based on point-based registration was used to improve the accuracy of the model registration process. The main advantages of this method are that it is accurate, reliable and the entire 3D model surface is used for registration instead of landmarks. Also, since the procedure is fully automated, the influence of the observer's variability on measurements accuracy is completely eliminated. A complex shape like the mandibular surface is more difficult to assess than a uniform geometric object. The arch curved shape causes blurring of object boundaries.[10] In the present study, the differences were measured at 25

Figure 3: *The isometric views of the colour mapping from the two groups. The differences between the group Commercial segmentation vs. laser surface scan and the group Doctor's segmentation vs. laser surface scan of mandibles 1 to 7 can be visually compared. The different colours represents the amount of deviation from the gold standard (laser surface scan), see the colour bar at the bottom for amount of deviation in millimeter (mm).*

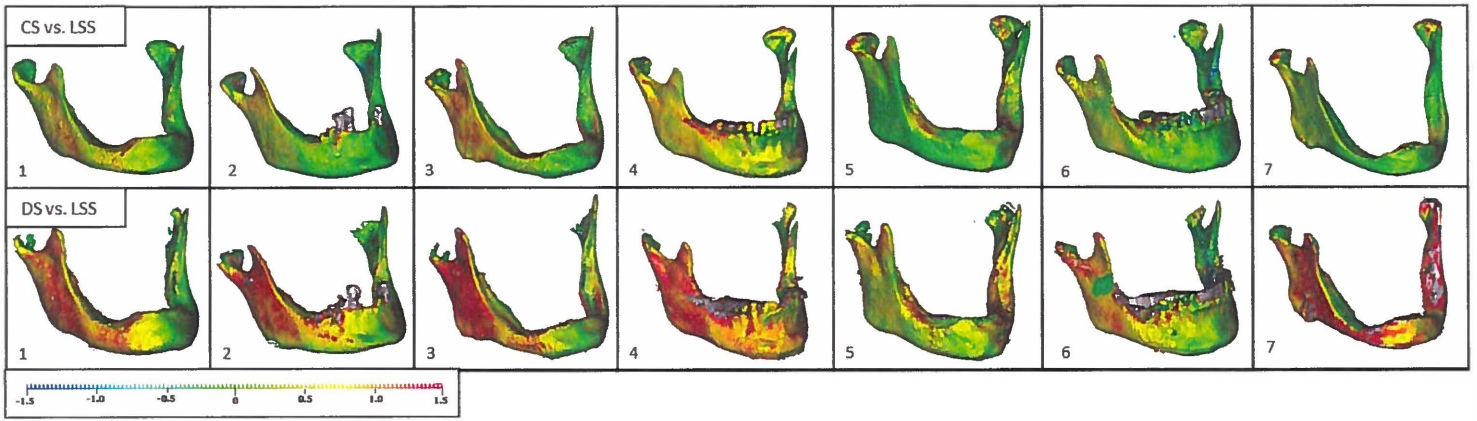

Table 4 The mean distance in millimetres (mm), standard deviation (SD) and 95% confidence interval (CI) of Commercial segmentation and the Doctor's segmentation vs. the gold standard LSS. If (-) negative values in the differences indicate that the CS or DS models is smaller than the LSS, see Figure 2. The differences between the CS and DS groups were indicated with P value.

Direction of interest		Difference with LSS models						
		Commercial segmentations (CS)			Doctors segmentations (DS)			
Axial		**Mean**	**SD (±)**	**CI (95%)**	**Mean**	**SD (±)**	**CI (95%)**	**P**
1	ConLatR	0.75	0.06	0.70 - 0.80	1.03	0.27	0.83 - 1.23	0.05
2	ConLatL	0.71	0.22	0.55 - 0.88	0.78	1.96	-0.68 - 2.23	0.01
3	ConMedR	0.18	0.36	-0.09 - 0.45	-0.46	3.66	-3.16 - 2.25	0.02
4	ConMedL	0.15	0.38	-0.14 - 0.43	0.83	1.52	-0.29 - 1.96	0.21
5	LingMandR	0.29	0.27	0.09 - 0.49	0.66	0.45	0.32 - 0.99	0.07
6	LingMandL	0.17	0.14	0.07 - 0.28	0.52	0.23	0.34 - 0.69	0.04
7	MentalisR	0.44	0.30	0.22 - 0.66	0.88	0.34	0.63 - 1.14	0.03
8	MentalisL	0.42	0.17	0.30 - 0.55	0.81	0.21	0.66 - 0.96	0.01
Saggital								
9	B	0.23	0.13	0.13 - 0.32	0.56	0.23	0.39 - 0.73	0.02
10	Pog	0.09	0.11	0.01 - 0.17	0.43	0.20	0.28 - 0.58	0.01
11	Gn	-0.11	0.19	-0.25 - 0.03	0.16	0.28	-0.04 - 0.37	0.53
12	Me	0.07	0.11	-0.01 - 0.16	0.41	0.15	0.29 - 0.52	0.00
13	Spina	0.93	0.25	0.74 - 1.11	1.74	0.74	1.19 - 2.28	0.01
14	GoR	0.39	0.22	0.22 - 0.55	0.87	0.45	0.54 - 1.21	0.07
15	GoL	0.43	0.27	0.22 - 0.63	0.90	0.33	0.66 - 1.15	0.10
16	ConAntR	0.23	0.45	-0.10 - 0.56	0.23	0.87	-0.41 - 0.87	0.05
17	ConAntL	0.43	0.27	0.23 - 0.63	1.27	0.58	0.84 - 1.69	0.01
18	ConPostR	0.73	0.17	0.60 - 0.85	1.02	0.95	0.32 - 1.73	0.04
19	ConPostL	0.45	0.33	0.21 - 0.70	1.16	2.32	-0.56 - 2.87	0.01
Coronal								
20	ConSupR	0.28	0.29	0.06 - 0.49	0.17	1.74	-1.12 - 1.47	0.05
21	ConSupL	0.92	0.81	0.32 - 1.51	1.72	1.99	0.24 - 3.19	0.32
22	CorR	0.77	0.70	0.25 - 1.29	0.74	1.00	-0.01 - 1.48	0.80
23	CorL	0.22	0.25	0.03 - 0.40	1.02	0.71	0.49 - 1.55	0.02
24	RetMolR	0.73	0.36	0.46 - 1.00	1.32	0.64	0.84 - 1.80	0.10
25	RetMolL	0.33	0.39	0.03 - 0.62	0.90	0.55	0.49 - 1.30	0.07

commonly used anatomical and cephalometric landmarks and the results are clinically relevant suggesting that the segmentation process significantly influences the cephalometric measurements especially at the condylar region.

Image artefacts associated with the CBCT affect the segmentation accuracy.[18] In the current study, the artefacts were mostly located at the lingual parts of mandible, the condyle and around alveolar crest. Liang et al. [10] found artifacts at the mandibular border and the posterior margin of the scan volume. Those parts were mostly located near the periphery of the scan volume. These "halation defects" whether streak or ring artefacts may cause considerable image distortions at the periphery of the scan volume, which could influence the segmentation accuracy.[10] Moreover, these areas are of less interest for surgical implant applications compared to the body of the mandible and important anatomical structure like the mental foramen. However, they might influence cephalometric measurements. Katsumata et al.[18] and Van Daatselaar et al.[19] reported specific artifacts when data discontinuity using limited-volume CBCT system. This phenomenon was thought to be a CBCT artefact related to halation from the image intensifier (II). This artefact appeared only when the area to be imaged was positioned near the facial surface. In addition, this artefact will not appear in CBCT systems using image II which are designed to scan large fields of view (FoV) whereby larger II tubes are used. In limited volume CBCT imaging, the size of the FoV is small as compared to the entire head and the intensity of transparent x-radiation fluctuates during the 360° scan. When an incident occurs in which some part of the x-ray beam reaches the fluorescent surface without passing through the patient's head, presumed halation from II occurs. In practice possible solutions might be a lower voltage. Another possibility involving more radiation is a reduction in the sensitivity or brightness setting of the II unit. However, it is clear that insufficient x-ray intensity leads to reduced image quality.[10] Hassan et al.[7] also reported more image artifacts associated with the smaller scan field. This was not the case in this present study as we used a large FoV (17mm).

Although the 3D models of the CS group were more accurate at the condylar region, it must be kept in mind that measurement error can be cumulative. Incorporation of deviations from all the landmarks used for the measurement ultimately resulting in clinically significant measurement error.[20] In the present study, there was a big difference between the left and right sides of the condylar measurements in the DS group (Table 4). This was not the case in the CS group. This indicates the unreliability of the surface model at condylar region in the DS group. If that is the region of interest, CS

should be considered. Therefore, the results of the present study suggest that care has to be taken when drawing conclusions from measurements and comparisons made from different segmentations, especially at the condylar region.

The present study did not include the maxilla because laser surface scanning of the maxilla is challenging and unreliable. The maxilla is an air-filled structure and structures like the lateral wall of the maxillary sinus and the walls of the orbit are extremely thin which allows for the laser to pass through it without being detected.[10] This makes the resulting maxillary surface model unreliable. In addition, the extremely complex geometry of the maxilla makes scanning with a surface laser scanner challenging.[10] The relatively small sample size and only including the mandible, might be seen as limitations of this study. In future, more accurate 3D measurements might be obtained when image segmentation procedures, based on both intensity and gradient magnitude of the signals, will be implemented rather than the current threshold based methods.

2.5 Conclusion

Producing 3D surface models from CBCT datasets is still less accurate than the reality when using threshold based methods. The 3D models are the least accurate at the condyle region and the lingual side of the mandible. If 3D models are needed for high precision, the additional cost of CS models seems to be justified to produce a more accurate surface model.

2.6 References

1. Hofrath H. Bedeutung der Röntgenfern und Abstands Aufnahme für die Diagnostik der Kieferanomalien. Fortschr Orthod 1931;1:231–258
2. Hashimoto K, Arai Y, Iwai K, Araki M, Kawashima S, Terakado M. A comparison of a newlimited cone beam computed tomographymachine for dental use with a multidetector row helical CT machine. Oral Surg Oral Med Oral Pathol Oral Radiol Endod 2003;95:371–437
3. Pohlenz P, Blessmann M, Blake F, Gbara A, Schmelzle R, Heiland M. Major mandibular surgical procedures as an indication for intraoperative imaging. J Oral Maxillofac Surg 2008;66:324–329
4. van Steenberghe D, Ericsson I, Van Cleynenbreugel J, Schutyser F, Brajnovic I, Andersson M. High precision planning for oral implants based on 3-D CT scanning. A new surgical technique for immediate and delayed loading. Appl Osseointegration Res 2004;4:27–31

5. Cevidanes LHS, Styner MA, Proffit WR. Image analysis and superimposition of 3-dimensional cone-beam computed tomography models. Am J Orthod Dentofacial Orthop 2006;129:6111-618
6. Mischkowski RA, Pulsfort R, Ritter L, Neugebauer J, Brochhagen HG, Keeve E, Zoller JE. Geometric accuracy of a newly developed cone-beam device for maxillofacial imaging. Oral Surg Oral Med Oral Pathol Oral Radiol Endod 2007; 104: 551-559
7. Hassan B, Couto Souza PC, Jacobs R, de Azambuja Berti S, van der Stelt P. Influence of scanning and reconstruction parameters on quality of three-dimensional surface models of the dental arches from cone beam computed tomography. Clin Oral Inverstig 2010;3:303-310
8. Halazonetis DJ. From 2-dimensional cephalograms to 3-dimensional computed tomography scans. Am J Orthod Dentofacial Orthop 2005;127:627-637
9. Loubele M, Jacobs R, Maes F, Denis K, White S, Coudyser W et al. Image quality vs radiation dose of four cone-beam computerized scanners. Dentomaxillofac Rad 2008; 37; 309-319
10. Liang X, Lambrichts I, Sun Y, Denis K, Hassan B, Li L, Pauwels R, Jacobs R. A comparative evaluation of Cone Beam Computed Tomography (CBCT) and Multi-Slice CT (MSCT). Part II: On 3D model accuracy. Eur J Radiol;2010: 270–274
11. Fourie Z, Damstra J, Gerrits PO, Ren Y. Evaluation of anthropometric accuracy and reliability using different three-dimensional scanning systems. Forensic Sci. Int 2011;207:127-134
12. Fourie Z, Damstra J, Gerrits PO, Ren Y. Accuracy and reliability of facial soft tissue depth measurement using cone beam computed tomography. Forensic Sci Int 2010;199:9-14
13. Besimo CE, Lambrecht JT, Guindy JS. Accuracy of implant treatment planning utilizing template guided reformation computed tomography. Dentomaxillofacial Radiology 2000;29:46-51
14. Ballrick JW, Palomo JM, Ruch E, Amberman BD, Hans MG. Image distortion and spatial resolution of a commercially available cone-beam computed tomography machine. Am J Orthod Dentofacial Orthop 2008; 134: 573-582
15. Hassan B, van der Stelt P, Sanderink G. Accuracy of three-dimensional measurements obtained from cone beam computed tomography surface-rendered images for cephalometric analysis: influence of patient scanning position. Eur J Orthod 2008 [E-pub ahead of print]
16. Damstra J, Fourie Z, Huddleston Slater JJR, Ren Y. Accuracy of linear measurements form cone-beam computed tomography-derived surface models of different voxel sizes. AJO-DO 2010;137:16.e1-16.e6
17. Van Vlijmen OJ, Rangel FA, Berge SJ, Bronkhorst EM, Becking AC, Kuiper-Jagtman AM. Measurements on 3D models of human skulls derived from different cone beam scanners. Clin Oral Investig 2010, Jun
18. Katsumata A, Hirukawa A, Noujeim M, Okumura S, Naitoh M, Fujishita M, Ariji E, Langlais RP.Image artifact in dental cone-beam CT. Oral Surg Oral Med Oral Pathol Oral Radiol Endod. 2006 May;101(5):652-657
19. Van Daatselaar AN, Dunn SM, Spoelder HJ, Germans DM, Renambot L, Bal HE. Feasibility of local CT of dental tissues. Dentomaxillofac Radiol 2003;32:173-180

20. Damstra J, Huddleston Slater JJR, Fourie Z, Ren Y. Reliability and the smallest detectable difference of lateral cephalometric measurements. Am J Orthod Dentofacial Orthop 2010: 138; 546e1-8; discussion 546-547

Chapter 3

The Influence of the Segmentation Process on 3D Measurements from Cone Beam Computed Tomography-derived Surface Models

This chapter is based on the following publication:
Fourie Z, Engelbrecht WP, Damstra J, Gerrits PO, Ren Y. The Influence of the Segmentation Process on 3D Measurements from Cone Beam Computed Tomography-derived Surface Models. Clin Oral Investig, 2011; Accepted

Abstract

Objectives: To compare the accuracy of linear and angular measurements between cephalometric and anatomic landmarks on surface models derived from 3D Cone Beam Computed Tomography (CBCT) with two different segmentation protocols.

Materials and methods: CBCT scans were made of cadaver heads and 3D surface models were created of the mandible using two different segmentation protocols. A high resolution laser surface scanner (LSS) was used to make a 3D model of the macerated mandibles. Twenty linear measurements at 15 anatomic and cephalometric landmarks between the laser surface scan and the 3D models generated from the two segmentation protocols (CS and DS groups) were measured.

Results: The interobserver agreement for all the measurements of all three techniques was excellent (ICC: 0.97 – 1.00). In the CS and DS groups, the biggest mean AE differences with the LSS models were found at the condylar measurements and the measurement between the mandibular width at the mental foramen.

Conclusion: 3D surface models derived from CBCT datasets are less than reality when using threshold based methods. Differences in the segmentation process resulted in significant clinical differences between the measurements.

Clinical implications: Care has to be taken when drawing conclusions from measurements and comparisons made from different segmentations, especially at the condylar region and the lingual side of the mandible as differences of these measurements may be clinically significant.

3.1 Introduction

For an increasing number of indications, cone beam computed tomography (CBCT) is currently the three-dimensional (3D) imaging modality of choice in oral and maxillofacial radiology [1,2]. Subsequently, oral radiologists are equipped with DICOM data sets, which open new possibilities of data transfer, segmentation, planning, simulation, and image fusion in the field of oral and maxillofacial radiology [3]. CBCT images provide useful datasets to generate both two-dimensional (2D) planar projections and 3D surface or volume rendered images for the use in orthodontic assessment and treatment planning [4,5].

Rendering is the process performed by a 3D software program where an object is given particular characteristics to make it appear like a real world object with shadows and transparencies. A volumetric rendering program is needed to construct the 3D surface models from CBCT data sets imported from the CBCT scanner. Each rendering program has its own unique algorithm that transform the raw CT data to vector data by constructing a surface of triangles covering the object of interest [6]. CBCT has many applications in the maxillofacial region. It is used for locating impacted teeth, dental development, limits of tooth movement, airway assessment, diagnostics of the temporomandibular joint (TMJ) [7]. The 3D surface model can be used to indicating landmarks, making measurements, craniofacial morphology and superimposition as well as pre-operative osteotomy and dental implant planning [6-8].

The accuracy of the derived surface model is of extreme importance for diagnostic purposes, treatment planning, and outcome evaluation. The accuracy of the segmented 3D surface model depends on the gray-value and the threshold value that are chosen by the operator during the segmentation process [6]. Automatically determined and operator independent threshold values can be applied to possibly overcome this problem. However, this process is complicated because CBCT imaging suffers from beam inhomogeneity. This results in variation of image quality among different manufacturers [9,10]. In practice, variations of image quality can result in differences during the segmentation process due to differences of the grey levels of the same object imaged by different scanners.

The accuracy of CBCT images has been confirmed with various CBCT scanners [11-16]. However, the accuracy of surface models derived from CBCT seems to vary [12-16]. Recently, the accuracy of CBCT 3D surface and volume reconstructions based on linear cephalometric measurements have been established to be within 1-2mm [13,16]. However, according to our knowledge the measurement accuracy made on 3D surface

models derived from different segmentation protocols have not been reported yet. In addition, it is questionable if segmentations produced by clinicians are clinically viable because the segmentation process could be very time consuming and arduous. To overcome the segmentation problems regarding accuracy and time-management, companies specialized in 3D imaging technology now offers a commercial segmentation service. However, to justify the additional cost of this service, the perceived benefits of improved accuracy warrants further investigation. Therefore, the aims of this study are to assess the clinical difference of linear and angular measurements made on 3D CBCT derived surface models from different segmentation protocols. This will be achieved by comparing models segmented by a commercial rendering company and by an experienced clinician to 3D models derived from a laser surface scanner.

3.2 Materials and Methods

Our study sample consisted of seven fresh cadaver heads supplied by the Department of Anatomy, University Medical Centre Groningen, Groningen, The Netherlands. Ethical approval was granted before starting with this project. In the present study only surface models of the mandible were used for comparison. A high resolution laser surface scanner was used to create the reference or gold standard 3D model [17].

Cone beam computed tomography (CBCT) imaging and segmentation protocols

The cadaver heads were scanned with the KaVo 3D exam scanner (KaVo Dental GmbH, Bismarckring, Germany) according to the manufacturer's instructions. The head was positioned and fixated in the scanner with the head facing forward and Frankfurt horizontal plane parallel to the floor. The head was scanned with a 0.3 mm voxel size with a 17 mm field of view [18,19]. The acquired CBCT DICOM datasets were transferred to a laptop computer before performing the segmentations. Two segmentation protocols were followed. 1: the acquired CBCT DICOM files were sent to Materialise Dental, (Leuven, Belgium) for segmentation. The surface models were segmented by experienced 3D technicians and are referred to as the commercial segmentation (CS) group in this study; The aims of this study was not known to the 3D technicians. 2: CBCT images were exported in DICOM multi-file format and imported into SimPlant Ortho Pro® 2.1 (Materialise Dental, Leuven, Belgium) software on an Acer Aspire 7730G laptop (Acer, s'Hertogenbosch, the Netherlands) with a dedicated 512 mb video card (Nvidia® Geforce ® 9600M-GT, NVIDIA, Santa Clara, California, USA). The 3D surface models of all CBCT images were generated by a clinician (R.S.) with 3 years' experience in 3D CBCT

imaging and segmentation using the same software. These segmentations are referred to as the doctor's segmentation (DS) group. To avoid any bias, the aims of this study were neither known to the commercial segmentation service nor to the clinician.

Figure 1: *Isometric and posterior views of the 3D surface models of the* ***A****- laser surface scan (LSS),* ***B****- Commercial segmentation (CS) and* ***C****- Doctor's segmentation (DS).*

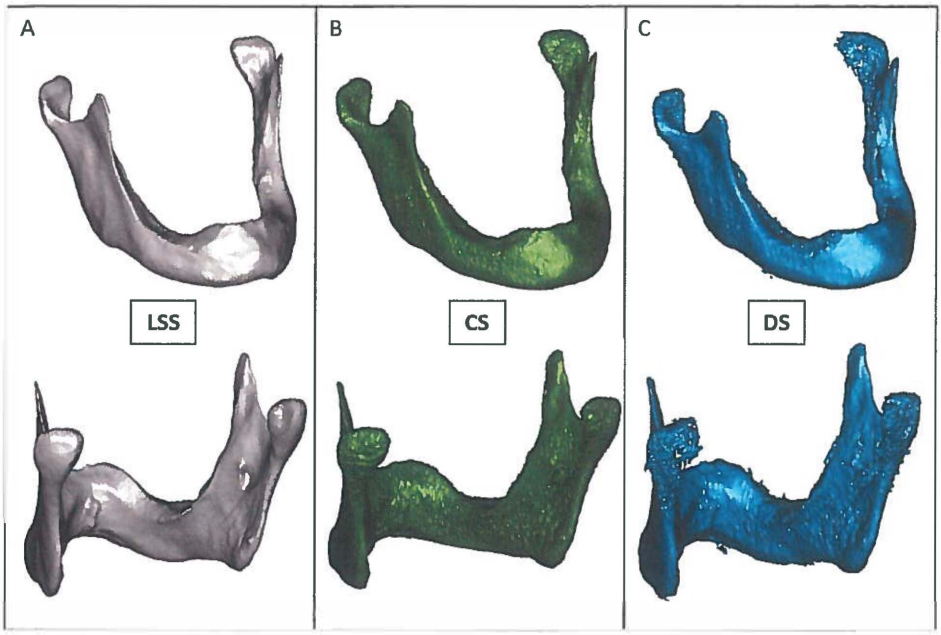

Laser surface scan procedure

Soft tissue was removed from all the cadaver heads by the dissectors of the Department of Anatomy at the University of Groningen. Thereafter, the cadaver heads were macerated following a standard protocol to remove the remaining soft tissue and to produce dry mandibles. The laser surface scan procedure was performed by a 3D scanning and 3D printing company (CNC consult, Den Bosch, The Netherlands). The dry mandibles were scanned individually using the Metris® ModelMarker D 100 with ESP2 laser surface scanner on a Metris®2400 M7 Measuring Coordinating Arm (Metris® HQ, Leuven, Belgium). The scanning was performed by an experienced 3D technician. The

laser scanner allows obtaining surfaces in the form of a point cloud with an accuracy of 23 µm. The top and the bottom halves of the mandibles were scanned individually and then joined together using Geomagic® Studio 11 (Geomagic® International, NC, America) by the same technician. The resulting 3D surface models were extracted as an STL file. The laser surface scanning models were regarded as the reference or "gold standard" and are referred to as the laser surface scanning (LSS) group (Figure 1).

Measuring procedure

Thirteen linear and seven angular measurements were made between 15 anatomical and cephalometric landmarks (14 bilateral and 1 unilateral) on the LSS, CS and DS (Figure 2; Table 1 and 2). These landmarks were chosen to represent the whole surface of the mandible, with the emphasis on landmarks commonly used in cephalometry. These measurements were performed on the LSS, CS and DS groups separately using the measuring tool of the SimPlant Ortho Pro® 2.1 software. These were repeated 5 times by one operator (PE) with one week apart for all seven mandibles. All the measurements were done on the 3D surface model view of the software.

Statistical analysis

To measure the intraobserver reliability, the intraclass correlation coefficient (ICC) for absolute agreement based on a 2-way random effects analysis of variance (ANOVA) was calculated between the five measurement sessions for variable of each 3D surface model technique (e.g. LLS, CS and DS). The results of the ICCs showed that the interobserver agreement for all the measurements of the all three techniques was excellent (ICC: 0.97 – 1.00). Therefore, the mean of the five repeated measurements was calculated and represented the actual values for each variable of each 3D surface model technique. Mean values and standard deviations were calculated and reported in Table 1.

To determine the clinical accuracy of the CS group and the DS group, the absolute error (AE) was used. Absolute error was defined as the CS or DS value subtracted by the LS value.[7] Mean values, standard deviations and 95% confidence intervals of the AE were calculated and reported in Table 2. All statistical analysis was performed with a standard statistical software package (SPSS version 14, Chicago, IL, USA).

Figure 2: *Measurements used in this study.* ***Bilateral measurements****:* ***(1+2)*** *Condylar width, left(L) and right(R);* ***(3+4)*** *Ramus length, L and R;* ***(5+6)*** *Mandibular body length, L and R;* ***(7+8)*** *Total mandibular length, L and R;* ***(9+10)*** *Gonion angle, L and R;* ***(11+12)*** *Co-Me-Go angle, L and R;* ***(13+14)*** *Go-Co-Me angle, L and R.* ***Unilateral measurements****:* ***(15)*** *Inter-condylar width;* ***(16)*** *Mandibular width at Gonion;* ***(17)*** *Mandibular width at Antegonion;* ***(18)*** *Mandibular width at Mentalis;* ***(19)*** *Mandibular width at Lingula;* ***(20)*** *Co-Me-Co angle.*

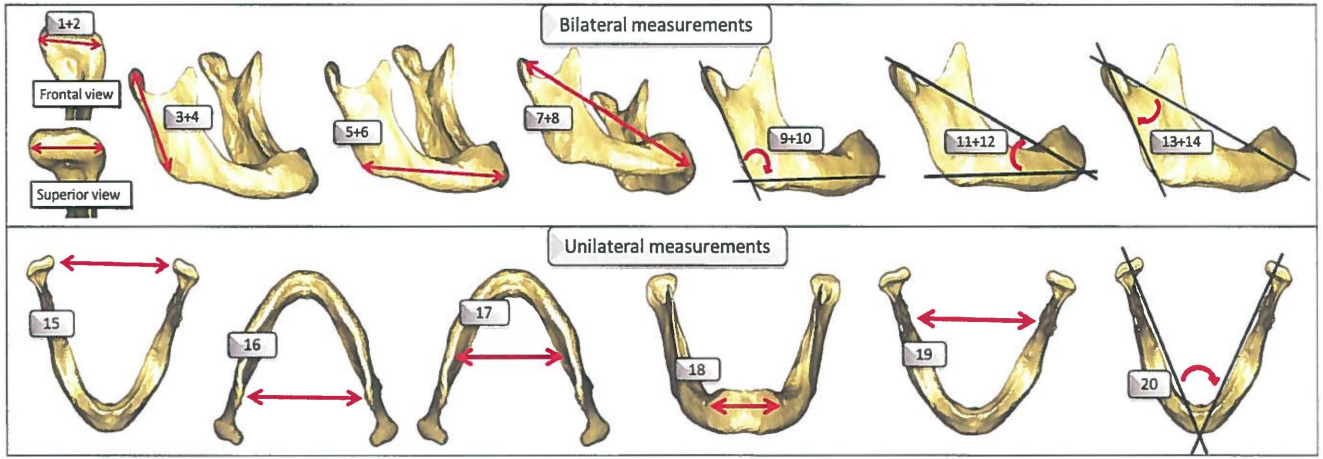

Table 1		Landmarks used in this study
Landmark and Abbreviation		**Definition**
Me	Menton	Menton is the most inferior midpoint of the chin on the outline of the mandibular symphysis
Co	Condylion	Condylion is the most superior point of each mandibular condyle in the sagittal plane
Go	Gonion	Gonion is the point at each mandibular angle that is defined by dropping a perpendicular from the intersection point of the tangent lines to the posterior margin of the mandibular vertical ramus and inferior margin of the mandibular body or horizontal ramus
AG	Antegonion	Most inferior midpoint of the antegonion notch
CoLat	Condylion laterale	Condylion laterale is the most lateral point of each mandibular condyle in the coronal plane
CoMed	Condylion mediale	Condylion mediale is the most medial point of each mandibular condyle in the coronal plane
Men.for	Mental foramen	The distal part of the mental foramen
Lingula	Lingula Mandibulae	The tip of the lingula mandibulæ, a sharp spine superior presents in front a prominent ridge at the foramen mandibulae

Table 2 Linear and angular measurements. Linear measurements in millimeters (mm) and angular measurements in degrees (°)

No	Measurement	Unit		Description
Bilateral measurements				
1+2	CoLat-CoMed	mm	Condyle width	Distance between right points CoLat and CoMed
3+4	Co-Gn	mm	Ramus length	Distance in mm between the point Co and point Gn
5+6	Me-Go	mm	Mandibular body length	Distance in mm between the point Me and point Go
7+8	Co-Me	mm	Total mandibular length	Distance in mm between the point Co and point Me
9+10	Co-Go-Me	°	Gonion angle	Angle between a line through the points Co and Go and Me
11+12	Co-Me-Go	°		Angle between a line through the points Co and Me and Go
13+14	Go-Co-Me	°		Angle between a line through the points and Go Co and Me
Unilateral measurements				
15	Co-Co	mm	Inter-condylar width	Distance between the left and right point Co
16	Go-Go	mm	Mandibular width at Go	Distance between the left and right points Go
17	AG-AG	mm	Mandibular width at AG	Distance between the left and right points Go
18	Men.for – Men.for	mm	Mandibular width at Men.for	Inter mental foramen width
19	Lingula-Lingula	mm	Mandibular width at Mandibular foramina	Intermandibular canal width
20	Co-Me-Co	°		Angle between a line through the points Co (right)and Me and Co (left)

3.3 Results

Means, standard deviations and confidence intervals for the differences of the CS and DS groups from the LSS are summarized in Table 3 and 4. The linear measurements from both CS and DS groups were generally larger when compared to the LSS model group.
The clinical differences of the measurements were determined with the AE. The results from this study showed that the accuracy was really high for most measurements with around 0.5mm deviation which is clinically irrelevant, since there is always the observer error in choosing landmark points. In the CS group, the biggest mean AE differences with the LSS models were found at the condylar measurements: condylar width left (CI:0.91 - 1.66), right (CI: 0.99 - 1.90), inter-condylar width (CI: 0.96 - 3.00) and the measurement between the mandibular width at the mental foramen (CI: 0.11 - 3.32). In the DS group, the same pattern was seen with the biggest mean AE differences at condylar measurements: condylar width left (CI: 1.26 - 2.61), right (CI: 0.92 - 2.65), inter-condylar width (CI: 1.19 - 3.12) and measurements like mandibular body length (CI: 0.63 - 2.73) as well as angular measurements: Go angle (CI: 0.85 - 2.18) and Go-Co-Me (CI:0.55 – 2.82).

3.4 Discussion

The aims of this study was to assess the linear and angular accuracy measurements done on 3D surface models generated from two segmentation protocols (CS and DS) and to compare these measurements with the LSS that was seen as the gold standard. The results show that the measurements from the CS group resemble the LSS more closely that the DS group (Table 4). In the current study, the biggest deviation from the LSS in both the CS and DS groups were found in the measurements from the condylar area and measurements relating to the lingual side of the mandible. This agrees with the results from a previous study performed by our group [20]. There are a few explanations why it is difficult to perform an accurate segmentation of the condylar area. The lower density of the bone in the condylar area compared to the rest of the mandible, a lot of overlapping bony structures and the difficulty to separate the condyle with the discus articulare during segmentation could explain the inaccuracies of condylar segmentations. The inaccuracies of the lingual area might be a result of the scattering of the beam and artifacts caused when the beam passes through the buccal cortical bone during the acquisition. The image artefacts associated with the CBCT affect the segmentation accuracy which directly influences the landmark identification and the resulting measurements [18]. Specific artifacts at the mandibular border and the

posterior margin of the scan volume were also described by Liang et al. [17]. Those parts were mostly located near the periphery of the scan volume.

The soft-tissue attenuation, metallic artifacts, and patient motion, voxel size, field of view (FoV), patient scanning position, and beam inhomogeneity of CBCT scanners are factors that can significantly influence the quality of the CBCT derived 3D segmented models and ultimately the measurement distance between landmarks [11,16,21]. Although number of basis projection images may also influence measurement accuracy of CBCT images, Damstra et al. [21] found that the voxel size did not have a significant influence on the accuracy of linear measurements of 3D models derived from CBCT for orthognatic surgery purposes [24]. Conversely, the effect of the scanner type on 3D images had a significant influence in the image quality and resulting accuracy of the segmented surface models [22-24].

At present, 3D volumetric representation of a structure depends on accurate segmentation. The threshold can be chosen to improve the bone voxel values and suppress the surrounding tissue values to enhance the structure of interest. Our results suggest that probably one of the most significant factors determining the clinical difference of the measurements on the surface models is likely to be the differences between the threshold dependant methods. Standard pre-set thresholds for bone, soft tissue and teeth are often specified and suggested by the software. However, the threshold should still be adjusted by the operator to enhance the quality of a certain region of interest. This process is dependent on the software algorithm, the spatial and contrast resolution of the scan, the thickness and degree of calcification or cortication of the bony structure, and most importantly, the technical skill of the operator [13]. This is why the segmentation process is a very subjective method. In order to overcome this problem, a threshold value automatically determined and observer independent values can be used. Clinically, the threshold value of the mandible is less than the value of the maxilla [9,10]. Cortical bone in the mandible is thick enough to keep the attenuation profile inform across the entire bone surface except for the condylar region. In the maxilla the variations of cortical bone thickness especially in the palate and tuberosity regions creates significant bone dehiscence and fenestrations artefacts in the 3D model [6]. It is therefore impossible to choose a single threshold value for bone tissue in single jaw. Due to the differences in bone density of the jaws itself, a single threshold will most likely result in inaccuracies of the resulting segmentation.

Table 3 Average and standard deviation (SD) of the 7 mandibles used for each 3D model technique

	Measurement	Unit	Surface model technique					
			Laser surface (LLS)		Commercial Segmentation (CS)		Doctor Segmentation (DS)	
			Mean	SD	Mean	SD	Mean	SD
Bilateral measurements								
1	Condyle width (L)	mm	20.26	2.93	21.55	2.74	22.00	3.90
2	Condyle width (R)	mm	20.81	2.40	22.25	2.33	22.59	2.35
3	Ramus length (L)	mm	58.24	3.47	58.21	3.93	58.33	4.16
4	Ramus length (R)	mm	58.74	3.93	58.72	4.21	58.57	4.67
5	Mand body length (L)	mm	84.97	5.95	85.44	5.83	86.50	5.14
6	Mand body length (R)	mm	85.15	5.55	86.04	5.71	86.23	5.68
7	Total Mand length (L)	mm	122.53	7.17	122.91	7.26	122.58	7.48
8	Total Mand length (R)	mm	122.45	6.64	122.89	6.99	122.96	6.72
9	Gonion angle (L)	°	116.43	3.88	116.45	4.02	114.92	3.93
10	Gonion angle (R)	°	115.39	3.36	114.84	3.66	114.86	3.83
11	Angle 1 L (Co-Me-Go)	°	25.21	2.13	25.12	2.38	26.76	4.11
12	Angle 1 R (Co-Me-Go)	°	25.72	2.38	25.72	2.32	25.63	2.60
13	Angle 2 L (Go-Co-Me)	°	38.35	2.64	38.43	2.42	40.04	2.62
14	Angle 2 R (Go-Co-Me)	°	38.89	2.22	39.44	2.73	39.50	2.85
Unilateral measurements								
15	Intercondylar width	mm	104.65	5.29	105.59	5.72	104.39	6.91
16	Mand width (Go)	mm	95.46	5.46	95.90	6.06	96.47	5.75
17	Mand width (AG)	mm	82.95	2.98	83.12	3.29	82.72	3.38
18	Mand width (Men.for)	mm	46.59	3.51	47.70	4.96	46.64	3.66
19	Mand width (Lingula)	mm	82.33	4.11	82.45	3.88	82.24	4.34
20	Angle 3 (Co-Me-Co)	°	50.64	2.21	50.95	2.43	50.38	2.96

Table 4 Clinical differences between the laser surface models and the commercial (CS) and doctor segmentations as determined by the absolute error (AE). The laser surface models (LS) were used as the reference for comparison. SD – Standard deviation. 95% CI AE – 95% Confidence interval of the AE

	Measurement	Unit	LLS vs. CS			LLS vs. DS		
			Mean AE	SD	95% CI AE	Mean AE	SD	95% CI AE
Unilateral measurements								
1	Condyle width (L)	mm	1.28	0.51	0.91 - 1.66	1.93	0.91	1.26 - 2.61
2	Condyle width (R)	mm	1.44	0.61	0.99 - 1.90	1.79	1.17	0.92 - 2.65
3	Ramus length (L)	mm	0.62	0.32	0.38 - 0.86	0.99	0.79	0.41 - 1.58
4	Ramus length (R)	mm	0.43	0.49	0.07 - 0.79	0.83	0.73	0.30 - 1.37
5	Mandibular body length (L)	mm	0.58	0.70	0.06 - 1.10	1.68	1.42	0.63 - 2.73
6	Mandibular body length (R)	mm	1.06	0.53	0.67 - 1.46	1.35	0.83	0.74 - 1.97
7	Total Mandibular length (L)	mm	0.55	0.40	0.26 - 0.85	1.21	0.81	0.61 - 1.81
8	Total Mandibular length (R)	mm	0.63	0.47	0.28 - 0.97	0.95	0.73	0.41 - 1.49
9	Gonion angle (L)	°	0.99	0.71	0.46 - 1.51	1.51	0.89	0.85 - 2.18
10	Gonion angle (R)	°	0.78	0.80	0.19 - 1.37	0.68	0.81	0.08 - 1.28
11	Angle 1 L (Co-Me-Go)	°	0.36	0.24	0.18 - 0.53	0.55	0.64	0.08 - 1.03
12	Angle 1 R (Co-Me-Go)	°	0.32	0.28	0.12 - 0.52	0.41	0.27	0.22 - 0.61
13	Angle 2 L (Go-Co-Me)	°	0.68	0.63	0.21 - 1.14	1.68	1.53	0.55 - 2.82
14	Angle 2 R (Go-Co-Me)	°	0.73	0.56	0.32 - 1.15	0.84	0.61	0.39 - 1.29
Bilateral measurements								
15	Inter-condylar width	mm	1.98	1.37	0.96 - 3.00	2.15	1.30	1.19 - 3.12
16	Mandibular width (Go)	mm	0.88	0.53	0.48 - 1.27	1.01	0.54	0.60 - 1.41
17	Mandibular width (AG)	mm	0.58	0.42	0.26 - 0.89	1.09	0.79	0.50 - 1.68
18	Mandibular width (Men.for)	mm	1.71	2.17	0.11 - 3.32	1.04	0.73	0.50 - 1.59
19	Mandibular width (Lingula)	mm	0.53	0.24	0.36 - 0.71	0.44	0.34	0.19 - 0.69
20	Angle 3 (Co-Me-Co)	°	0.95	0.49	0.59 - 1.31	1.02	0.91	0.35 - 1.61

In this present study a laser surface scan was made of the dry mandible. This was regarded as the gold standard for comparison. Laser scanning is a commonly used technique in the engineering industry for acquiring 3D data from objects [25]. It is a valid and reliable technique that is used to detect minute and microscopic defects [21]. It is increasingly being used in medicine, forensic science, physical anthropology , and conservators to document, reconstruct, and analyse objects and human remains, including craniofacial features [18,25]. Laser surface scanning is reliable and accurate for producing mandibular surface models [17]. The present study did not include the maxilla. This is due to the fact that laser surface scanning of the maxilla is challenging and unreliable. The extremely thin lateral wall of the maxillary sinus and the walls of the orbit allows for the laser to pass through it without being detected [17]. Laser surface scanning of the maxilla is further complicated by the extremely complex geometry of the maxilla.

In this present study 95% confidence interval (CI) was used instead of the *P* values to determine clinical differences. In most research studies, where comparisons are made between groups, some form of statistical analysis is performed and a test or a number of tests of significance are reported with corresponding *P* values. However, *P* values do not always give an indication regarding the clinical importance of the observed results [26]. A more appropriate presentation of the trial results would focus on the size of the difference between the treatment groups and its range, i.e. the 95% CI [27]. The CIs provide a range of values within which the true difference of the study groups is believed to exist, thus giving the reader the opportunity to interpret the results in relation to clinical practice [26].

Inherent clinical inaccuracies of both landmark identification and measurement associated with the 3D images are a major source of measurement error [13,28]. Therefore, efforts should be made to minimize the effect of errors in landmark identification [15,28]. In previous studies fiducial reference markers were placed to establish a consensus landmark location. However, this was not possible in our study as the soft tissue was still intact when the CBCT scans were made. In the present study, all measurements were performed by one observer. If systematic errors were made by the observer in identification of the landmarks, it would have been the same for all three types of surface models, and therefore have no influence on reproducibility of the measurements. This was confirmed by the ICCs of repeated measurements. Hence it is justified to have one observer for this type of study.

The present study is unique because fresh cadaver heads were used to make the CBCT scan. After maceration of the skulls, laser surface scanning were applied to produce true surface models of the mandibles. With this method, all data from the same head could be compared and no artificial media was needed to mimic soft tissues. Moreover, if only the mandible is scanned, the missing cervical vertebra and skull base could influence the results [17]. For this reason Liang et al. suggested that full cadaver skull including both lower and upper jaws with soft tissue and cervical vertebra should be used [17]. In the present study a full fresh cadaver heads with cervical vertebrae were used for the CBCT scans which overcame problems associated with methods previously described using dry skulls.

The results of the present study confirm that measurements derived from landmarks on the condyle and lingual region of the mandibula are less accurate than reality. These differences might be clinically relevant depending on the accuracy required. In addition, the measurements of 3D models of the CS group were more accurate at the condylar region when compared to the DS group. Therefore, differences in the segmentation process have a significant influence on the accuracy of the 3D models. Provided that the commercial company performs accurate segmentations, the improved accuracy of commercially segmentations may therefore justify the additional cost of outsourcing the production of surface models. Therefore, commercially segmented surface models should be considered if more accurate measurements are required i.e. for orthognathic surgical treatment planning or evaluation of treatment outcome.

3.5 Conclusion

Producing 3D surface models from CBCT datasets is still less accurate than the reality when using threshold based methods. Differences in the segmentation process resulted in significant clinical differences between the measurements. The results of the present study suggest the commercially segmented surface models were more accurate than the experienced clinician's segmented surface models when compared to the laser surface models. However, equal quality may also be reached by a clinician if sufficient training and time is taken to segment a CBCT surface model. Importantly, care has to be taken when drawing conclusions from measurements and comparisons made from different segmentations, especially at the condylar region and the lingual side of the mandible as differences of these measurements may be clinically significant.

3.6 Reference

1. Scarfe WC, Farman AG, Sukovic P. Clinical applications of cone-beam computed tomography in dental practise. J Can Dent Assoc 2006;72:75-80.
2. Guerrero ME, Jacobs R, Loubele M, Schutyser F, Suetens P, van Steenberghe D. State-of-the-art on cone beam CT imaging for preoperative planning of implant placement. Clin Oral Invest 2006;10:1-7
3. Cevidanes LH, Styner MA, Proffit WR. Image analysis and superimposition of 3-dimensional cone-beam computed tomography models. Am J Orthod Dentofacial Orthop 2006;129:611-618
4. Farman AG, Scarfe WC. Development of imaging selection criteria and procedures should precede cephalometric assessment with cone-beam computed tomography. Am J Orthod Dentofacial Orthop. 2006;130:257–265
5. Lagravere MO, Hansen L, Harzer W, Major PW. Plane orientation for standardization in 3-dimensional cephalometric analysis with computerized tomography imaging. Am J Orthod Dentofacial Orthop. 2006;129:601–604
6. Halazonetis DJ. From 2-dimensional cephalograms to 3-dimensional computed tomography scans. Am J Orthod Dentofacial Orthop 2005;127:627-637.
7. Mah JK, Huang JC, Choo H. Practical applications of cone-beam computed tomography in orthodontics. JADA 2010;141:7S-13S
8. van Steenberghe D, Ericsson I, Van Cleynenbreugel J, Schutyser F, Brajnovic I, Andersson M. High precision planning for oral implants based on 3-D CT scanning. A new surgical technique for immediate and delayed loading. Appl Osseointegration Res 2004;4:27–31
9. Hassan B, Couto Souza PC, Jacobs R, de Azambuja Berti S, van der Stelt P. Influence of scanning and reconstruction parameters on quality of three-dimensional surface models of the dental arches from cone beam computed tomography. Clin Oral Inverstig 2010;3:303-310
10. Loubele M, Jacobs R, Maes F, Denis K, White S, Coudyser W et al. Image quality vs radiation dose of four cone-beam computerized scanners. Dentomaxillofac Rad 2008; 37; 309-319
11. Ballrick JW, Palomo JM, Ruch E, Amberman BD, Hans MG. Image distortion and spatial resolution of a commercially available cone-beam computed tomography machine. Am J Orthod Dentofacial Orthop 2008;134:573-82
12. Brown AA, Scarfe WC, Scheetz JP, Silveira AM, Farman AG. Linear accuracy of cone beam CT 3D images. Angle Orthod 2009;79:150-7
13. Periago DR, Scarfe WC, Moshiri M, Scheetz JP, Silveira AM, Farman AG. Linear accuracy and reliability of cone beam CT derived 3-dimensional images using an orthodontic volumetric rendering program. Angle Orthod 2008;78:387-395
14. Mischkowski RA, Pulsfort R, Ritter L, Neugebauer J, Brochhagen HG, Keeve E, et al. Geometric accuracy of a newly developed cone-beam device for maxillofacial imaging. Oral Surg Oral Med Oral Pathol Oral Radiol Endod 2007;104:551-559

15. Lagravere MO, Carey J, Toogood RW, Major PW. Three-dimensional accuracy of measurements made with software on cone beam computed tomography images. Am J Orthod Dentofacial Orthop 2008;134:112-116
16. Hassan B, van der Stelt P, Sanderink G. Accuracy of three-dimensional measurements obtained from cone beam computed tomography surface-rendered images for cephalometric analysis: influence of patient scanning position. Eur J Orthod 2009;31: 129-34
17. Liang X, Lambrichts I, Sun Y, Denis K, Hassan B, Li L, Pauwels R, Jacobs R. A comparative evaluation of Cone Beam Computed Tomography (CBCT) and Multi-Slice CT (MSCT). Part II: On 3D model accuracy. Eur J Radiol;2010: 270–274
18. Fourie Z, Damstra J, Gerrits PO, Ren Y. Evaluation of anthropometric accuracy and reliability using different three-dimensional scanning systems. Forensic Sci. Int 2011;207:127-134
19. Fourie Z, Damstra J, Gerrits PO, Ren Y. Accuracy and reliability of facial soft tissue depth measurement using cone beam computed tomography. Forensic Sci Int 2010;199:9-14.
20. Fourie Z, Damstra J, Schepers RH, Gerrits PO, Ren Y. Segmentation Process Significantly Influences the Accuracy of 3D Surface Models Derived from Cone Beam Computed Tomography. Euro J Radiology 2011; submitted
21. Damstra J, Fourie Z, Huddleston Slater JJR, Ren Y. Accuracy of linear measurements form cone-beam computed tomography-derived surface models of different voxel sizes. Am J Orthod Dentofac Orthop 2010;137:16.e1-16.e6
22. Loubele M, Maes F, Schutyser F, Marchal G, Jacobs R, Suetens P. Assessment of bone segmentation quality of cone-beam CT versus multislice spiral CT: a pilot study. Oral Surg Oral Med Oral Pathol Oral Radiol Endod 2006;102:225–234
23. Van Vlijmen OJ, Rangel FA, Berge SJ, Bronkhorst EM, Becking AC, Kuiper-Jagtman AM. Measurements on 3D models of human skulls derived from different cone beam scanners. Clin Oral Investig 2010, Jun
24. Hassan B, Metska ME, Ozok AR, van der Stelt P, Wesselink PR. Comparison of Five Cone Beam Computed Tomography Systems for the Detection of vertical root fractures. JOE 2010;36:126-129
25. Kau CH, Richmond S, Incrapera A, English J, Xia JJ. Three-dimensional surface acquisition systems for the study of facial morphology and their application to maxillofacial surgery. Int J Med Robotics Comput Assist Surg 2007;3: 97–110
26. Polychronopoulou A, Pandis N, Eliades T. Appropriateness of reporting statistical results in orthodontics: the dominance of P values over confidence intervals. European Journal of Orthodontics 2011;33:22–25
27. De Angelis D, Sala R, Cantatore A, Grandi M, Cattaneo C. A new computer- assisted technique to aid personal identification. Int. J. Legal Med 2009;123:351–356
28. Damstra J, Fourie Z, Huddleston Slater JJR, Ren Y. Reliability and the smallest detectable difference of three-dimensional cephalometric measurements. Am J Orthod Dentofacial Orthop 2010; 137: 16.w1-16.e6

Chapter 4

Reliability and the smallest detectable differences of measurements made on three-dimensional cone-beam computed tomography images

This chapter is based on the following publication:

Damstra J*, Fourie Z*, Huddleston Slater JJR and Ren Y. Reliability and the smallest detectable differences of measurements made on three-dimensional cone-beam computed tomography images. Am J Orthod Dentofacial Orthop 2010; Accepted
(*Shared first authorship)

Abstract

Introduction: The aim of this study was to determine the reliability and the measurement error (by means of the smallest detectable error or SDD) of 17 commonly used cephalometric measurements made on three-dimensional (3D) cone-beam computed tomography images. Methods: 25 Cone-beam computer tomography (CBCT) scans were randomly selected. 3D images were rendered, segmented and traced with the SimPlant Ortho Pro® 2.1 (Materialise Dental, Leuven, Belgium) software. This was repeated two times by two observers during two sessions with at least one week apart. Measurement error was determined by means of the smallest detectable difference (SDD). Differences were analyzed by means of the Wilcoxon signed-rank tests. Intra- and interobserver reliability was calculated by means of intraclass correlation coefficients (ICC) based on absolute agreement. Results: There was a large variation of measurement error between the angular (range: 0.88° – 6.29°) and linear (range: 1.33 mm – 3.56 mm) variables. The largest measuring error was associated with the dental measurements U1-FHPL, L1-MdPL and L1-FHPL (range: 3.80° – 6.29°). The ANB angle was the only variable with a measuring error of one or less measuring unit for both observers. The intraobserver agreement of all measurements was very good (ICC: 0.86 - 0.99). Except for SN-FHPL (ICC = 0.76), the interobserver agreement was very good (ICC > 0.88). Conclusion: The measurement error of 3D cephalometric measurements (except for the ANB angle) can be considered clinically relevant. This questions the use of linear and angular 3D measurements to detect true treatment effect when a high level of accuracy required.

4.1 Introduction

Since the introduction of three-dimensional (3D) cone-beam computed tomography (CBCT) for imaging of the maxillofacial region a decade ago, the ability to show spatial relationships in all three planes have expanded the possibilities for diagnosis, craniofacial surgery planning and outcome evaluation in orthodontics and oral maxillofacial surgery.[1-3] The main advantage of CBCT technology is the significant reduction of radiation exposure compared to conventional CT.[3,4] With CBCT it is possible to perform a full scan of the head in a few seconds with an effective dose of only 50uSv compared to 2000uSv from conventional CT.[5,6] Other advantages promoting the use of CBCT are less cost, increased accessibility to orthodontic practices, flexibility in the field of view and sub-millimeter spatial resolution.[3,4] In fact, it can be argued that the routine use of CBCT images in orthodontics and craniofacial surgery might not be far away.[3,4,7]

Due to their absolute accuracy [8-13], CBCT images have become powerful tools for evaluation of craniofacial morphology and treatment outcome.[3] Accuracy is of utmost importance when the data from CBCT are used for pre-surgical planning to assure correct jaw repositioning.[14-16] However, accurate CBCT images or precise location of landmarks do not guarantee accurate measurements as geometric factors may have a significant influence on 3D measurements.[17] Moreover, each 3D landmark has its own unique configuration and envelope of error which contributes to measurement error.[14] Recent studies showed the reliability of 3D landmark identification to be very good and even more precise than conventional cephalograms when it is done by trained and experienced operators using the renderings and the cross sectional slices in all three planes of space. [15, 16] In contrast to 2D cephalometry where lines are used for measurements, 3D measurements are often made to planes which may have a different orientation to each other from the frontal view. This means that the measurement between the planes might differ depending on the location of the measurement and can therefore be an additional source of error (Figure 1).

Reliability of 3D measurements reported as correlation coefficients may have limited clinical value as very good correlation does not imply a small measuring error.[18, 19] Unfortunately, only few articles have reported the intra- and interobserver measurement errors associated with 3D measurements. However, It is difficult to draw conclusions from these articles because they used different methods and variables to describe 3D measurement error.[20-24] Nevertheless, the reported 3D measurement errors seem to be clinically relevant (> 1.00 mm or degree) considering the absolute level of accuracy required for surgical planning and outcome evaluation. Recently, we

introduced the concept of the smallest detectable difference (SDD) in cephalometry to describe the measurement error.[18] The SDD implies that in order to be able to detect real change, the difference between two observations must be at least equal or larger than the SDD for the specific measurement.[18, 19]

Since CBCT images are accurate, it is necessary to determine if the numerical data of 3D cephalometric variables derived from the images are sufficiently accurate and reliable for surgical planning and outcome evaluation. The aim of this study was to determine the reliability and the measuring error by means of the SDD of angular and linear measurements commonly used in 3D cephalometric analysis.

Figure 1 *An illustration to show that due to the variation in orientation of the mandibular plane (MdPL) and the Frankfort horizontal plane (FHPL) from the frontal view, the angle between the planes may differ depending on where the measurement is made.*

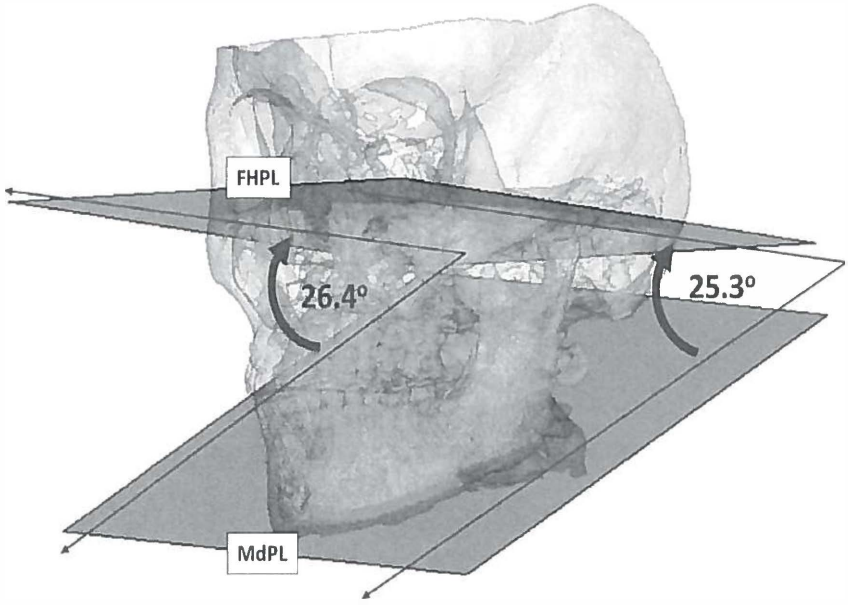

4.2 Methods and Materials

The sample consisted of 25 (13 male, 12 female) CBCT scans randomly selected at the Department of Orthodontics of the University Medical Center Groningen (UMCG). The average age of the subjects in the sample was 25.8 years (range: 11.7-49.5 years). Informed consent was obtained from the patients and no identifying marks were used after selection of the CBCT scans. Cleft patients and patients with visible asymmetry (defined by 4.00 mm deviation of point Menton from the midsagittal plane[25]) were not considered. The CBCT images were acquired with the KaVo 3D eXam scanner (KaVo Dental GmbH, Bismarckring, Germany) at a 0.30 voxel resolution. The CBCT data was exported from the eXamVisionQ (Imaging Sciences International LCC, Hatfield, Pennsylvania, USA) software in DICOM multi-file format and imported into SimPlant Ortho Pro® 2.1 (Materialise Dental, Leuven, Belgium) software on an Acer Aspire 7730G laptop (Acer, s'Hertogenbosch, the Netherlands) with a dedicated 512 MB video card (Nvidia® Geforce ® 9600M-GT, NVIDIA, Santa Clara, California, USA).

The 3D surface models of all of the CBCT images were generated by means of a threshold based method performed by one operator (ZF). The surface model was saved and the same surface model was used for each measuring session. All measurements were performed on a 17-inch Acer CrystalBrite™ LCD flat panel colour screen with a maximum resolution of 1440 x 900 pixels. The SimPlant Ortho Pro® 2.1 software provides various views using the rotation and translation of the rendered image. Prior to measurement, two experienced observers (with more than 3 years' experience in 3D cephalometry) discussed and reviewed the definitions of the anatomical landmarks (Table I) during a consensus meeting. The definitions of the landmarks and planes as defined by Swennen et al.[26] were used for this study. The two observers performed the measurements separately. The same patient was measured two time intervals (T1 and T2) by each observer during two different sessions with at least two weeks apart. The anatomical landmarks were identified by using a cursor-driven pointer on the volume renderings and the cross sectional slices in all three planes of the CBCT images.[14] After landmark identification, a preprogrammed analysis provided the distances to the nearest one-hundredth of a millimeter of the measurements described in Table II. The values were then exported and saved as Excel® file format.

Statistical analysis

The standard error of measurement (SEM) of the repeated measurements was calculated as the square root of the variance of the random error from a 2-way

Table I The 3D landmarks and planes used in this study

Landmark and Abbreviation		Definition
Unilateral landmarks		
1. Sella	S	Sella is the center of the fossa hypophysialis
2. Nasion	N	Nasion is the midpoint of the frontonasal suture
3. Anterior nasal spine	ANS	Anterior Nasal Spine is the most anterior midpoint of the anterior nasal spine of the maxilla
4. A-point	A	A-Point is the point of maximum concavity in the midline of the alveolar process of the maxilla
5. Upper incisor tip	Isi	Upper incisor tip is the middle point of the tip of the crown of the most prominent upper central incisor
6. Upper incisor apex	Isa	The middle point of the tip of the apex of the most prominent upper central incisor
7. Lower incisor incisal tip	Iii	Lower incisor tip is the middle point of the tip of the crown of the most prominent lower central incisor
8. Lower incisor apex	Iia	The middle point of the tip of the apex of the most prominent lower central incisor
9. B-point	B	B-Point is the point of maximum concavity in the midline of the alveolar process of the mandible
10. Pogonion	Pog	Pogonion is the most anterior midpoint of the chin on the outline of the mandibular symphysis
11. Gnathion	Gn	Gnathion is the midpoint between points Pog and Me on the outline of the mandibular symphysis
12. Menton	Me	Menton is the most inferior midpoint of the chin on the outline of the mandibular symphysis
13. Basion	Ba	Basion is the most anterior point of the foramen magnum
*Bilateral landmarks**		
14. Gonion	Go	Gonion is the point at each mandibular angle that is defined by dropping a perpendicular from the intersection point of the tangent lines to the posterior margin of the mandibular vertical ramus and inferior margin of the mandibular body or horizontal ramus.
15. Condylion	Co	Condylion is the most posterior-superior point of each mandibular condyle in the sagittal plane
16. Orbitale	Or	Orbitale (Or) is the most inferior point of each infra-orbital rim
17. Porion	Po	Porion is the most superior point of each external acoustic meatus
18. Posterior maxillary point	PMP	Posterior Maxillary Point is the point of maximum concavity of the posterior border of the palatine bone in the horizontal plane
Planes and Abbreviation		**Definition**
1. Frankfort horizontal	FHPL	The Frankfort horizontal plane is defined by a plane that passes both Orbital (Or left and Or right) landmarks and the mean of the two Porion (Po left and Po right) landmarks
2. Palatal plane	PPL	The palatal plane is defined by a plane that passes the Anterior Nasal Spine (ANS) and both Posterior Maxillary Point (PMP left and PMP right) landmarks
3. Mandibular plane	MdPL	The mandibular plane is defined by a plane that passes the Menton and both Gonion (Go left and Go right la

*, left and right landmarks used

random effect ANOVA. The SEM was calculated for each of the angular and linear measurements. The SDD was then calculated with the formula: 1.96 x √2 x SEM.18, 19 The SDD was used to calculate intraobserver and interobserver measurement error. As a measure of intraobserver and interobserver reliability, the intraclass correlation

Table II The 3D measurements used in this study

Measurement	Description
Angular measurements	
1. SNA	Angle between points S and A with its vertex at point N
2. SNB	Angle between points S and B with its vertex at point N
3. ANB	Angle between points A and B with its vertex at point N
4. SN-FHPL	Angle between a line through the points S and N and the FHPL in the sagittal plane
5. SN-PPL	Angle between a line through the points S and N and the PPL in the sagittal plane
6. SN-MdPL	Angle between a line connection the points S and N and the MdPL in the sagittal plane
7. PPL-MdPL	Angle between the PPL and the MdPL in the sagittal plane
8. Y-Axis	Angle between points N and Gn with its vertex at point S
9. U1-FHPL	Angle between a line through the points Isi and Isa and the FHPL in the sagittal plane
10. L1-MdPL	Angle between a line through the points Iii and Iia and the MdPL in the sagittal plane
11. L1-FHPL	Angle between a line through the points Iii and Iia and the FHPL in the sagittal plane
12. BaSN	Angle between points and Ba with its vertex at point S
Linear measurements	
13. ANS-Me	Distance in mm between the point ANS and point Me
14. Co-A	Distance in mm between the right point Co and point A
15. Co-Gn	Distance in mm between the right point Co and point Gn
16. AFH	Distance in mm between point Me and point N
17. PFH	Distance in mm between point S and the mean point between the left and right points Go

coefficient (ICC) for absolute agreement based on a 2-way random effects analysis of variance (ANOVA) was calculated. Interobserver reliability was tested by comparison of the first measuring sessions. Interobserver reliability was tested by comparison of the first measuring sessions. Because not all variables were normally distributed (Shapiro-Wilk tests), non-parametric tests were performed. The Wilcoxon signed-rank sum tests were performed to compare the repeated measurements of each observer. In addition, Wilcoxon signed-rank sum tests were performed to compare first measuring sessions between the observers. P values less than 0.05 were considered significant. All statistical analyses were performed with a standard statistical software package (SPSS version 16, Chicago, IL).

4.3 Results

The results are reported in Table III. There were no significant statistical differences ($P < 0.05$) between the measuring sessions or observers. The intraobserver reliability of the cephalometric measurements was very good (ICC: 0.86 – 0.99). The interobserver reliability of the 3D measurements was also very good. Except for PPL-MdPL (ICC = 0.76)

the interobserver ICCs were all higher than 0.88. The measurement error (SDD) followed the same trends for both observers. The largest angular SDDs for both observers (3.80° – 6.29°) were all dental measurements (U1-FHPL, L1-MdPL, and L1-FHPL). The smallest angular SDD for both observers was the ANB angle (0.88° and 0.98° respectively). Only the ANB angle had an intraobserver measuring error of less than 1.00° which is usually regarded as clinically relevant in cephalometry.[27] The linear variable with the smallest SDD for observer 1 was the Co-A (1.52 mm) whilst ANS-Me (1.33 mm) was the linear variable with the smallest SDD for observer 2. The interobserver measuring error did not increase as expected and were in the same range as the interobserver measuring errors and followed the same trend as the intra-observer measuring errors.

5.4 Discussion

The clinical relevance of the SDD implies that if the SDD exceeds the observed difference, one cannot conclude with certainty that the observed change is a result of the treatment instead of a result of the landmark errors. In cephalometry it means that if the measured difference between pre- and post-treatment cephalograms does not exceed the SDD, the measured change is not due to treatment effect but most likely due to measurement error. The SDD is used in all fields of medicine for reliability testing of measurements because it is sensitive enough to determine significant (α=0.05) changes not caused by measurement error.[18, 19, 28-33] This is not the case with Dahlberg's formula (the current accepted method for determining measuring error in cephalometry) which may not set limits strict enough to detect real change.[18]

No studies reporting the 95% confidence level of the 3D measuring error could be found in the literature. In the present study we used 3D measurements commonly used in 2D and 3D cephalometry. This might serve as reference for other studies but it also allows for comparison between 2D and 3D of the corresponding variables. Conversely, the SDD of linear measurements Co-A and Co-Gn were smaller in 3D (average: 1.92 mm and 2.33 mm) than in 2D (average: 4.70 mm and 3.61 mm).[18] The differences in the range of the SDD of the dental angular measurements between 2D (4.21° – 5.27°) and 3D (3.80° – 6.29°) were small.[18] In the present study, the magnitude of the 3D measuring error did not increase as much as the 2D measuring error between two observers.[18] The same geometric principles that have an effect on 2D measurements also apply to 3D measurements.[18] However, the effects differ for certain variables. The

Table III Means, standard deviations (SD) and comparison of the intra- and interobserver measurements.

Measurement	Intra-observer													Interobserver		
	Observer 1							Observer 2								
	T1		T2		Comparison (T1-T2)			T1		T2		Comparison (T1-T2)			Comparison (T1-T1)		
	Mean	SD(±)	Mean	SD(±)	ICC	*P*	SDD	Mean	SD(±)	Mean	SD(±)	ICC	*P*	SDD	ICC	*P*	SDD
Angular measurements																	
1. SNA	81.73	3.72	82.18	3.77	0.96	0.79	2.08	82.98	3.70	82.32	3.91	0.95	0.48	2.34	0.88	0.26	3.63
2. SNB	78.13	4.15	78.41	4.29	0.98	0.82	1.74	79.04	4.26	78.38	4.27	0.95	0.52	2.75	0.93	0.41	3.28
3. ANB	3.60	3.21	3.77	3.16	0.99	0.69	0.88	4.11	3.22	3.87	3.16	0.99	0.70	0.98	0.97	0.57	1.47
4. SN-FHPL	10.36	2.46	10.36	2.05	0.91	0.66	1.86	9.64	2.39	10.10	2.35	0.86	0.32	2.46	0.76	0.21	3.38
5. SN-PPL	7.20	3.37	6.73	3.52	0.90	0.68	3.06	6.65	3.61	6.94	3.67	0.92	0.95	2.91	0.86	0.67	3.60
6. SN-MdPL	31.59	8.07	31.70	8.19	0.98	0.95	3.39	31.17	8.32	31.85	8.44	0.98	0.87	3.31	0.97	0.80	3.64
7. PPL-MdPL	24.46	7.92	25.04	8.02	0.98	0.82	3.25	24.73	7.94	25.02	8.17	0.97	0.85	3.66	0.98	0.93	2.77
8. Y-Axis	67.59	4.91	67.54	4.87	0.98	0.99	2.11	67.29	5.14	67.97	4.98	0.95	0.50	2.87	0.96	0.71	2.96
9. U1-FHPL	67.32	8.69	66.35	8.47	0.96	0.68	4.81	66.38	9.27	67.22	8.32	0.98	0.63	3.80	0.97	0.55	4.57
10. L1-MdPL	80.44	6.47	80.21	6.95	0.89	0.93	6.29	80.73	6.57	81.21	6.30	0.93	0.76	5.77	0.89	0.91	6.11
11. L1-FHPL	63.63	8.10	64.21	8.25	0.95	0.82	4.93	64.05	7.90	64.11	7.48	0.96	0.89	4.46	0.96	0.85	4.56
12. BaSN	132.21	5.60	131.97	5.74	0.96	0.82	3.17	131.75	5.95	132.53	5.46	0.96	0.46	3.27	0.93	0.63	4.22
Linear measurements																	
13. ANS-Me	66.95	8.66	67.38	8.67	0.99	0.82	2.00	67.34	8.68	67.06	8.79	0.99	0.86	1.33	0.99	0.84	2.12
14. Co-A	96.08	5.62	95.87	5.75	0.99	0.88	1.52	95.87	5.76	95.69	5.49	0.98	0.95	2.33	0.99	0.79	1.42
15. Co-Gn	122.21	8.13	122.08	8.34	0.99	0.98	1.80	121.97	8.36	122.58	8.34	0.99	0.74	2.85	0.99	0.90	2.20
16. AFH	116.72	10.66	116.73	10.85	0.99	0.97	1.89	116.59	10.99	116.85	11.04	0.99	0.90	2.13	0.99	0.96	2.68
17. PFH	75.78	6.51	75.88	6.02	0.97	0.94	2.79	76.21	6.30	76.00	6.37	0.96	0.85	3.56	0.96	0.66	3.60

Statistically significant at $P < 0.05$
ICC Intraclass correlation coefficient
SDD Smallest detectable difference

following discussion offers an explanation why variation of 3D measurement error occurs and why it may differ from the corresponding 2D measurement error.

In 2D and 3D cephalometry, landmarks have a district shape of distribution (envelope of error) depending on the clarity of the definition, the quality of the image and the geometry of the object.[14,15] Importantly, differences existed between the envelopes of error of corresponding landmarks of 2D and 3D images. This is due to the fact that certain landmarks can be more accurately identified on 3D views.[16] The bilateral landmarks of Co, Go and Or show greater variations in 2D cephalometry due to overlapping of structures and is therefore associated with large measurement error.[34] These bilateral landmarks can be more precisely located on 3D images probably due to better visualization in all three planes of space.[16]

Variation of landmark identification increases the measurement error because the errors in location are cumulative.[18,35] In 3D cephalometry, the addition of an extra dimension introduces an additional source of error in the mediolateral direction. This offers an explanation why certain angular measurements show greater measurement error in 3D than 2D. For example, the larger SDD of SNB in 3D is due to the added variability in the mediolateral direction. Although the anteroposterior variability of point B was only 0.69 mm, mediolateral variation was 1.32 mm in 3D.[16] Therefore, when constructing an angle between the three points of S, N and point B, the added mediolateral variability of point B resulted in a greater measurement error. The mediolateral variation is also one of the contributing factors to the larger measurement error of the 3D dental measurements. Although the variability of the Isi is very small in the anteroposterior (0.63 mm) and cranial-caudal (0.76 mm) direction, the variability in the mediolateral direction is significantly larger (1.99 mm).[16] Greater variability of certain landmarks in the mediolateral direction in 3D was probably related to inadequate definition of the landmarks.[16] The addition of the extra dimension also means that 3D cephalometry relies on planes rather than lines for reference. Because the human face is inherently asymmetric and the planes are often constructed by connection of two bilateral structures, the orientation of the planes might differ when assessing the patient from the frontal view (Figure 1). This could be an additional source of error because the 3D software automatically calculates the smallest value between the planes. Therefore, the reference for the angular measurement is not standardized and can vary depending on the plane orientation. Although this effect is likely to be small in a symmetric sample, the effect is clinically significant in asymmetric cases. A possible solution to overcome this problem is to select an anteroposterior plane (e.g.

midsagittal plane) to serve as reference for angular measurements between planes to allow for more accurate comparison.

Nagasaka et al.[36] illustrated that the more closely two landmarks are, the greater the linear and angular measurement error tends to be. This geometric principal plays a significant role in 3D cephalometry. For example; due to the short distance of the landmarks used to construct the axis of the maxillary incisor, a small variation in the anteroposterior location of the apex will result in a significantly larger measuring error.[18] In 3D cephalometry this effect also becomes more apparent when two landmarks in close proximity are used to construct reference planes e.g. PMP left and right to construct the PPL. If one of the landmarks varies by a minor amount, the resulting change in the orientation of the plane is significant (Figure 2). Therefore, constructing 3D planes through two landmarks in close relation to each other could result in larger measuring errors and should be avoided.

Another source of measurement error in 3D cephalometry, not investigated in the present study, is the possible effects of segmentation process. The surface models are constructed from voxel based data, requiring the input of a threshold value which specifies what the structure of interest (e.g. bone or soft-tissue) is or is not. The accuracy of segmentation therefore relies on the gray-value and the user entered threshold value by the operator. This process is further complicated because CBCT imaging suffers from beam inhomogeneity which results in variation of image quality and accuracy among different manufactures and reconstruction parameters.[37-39] This means that the grey levels of the voxels of the same object imaged by at two different times are likely to differ, resulting in differences during the segmentation process. We eliminated this problem by using the same surface model for all the measurements. However, in practice the differences between pre- and post-treatment CBCT segmentations might introduce additional measuring error. A possible solution to minimize this problem is to verify the location of each landmark on the axial, coronal and sagittal slices of each CBCT scan rather that to rely on the surface model alone for landmark identification. However, this may not always be possible. Due to geometry, certain landmarks like Gonion (Go) are better visualized and located on the 3D model than on the cross sectional slices.

The clinical significance of the measurement error depends on the level of accuracy required. If the goal is to assess growth changes or to perform surgical planning, a very high degree of accuracy is required.[1-3] In the present study, the overall intraobserver agreement was good. However, the SDD illustrated that the measurement errors of

most measurements were considerable and clinically relevant (more than one measuring unit [27]). The 3D measurement error can be a result of accuracy of the landmarks but is influenced by the geometric principles as discussed above. Interplay between the variations in landmark identification and geometric principles exist which explains the variability of the measurement error.

Figure 2.a: The PPL constructed through 3 points as described by Swennen et al.[26] (ANS, PMP left and PMP right). Note the close proximity of PMP left and right to each other. b: Minor cranial-caudal variation of point PMP left (< 0.05 mm) results in a significant change in the orientation of the FHPL and PPL from the frontal view.

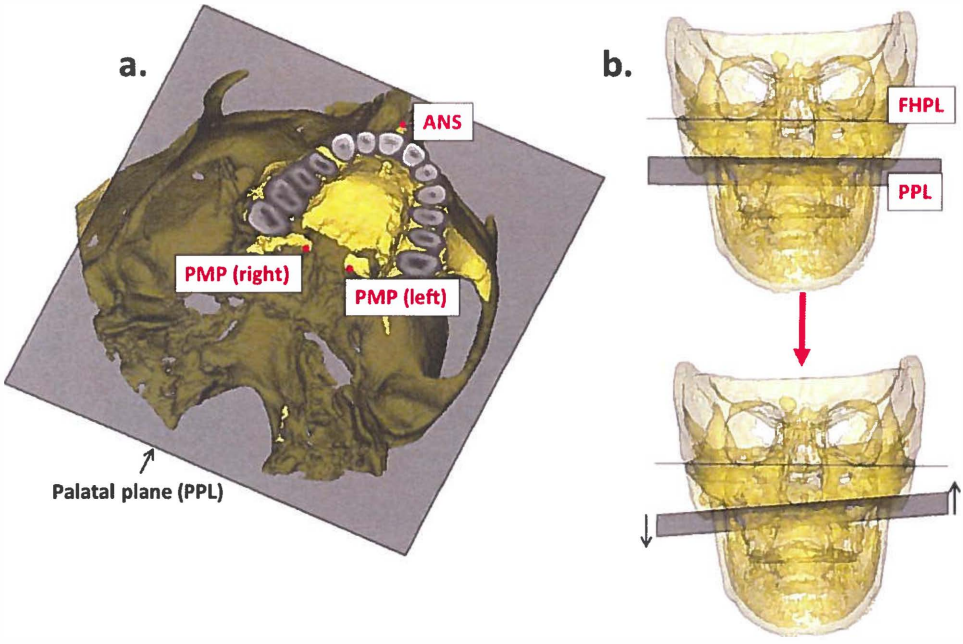

Our results confirm that most 3D cephalometric measurements are possibly not sensitive enough for small changes between the start and end of an active treatment. Reducing the measurement error by repeated measurement is arduous and unrealistic in daily practice because 3D landmark identification can be time consuming.

Superimposition of 3D surface models is an alternative method to evaluate growth or treatment outcome and quantifies change by means of colour maps.[40] Future research need to assess if superimposition of surface models is a more reliable method than linear and angular measurements to quantify 3D change. Unfortunately it is currently very time-consuming and computer-intensive to perform 3D superimposition. However, new advances will undoubtedly make a simplified analysis available in the future.[40] In addition; more accurate 3D measurements might be obtained when future image segmentation procedures, based on both intensity and gradient magnitude of the signals, will be implemented rather than the current threshold based methods.

5.5 Conclusion

The measurement error of 3D cephalometric measurements (except for the ANB angle) can be considered clinically relevant. This questions the use of linear and angular 3D measurements to detect true treatment effect when a high level of accuracy required

5.6 References

1. Cevidanes LHC, Tucker S, Styner M, Kim H, Chapuis J, Reyes M, Profitt, Turvey T, Jaskolka M. Three-dimensional surgical simulation. Am J Orthod Dentofacial Orthop 2010; 138: 361-71
2. Swennen GRJ, Mollemans W, Schutyser F. Three-dimensional treatment planning of orthognathic surgery in the era of virtual imaging. J Oral Maxillofac Surg 2008; 67: 2080-92
3. Swennen GRJ, Schutyser F. Three-dimensional cephalometry: Spiral multi-slice vs. cone-beam computed tomography. Am J Orthod Dentofacial Orthop 2006; 130: 410-6
4. Halazonetis DJ. From 2-dimensional cephalograms to 3-dimensional computed tomography scans. Am J Orthod Dentofacial Orthop 2005; 127: 627-37
5. Ngan DC, Kharbanda OP, Geenty JP, Darendeliler MA. Comparison of radiation levels from computed tomography and conventional dental radiographs. Aust Orthod J 2003; 19: 67-75
6. Mah JK, Danforth RA, Bumann A, Hatcher D. Radiation absorbed in maxillofacial imaging with a new dental computed device. Oral Surg Oral Med Oral Pathol Oral Radiol Endod 2003; 96:508-13
7. Hatcher DC, Aboudara CL. Diagnosis goes digital. Am J Orthod Dentofacial Orthop 2004; 125: 512-5
8. Brown AA, Scarfe WC, Scheetz JP, Silveira AM, Farman AG. Linear accuracy of cone beam CT 3D images. Angle Orthod 2009; 79: 150-7

9. Damstra J, Fourie Z, Huddleston Slater JJR, Ren Y. Accuracy of linear measurements from cone-beam computed tomography-derived surface models of different voxel sizes. Am J Orthod Dentofacial Orthop 2010;137:16.e1-16.e6)
10. Lagravere MO, Carey J, Toogood RW, Major PW. Three-dimensional accuracy of measurements made with software on cone-beam computed tomography images. Am J Orthod Dentofacial Orthop 2008;134:112-16
11. Hassan B, van der Stelt P, Sanderink G. Accuracy of three-dimensional measurements obtained from cone beam computed tomography surface-rendered images for cephalometric analysis: influence of patient scanning position. Eur J Orthod 2008;31:129-34
12. Mischkowski RA, Pulsfort R, Ritter L, Neugebauer J, Brochhagen HG, Keeve E, Zoller JE. Geometric accuracy of a newly developed cone-beam device for maxillofacial imaging. Oral Surg Oral Med Oral Pathol Oral Radiol Endod 2007;104:551-9
13. Grauer D, Cevidanes LSH, Profitt WR. Working with DICOM craniofacial images. Am J Orthod Dentofacial Orthop 2009; 136:460-70
14. Lou L, Lagravere MO, Compton S, Major PW, Flores-Mir C. Accuracy of measurements and reliability of landmark identification with computed tomography (CT) techniques in the maxillofacial area: a systematic review. Oral Surg Oral Med Oral Pathol Oral Radiol Endod 2007; 104: 402-11
15. De Oliviera AEF, Cevidanes LHS, Phillips C Motta A, Burke B, Tyndall D. Observer reliability of three-dimensional cephalometric identification on cone-beam computerized tomography. Oral Surg Oral Med Oral Pathol Oral Radiol Endod 2009; 107: 256-265
16. Ludlow JB, Gubler M, Cevidanes LHS, Mol A. Precision of cephalometric landmark identification: cone-beam tomography vs. conventional cephalometric views. Am J Orthod Dentofacial Orthop 2009; 136: 312e1-10; discussion 312-3
17. Lagravere MO, Major PW, Carey J. Sensitivity analysis for plane orientation in three-dimensional cephalometric analysis based on superposition of serial cone beam computed tomography images. Dentomaxillofac Radiol 2010: 39: 400-408
18. Damstra J, Huddleston Slater JJR, Fourie Z, Ren Y. Reliability and the smallest detectable difference of lateral cephalometric measurements. Am J Orthod Dentofacial Orthop 2010: 138; 546e1-8; discussion 546-547
19. Harris EF, Smith RN. Accounting for measurement error: A critical but often overlooked process. Arch of Oral Biol 2009;54 Suppl 1:S107-17
20. Van Vlijmen OJC, Maal T, Berge SJ, Bronkhorst EM, Katsaros AM, Kuipers-Jagtman. A comparison between 2D and 3D cephalometry on CBCT scans of human skulls. Int J Oral Maxillofac Surg 2010; 39: 156-160
21. Olszewski R, Zech F, Cosnard G, Nicolas V, Macq B, Reychler H. Three-dimensional computed tomography cephalometric craniofacial analysis: experimental validation in vitro. Int J Maxillofac Surg 2007; 36: 828-33
22. Swennen GRJ, Schutyser F, Barth EL, De Groeve P, De Mey A. A new method of 3-D cephalometry Part I: the anatomic Cartesian 3-D reference system. J Craniofac Surg 2006; 17: 314-25

23. Moerenhout BAMML, Gelaude F, Swennen GRJ, Casselman JW, Van der Sloten J, Mommaerts MY. Accuracy and repeatability of cone-beam computed tomography (CBCT) measurements used in the determination of facial indices in the laboratory setup. J Craniomaxillofac Surg 2009; 37:18-23
24. Suomalainen A, Vehmas T, Kortesniemi M, Robinson S, Peltola J. Accuracy of linear measurements using dental cone beam and conventional multislice computed tomography. Dentomaxillofac Radiol 2008; 37: 10-17
25. Haraguschi S, Takada K, Yasuda Y. Facial asymmetry in patients with skeletal class III deformity. Angle Orthod 2002; 72: 28-35
26. Swennen GJR, Schutyser F, Hausamne JE. Three-dimensional cephalometry. A colour atlas and manual. Heidelberg Springer, Berlin 2005
27. Richardson A. A comparison of traditional and computerized methods of cephalometric analysis. Eur J Orthod 1981;3:15-20
28. Lagerros YT. Physical activity – the more we measure, the more we know how to measure. Eur J Epidemiol 2009; 24: 119-122
29. Hopkins WG. Measures of reliability in sports medicine and science. Sports Med 2000;30:1-15
30. Smeulders MJ, Van den Berg S, Odeman J, Nederveen AJ, Kreulen M, Maas M. Reliability of in vivo determination of forearm muscle volume using 3.0 T magnetic resonance imaging. J Magn Reson Imaging 2010; 31: 1252-1255
31. Grunt S, Van Kampen PJ, Van der Krogt MM, Brehm MA, Doorenbosch CAM, Becher JG. Reproducibility and validity of video screen measurements of gait in children with spastic cerebral palsy. Gait Posture 2010; 31: 489-494
32. Kropmans TJ, Dijkstra PU, Stegenga B, Stewart R, de Bont LG. Smallest detectable difference in outcome variables related to painful restriction of the temporomandibular joint. J Dent Res 1999;78-784-789
33. Beckerman H, Roebroeck ME, Lankhorst GJ, Becher JG, Bezemer PD, Verbeek ALM. Smallest real difference, a link between reproducibility and responsiveness. Qual Life Res 2001;10:571-578
34. Marci V, Athanasiou AE. Sources of error in lateral cephalometry. In: Athanasiou AE. Orthodontic cephalometry. London, UK: Mosby-Wolfe: 1995: 125-140
35. Kamoen A Dermaut L, Verbeeck R. The clinical significance of error measurement in the interpretation of treatment results. Eur J Orthod 2001; 23: 569-578
36. Nagasaka S, Fujimora T, Segoshi K. Development of a non-radiographic cephalometric system. Eur J Orthod 2003;25:77-85
37. Loubele M, Jacobs R, Maes F, Denis K, White S, Coudyser W et al. Image quality vs radiation dose of four cone-beam computerized scanners. Dentomaxillofac Rad 2008; 37; 309-319
38. Hassan B, Metska ME, Ozok AR, Van der Stelt PF, Wesselink PR. Comparison of five cone beam computed tomography systems for the detection of vertical root fractures. J Endod 2010; 36: 126-129
39. Loubele M, Maes F, Schutyser F, Marchal G, Jacobs R et al. Assessment of bone segmentation quality of cone-beam CT versus multislice spiral CT: a pilot study. Oral Surg Oral Med Oral Pathol Oral Radiol Endod 2006; 102: 255-234

40. Cevidanes LHS, Styner M, Profitt WR. Three-dimensional superimposition for quantification of treatment outcomes. In: Nanda R, Kapila S. Current therapy in Orthodontics. London, UK: Mosby-Wolfe: 2010: 36-45

Chapter 5

The linear accuracy and repeatability of anthropometric facial measurements using cone-beam computed tomography

This chapter is based on the following publication:
Fourie Z, Damstra J, Gerrits PO, Ren Y. Linear accuracy and repeatability of anthropometric facial measurements using cone-beam computed tomography. Cleft-Palate Craniofac J 2010; doi: 10.1597/10-076

Abstract

The purpose of this study was to determine the accuracy and repeatability of linear anthropometric measurements on the soft tissue surface model generated from cone beam computed tomography (CBCT) scans. **Materials and Methods.** The study sample consisted of seven cadaver heads. The accuracy and repeatability were assessed by means of a series of 21 standardized, linear facial measurements derived from 11 landmarks taken both directly on the face with a set of digital callipers and indirectly from a 3D soft tissue surface model (STSM) generated from a CBCT scan of the heads using SimPlant® Ortho Pro software. The landmarks and measurements were chosen to cover various regions of the face with an emphasis on the oral-nasal region. The CBCT measurements were compared to the physical measurements. Statistical analysis for the repeatability was done by means of the intra-class coefficient (ICC). Accuracy was determined by means of the absolute error (AE) and absolute percentage error (APE). **Results.** The CBCT measurements were very accurate when compared to the physical measurements (0.962 - 0.999). Except for one measurement, between point tragion (t) and nasion (n) (mean 1.52 mm), all the measurements had a mean AE of less than 1.5 mm. **Conclusions.** The 3D surface models derived from CBCT images, is sufficiently precise and accurate for the anthropometric measurements.

5.1 Introduction

Many craniofacial anomalies are characterized by complex deviations in the shape and configuration of facial soft tissue structures. For affected individuals, extensive surgical interventions often are required to correct malformed or malpositioned facial structures, thereby normalizing their viscerocranial appearance. Effective treatment planning and postsurgical outcome assessment for such skeletal anomalies require an accurate, reliable, and objective system for quantifying the soft tissue of the face (Farkas et al., 1980; Arridge et al., 1985; Posnick and Farkas, 1994; Ayoub et al., 1998).

Anthropometry provides objective means to assess facial shape and detect shape changes over time. This is important to diagnose acquired malformations, to plan and evaluate surgery, to study normal and abnormal growth, and to differentiate between the results of treatment and normal growth. Although the term anthropometry covers measurement of any aspect of human form, the term surface anthropometry is used in this paper to refer to the measurement of the facial surface features (Douglas, 2004).
Until recently, anthropometry has been limited to measurements that use traditional manual instruments (e.g., slicing and spreading calipers) during an examination. These "direct" measurements are reliable and inexpensive to make. An extensive normative exists (Farkas 1994). Nevertheless, there are several limitations to the use of direct anthropometry. This includes prerequisite training of live subjects (which is painstaking) and the time-consuming nature of performing multiple direct measurements during an examination (Wong et al., 2008). Patient compliance must be maintained, requiring subjects to remain still. Additionally, there is no opportunity to archive craniofacial surface morphology. Furthermore, serial measurements are sometimes needed because three-dimensional (3D) abnormalities in craniofacial disorders may undergo substantial changes over time (Mullikan et al., 2001; Deutsch and Mulliken, 2008; Wong et al., 2008).

There is a growing interest in overcoming the limitations techniques. Anthropometry using two-dimensional (2D) images, such as photogrammetry and lateral cephalometry, would seem to hold obvious appeal over direct measurements of moving subjects (Grayson et al., 1988; Al-Omari et al., 2005). Disadvantages of these 2D-image techniques are measurement errors due to subjective analysis, magnification errors, parallax, variation in lighting, variation in head orientation, and projection errors (Farkas et al., 1980).

A number of relatively noninvasive, 3D imaging techniques have been developed over the last three decades. Examples include various forms of stereophotogrammetry

(Burke and Beard, 1967; Burke et al., 1983; Kobayashi et al., 1990; Motoyoshi et al., 1992; Meintjes et al., 2002), Moire´ topography techniques (Kawano, 1987; Kawai et al., 1990), surface scanning techniques (Moss et al., 1987; Moss et al., 1989). In addition to linear distances, these techniques potentially allow for the calculations of angles, surface arcs, surface areas, and volumes of the face (Weinberg et al., 2004). Image-processing algorithms applied to facial images have the potential to enhance anthropometric applications through reduction in the time spent on examinations and to improve the reliability of measurements. Automatic extraction of desired facial features or landmarks would enable automatic measurement of clinically relevant information (Douglas, 2004).

Cone beam computed tomography (CBCT) systems have been developed specifically for the maxillofacial region (Sukuvic, 2003). Many devices are capable of large field-of view imaging of the skull, including most anthropometric landmarks used in cephalometric analysis. Scanning time and radiation dose requirements have been suggested to be of the same order of magnitude as in other dental radiographic modalities (Ludlow et al., 2006). High dimensional accuracy has been reported for maxillofacial CBCT in measurements of facial structures (Kobayashi et al., 2004; Lascala et al., 2004; Hilgers et al., 2005). Reduced radiation exposure and sub-millimetre resolution are just some of the advantages CBCT-derived images have over conventional CT (Periago et al., 2008).

The ability to obtain reliable and accurate measurement data is perhaps the most important criterion upon which to evaluate any measurement technology. There have been multiple studies addressing the reliability and accuracy of surface scanning technology as both a clinical and a research tool (McCance et al., 1992; Bacja et al., 1994; Aung et al., 1995; Bush and Antonyshyn, 1996). Although the accuracy and reliability of linear measurements using CBCT on hard tissue has been shown (Damstra et al., 2010), there is a lack of data regarding the repeatability and accuracy of linear measurements obtained with CBCT from 3D facial soft tissue surface models (STSM). The purpose of this present study was to compare the repeatability and accuracy of linear measurements made on 3D STSM generated with SimPlant® Ortho Pro software (version 2.0, Materialise Dental, Leuven, Belgium).

Figure 1. *Soft tissue landmarks*

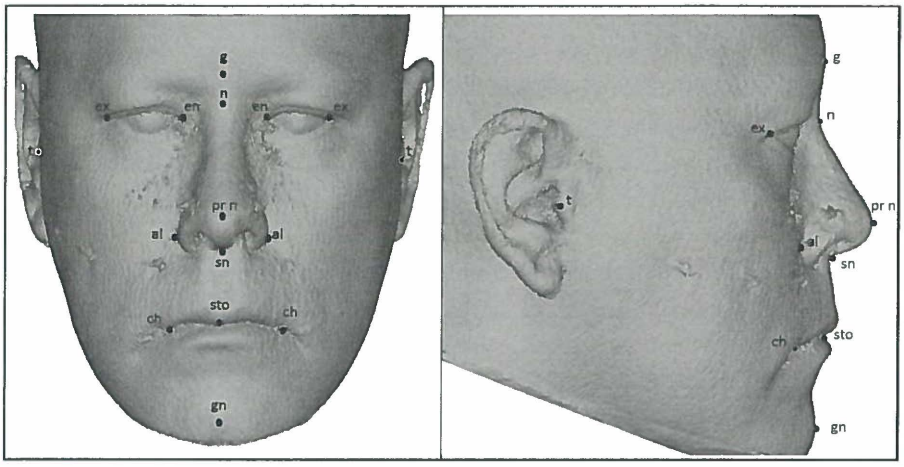

Table 1 Landmark descriptions

Abbreviation	Landmark	Description
g	glabella	Most prominent midpoint between eyebrows
n	soft tissue nasion	Midline depth
en	endocanthion	Inner commisure of palpebral fissure(left and right)
ex	exocanthion	Outer commisure of palpebral fissure(left and right)
prn	pronasale	Most prominent midpoint of nasal tip
sn	subnasale	Midpoint of columellar base at junction of upper lip
al	nasal alare	Most lateral point of alar contour (left and right)
ch	cheilion	Lateral extent of labial commisure (left and right)
sto	stomion	Midpoint of the labial fissure between gently closed lips
t	tragion	Positioned on the same level as the upper rim of the external meatus
gn	gnation	Most anterior inferior point on the soft tissue chin

5.2 Materials and Method

Our study sample consisted of seven fresh cadaver heads supplied by the Department of Anatomy, University Medical Centre Groningen, The Netherlands. Cadaver heads were used because for repeated physical measurements we needed a specimen that was not able to move with the same properties as a living person. We used a series of 11 landmarks (Fig. 1; Table 1) and 21 linear measurements (11 midline and 10 bilateral

measurements) (Fig. 2; Table 2) in all three planes of space on each subject. They were based on 17 standard anthropometric landmarks and 19 standard linear measurements used by Weinberg et al. (2004) and Wong et al. (2008) and originally defined by Farkas (1994). Some standard facial landmarks were excluded because they could not be identified well enough on the 3D rendered imaged made by the CBCT; two examples are supra auriculare (sa) and sub auriculare (sba), which were used by Weinberg et al. (2004) to determine the auricular length (length of the ear). The cadaver heads were placed in a special headrest supplied by the Department of Anatomy such that the Frankfort horizontal was at about 45° from the ground. This position makes it much easier to place the markers and make the physical measurements. One operator (Z.F.) used a sharp black permanent marker to make a dot for each landmark on the subjects' faces. Thereafter, a glass sphere with a diameter of 1.5 mm was glued to each black dot using superglue. The glass spheres were used because and give minimal scattering when surface models they rendered (Damstra et al., 2010). The midpoint of the outermost part of the sphere, opposite where it was glued to the skin surface, was the reference mark. The distances between the reference marks were determined manually with an electronic digital calliper (GAC, Bohemia, NY). The physical measurements were made three times by consensus of two operators (Z.F. and J.D.). The mean of the measurements was designated as the reference value, or anatomic truth. During the physical measurements, care was taken not to distort the soft tissue while measuring the linear distances. The readouts were not visible to the observer during the actual measurements.

The CBCT scans were made directly after making the physical measurements. For the scanning procedure, the KaVo 3D exam (KaVo Dental GmbH, Bismabring, Germany) CBCT scanner was used. The head was positioned and fixed in the scanner with the head facing forward and the Frankfort horizontal plane parallel to the floor. The specimen was handled carefully to prevent distortion of the soft tissues. The head was scanned with a 0.3 mm voxel size with a 17-mm field of view (Fourie et al., 2010). The acquired CBCT Digital Image and Communication in Medicine (DICOM) data sets were saved to an external hard disc (LaCie 120-GB hard disk; Haining, Hong Kong) and then transferred to a personal laptop computer (Aspire 5738ZG; Acer, Hertogenbosch, The Netherlands) with a dedicated 512-MB video card (Geforce 600MGT; NVIDIA, Santa Clara, CA). All measurements were performed on the surface models on a 16-in. CrystalBrite LCD flat-panel colour screen (Acer) with a maximum resolution of 1440 3 900 pixels. The DICOM files were then imported into SimPlant® Ortho Pro software (version 2.0; Materialise

Dental, Leuven, Belgium).The 3DSTSMwere all generated by the present threshold for soft tissues (2742 to 3055 Hounsfield units) as specified by the rendering software. The SimPlant® Ortho Pro software provides various views by rotating and transplanting the rendered image. The reference points were identified on the spherical glass markers by using a cursor-driven pointer (Fig. 3). After landmark identification, a preprogramed analysis provided the distances (to the nearest 0.01 mm) of the 21 linear measurements, as described in Figure 2 and Table 2. The values were then exported and saved in an Excel file format. Each CBCT image was rendered and measured on three occasions by one observer (Z.F.). To reduce the measurement error, glass spheres were used. The mean of the three measurements represented the CBCT measurement value (Table 3).

Statistical Analysis

Means and standard deviations were calculated for the direct caliper and CBCT measurements. As a measure of repeatability, the intraclass correlation coefficient (ICC) for absolute agreement based on a two-way random effects analysis of variance was calculated. The ICCs of the repeated measurements tested the repeatability of the direct caliper and CBCT measurements. The accuracy of the CBCT measurements was determined by comparison of the CBCT and direct caliper measurements. The intra-examiner reproducibility also was calculated by means of the ICC.

The accuracy of the CBCT measurements were expressed by means of the absolute error (AE) and absolute percentage error (APE). Absolute error was defined as the CBCT measurement value subtracted by the reference value (Mischkowski et al., 2007). Absolute percentage errors were calculated by means of the following equation: APE 5 100 3 (AE / Reference value) (Mischkowski et al., 2007). All statistical analyses were performed with a standard statistical software package (SPSS version 16; SPSS, Inc., Chicago, IL).

Figure 2. *Linear soft tissue measurement*

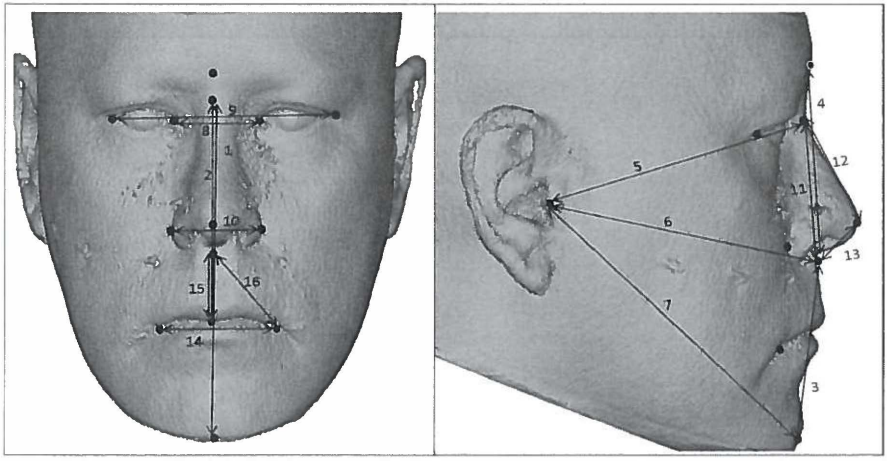

Table 2 List of measurements

No	Linear measurements	Region	Landmarks
1	Total facial height	face	n-gn
2	Upper facial height	face	n-sto
3	Lower facial height	face	sn-gn
4	Glabella-subnasale distance	face	g-sn
5	Upper facial depth (right)	face	t-n
6	Upper facial depth (left)	face	t-n
7	Midfacial depth right)	face	t-sn
8	Midfacial depth (left)	face	t-sn
9	Lower facial depth (right)	face	t-gn
10	Lower facial depth (left)	face	t-gn
11	Intercanthal width	eye	en-en
12	Biocular width	eye	ex-ex
13	Nasal width	nose	al-al
14	Nasal height	nose	n-sn
15	Nasal projection	nose	n-prn
16	Alar length (right)	nose	al-prn
17	Alar length (left)	nose	al-prn
18	Labial fissure width	mouth	ch-ch
19	Upper lip height	mouth	sn-sto
20	Upper lip length (right)	mouth	sn-ch
21	Upper lip length (left)	mouth	sn-ch

5.3 Results

All the scans were made with a 0.3 voxel size. The intraobserver reproducibility was very high for the physical measurements (.964 to .999) as well as for the CBCT measurements (.982 to .999) (Table 4). When comparing the CBCT measurements with the physical measurements, data proved to be very reliable with an ICC between .923 and .999 (Table 4). Accuracy of the measurements was determined by the AE and APE (Table 5). The means, standard deviations, and confidence intervals of the AE and APE were calculated and confirmed the accuracy of the measurements. For this study, we regarded a mean AE of more than 1.5 mm as clinically significant. Only one measurement (t-n) had a mean AE of more than 1.5 mm. The percentage error was more than 2% for only two measurements, namely no. 11 (en-en) with an APE of 2.27% and no. 19 (sn-sto) with an APE of 3.2%. However, the mean AE was less than 1 mm for both measurements.

Figure 3. *(A) An example of the rendered image of the nose. (B) Close up of the point Pronasale (prn) to illustrate the glass spheres without scattering on the rendered image.*

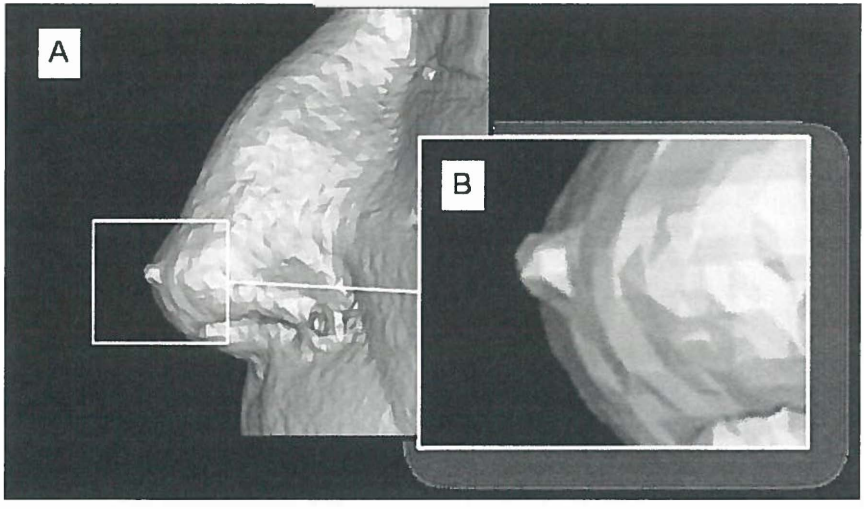

5.4 Discussion

The present study showed that 3D measurements on a computer-generated surface model created from a CBCT data set were accurate and reproducibility was excellent when compared with direct anthropometry. The introduction of maxillofacial CBCT

Table 3	Mean and standard deviation (SD) of the calliper and CBCT measurements in mm			
soft tissue measurements	measuring techniques			
	reference (calliper)		CBCT	
	mean	SD (±)	mean	SD (±)
1.(n-gn)	114.99	6.10	115.48	6.04
2.(n-sto)	77.68	3.92	78.16	3.69
3.(sn-gn)	60.27	5.89	60.20	5.72
4.(g-sn)	70.02	5.96	70.16	5.90
5.(t-n) - right	125.72	6.61	125.53	7.39
6.(t-n) - left	126.14	6.30	125.77	6.61
7.(t-sn) - right	130.89	8.76	128.93	7.37
8.(t-sn) - left	131.14	2.24	131.59	2.78
9.(t-gn) - right	149.79	12.07	149.27	11.76
10.(t-gn) - left	148.24	9.05	149.63	7.61
11.(en-en)	33.62	4.03	33.92	3.66
12.(ex-ex)	89.81	6.22	88.86	5.95
13.(al-al)	37.70	4.66	36.99	3.84
14.(n-sn)	56.44	3.39	55.33	3.20
15.(n-prn)	53.52	3.20	50.09	5.26
16.(al-prn) - right	33.28	5.23	33.46	4.82
17.(al-prn) - left	33.03	3.52	32.02	4.60
18.(ch-ch)	55.04	10.10	57.77	8.79
19.(sn-sto)	23.90	3.66	22.92	3.50
20.(sn-ch) - right	43.76	3.97	43.24	3.89
21.(sn-ch) - left	43.20	1.97	43.10	2.21

Table 4	Intraclass correlation coefficients (ICC): Intraobserver reliability and the accuracy of the CBCT measurements when compared to the reference values		
soft tissue measurements	intra-observer reliability		accuracy: reference vs. 3D CBCT
	reference (caliper)	3D CBCT	
1.(n-gn)	0.993	0.999	0.977
2.(n-sto)	0.981	0.999	0.982
3.(sn-gn)	0.988	0.998	0.976
4.(g-sn)	0.989	0.999	0.997
5.(t-n) - right	0.995	0.999	0.962
6.(t-n) - left	0.991	0.999	0.962
7.(t-sn) - right	0.998	0.999	0.976
8.(t-sn) - left	0.964	0.999	0.923
9.(t-gn) - right	0.999	0.999	0.989
10.(t-gn) - left	0.999	0.999	0.996
11.(en-en)	0.995	0.989	0.962
12.ex-ex)	0.992	0.999	0.995
13.(al-al)	0.990	0.987	0.989
14.(n-sn)	0.975	0.996	0.974
15.(n-prn)	0.992	0.998	0.976
16.(al-prn) - right	0.991	0.988	0.996
17.(al-prn) - left	0.976	0.998	0.995
18.(ch-ch)	0.998	0.998	0.999
19.(sn-sto)	0.988	0.996	0.966
20.(sn-ch) - right	0.984	0.989	0.994
21.(sn-ch) - left	0.987	0.982	0.974

Table 5	Absolute error (AE) and Absolute percentage error (APE)					
	absolute error (AE)			absolute percentage error (APE)		
soft tissue measurements	mean	SD	CI (95%)	mean	SD	CI (95%)
1.(n-gn)	0.76	0.73	0.22 - 0.78	0.78	0.92	0.09 - 1.46
2.(n-sto)	0.69	0.50	0.33 - 0.89	0.89	0.65	0.41 - 1.37
3.(sn-gn)	1.11	0.62	0.66 - 1.87	1.87	1.08	1.07 - 2.68
4.(g-sn)	0.40	0.20	0.25 - 0.56	0.56	0.27	0.36 - 0.77
5.(t-n)- right	1.52	1.21	0.62 - 1.21	1.21	0.95	0.50 - 1.91
6.(t-n)- left	1.20	1.05	0.42 - 0.94	0.94	0.82	0.33 - 1.55
7.(t-sn) - right	1.17	1.31	0.21 - 0.90	0.90	0.99	0.16 - 1.63
8.(t-sn) - left	1.10	0.55	0.69 - 0.83	0.83	0.41	0.52 - 1.13
9.(t-gn) - right	1.41	0.96	0.70 - 0.97	0.97	0.74	0.43 - 1.52
10.(t-gn) - left	0.58	0.45	0.25 - 0.34	0.34	0.37	0.06 - 0.61
11.(en-en)	0.94	0.54	0.54 - 2.97	2.97	2.00	1.49 - 4.45
12.ex-ex)	0.50	0.43	0.18 - 0.57	0.57	0.50	0.20 - 0.94
13.(al-al)	0.64	0.28	0.43 - 1.72	1.72	0.73	1.18 - 2.25
14.(n-sn)	0.63	0.42	0.32 - 1.11	1.11	0.74	0.56 - 1.66
15.(n-prn)	0.57	0.36	0.30 - 1.07	1.07	0.66	0.58 - 1.56
16.(al-prn) - right	0.39	0.39	0.10 - 1.23	1.23	1.42	0.17 - 2.28
17.(al-prn) - left	0.41	0.27	0.21 - 1.27	1.27	0.89	0.61 - 1.93
18.(ch-ch)	0.27	0.27	0.08 - 0.91	0.91	0.76	0.34 - 1.47
19.(sn-sto)	0.68	0.86	0.04 - 3.20	3.20	3.86	0.34 - 6.06
20.(sn-ch) - right	0.50	0.32	0.26 - 1.10	1.10	0.64	0.63 - 1.58
21.(sn-ch) - left	0.41	0.28	0.21 - 0.96	0.96	0.67	0.46 - 1.46

equipment provides clinicians with an opportunity to generate 3D volumetric renderings using third-party personal computer–based software (Periago et al., 2008). The rapidly emerging availability of this technology will undoubtedly expand the use and application of 3D imaging, particularly in the field of orthodontics (Danforth et al., 2003; Weinberg and Kolar, 2005). The aim of this study was to determine the reproducibility and accuracy of linear measurements made on 3D STSM generated from a CBCT data set made from human cadavers. It was found that the anthropometric surface measurements made on the CBCT 3D image are very reliable and accurate. One limitation of this study was the sample size, but although it was relatively small due to a lack of available human cadavers, the present study shows that this is a very good method for linear measurements. Damstra et al. (2010) compared linear measurements from CBCT surface models with physical measurements and also found the method to be very reliable and accurate. The accuracy of CBCT has been confirmed by other studies (Periago et al., 2008; Stratemann et al., 2008; Damstra et al., 2010; Fourie et al., 2010). However, Periago et al. EP (2008) and Cavalcanti et al. (1998) found that two thirds of CBCT measurements were statistically significantly different from the physical measurements. A number of factors could explain the inaccuracies they observed: The accuracy of 3D images of patients may be affected by a reduction in image quality due to soft tissue attenuation, metallic artifacts, and landmark identification error. In addition, they measured on the slices and not on the surface models. Wong et al. (2008) suggested that markers should be used, otherwise validity will be very difficult to achieve. Their opinion is shared by other authors (Ward and Jamison, 1991; Jamison and Ward, 1993). In the present study, the CBCT measurements were accurate because landmark identification error was reduced by using opaque glass spheres as fiducial markers. The reason we used markers was to measure the accuracy and reproducibility of linear measurements on the STSM and not the reproducibility of landmark identification. Although we did not measure the inter-observer reproducibility, the measurement error was reduced by the use of glass spheres. In addition, the spherical glass markers are likely to be less affected by the segmentation process due to their uniform density. The glass spheres we used were produced from soda-lime-silica glass, the most prevalent type of glass and commonly used for windows and containers (bottles and jars) (Damstra et al., 2010). The main advantage of glass versus metallic markers is that glass markers produce no scattering and artifacts when rendered to

surface models. This is because bone and glass spheres have similar values on the Hounsfield scale (Enomoto et al., 2009). The fact that glass spheres cannot be used in a clinical situation on a patient is a definite limitation of this study.

In their studies of the precision and reproducibility of coordinate data and distances made on stereophotogrammetry and laser surface scan images, Weinberg et al. (2004) and Wong et al. (2008) used several of the same landmarks used in our study and also found the method to be highly precise and reliable. Differences in study design, measurement protocols, and statistical analysis prevent comparison of our results with those of other studies (Douglas, 2004; Weinberg et al., 2004; Wong et al., 2008). Previous studies have demonstrated high levels of incongruence between simple indirect measurement methods and direct anthropometry (Farkas et al., 1980; Burke et al., 1983). Similar comparisons have been made between various 3D techniques and direct anthropometry, with mixed results (Bacja et al., 1994; Aung et al., 1995; Meintjes et al., 2002). Bacja et al. (1994) compared 21 measurements derived from laser surface scans with measurements from direct anthropometry taken on a sample of adult facial casts. They found a very high degree of correlation between the two methods (from .93 to 1) and mean difference scores in the sub-millimeter range in all but one variable (total facial height, or n-gn) (Bacja et al., 1994). The same pattern was seen in this present EQ study with all the mean AEs smaller than 1.5 mm except for the measurement n-g (mean AE, 1.51 mm). Aung et al. (1995) also compared laser surface scanning with direct anthropometry, but they used living subjects. However, their results were highly variable, ranging from 0.36 to 7 mm. The results of the present study were most comparable with those of Bacja et al. (1994).

Determining the accuracy of a feature extraction or segmentation method is difficult in medical imaging if no criterion standard of measurement exists for the complex structures being examined. New measurement methods for ER surface anthropometry are validated by comparison with direct measurements and their accuracy described in terms of their agreement with direct measurements (Douglas, 2004). Direct measurement using a ruler or calipers is subject to errors of parallax, interoperator variability, and instrument-dependent variability. Image-processing methods also can be validated by comparing their results with those of manual measurement on images displayed on a computer screen. In cephalometry, direct measurement is possible only on dry skulls, and validation of image processing algorithms relies on comparison with manual measurements on displayed images (Douglas, 2004). A difference of less than 1 mm between a new method and direct measurement in surface anthropometry is

generally regarded as acceptable (Farkas, 1996).

The literature varies on the accuracy acceptable for cephalometric landmarks: Rakosi (1982) suggested that an error of 2 mm is acceptable; whereas, Forsyth and Davis (1996) and Richardson (1981) have indicated that 1 mm is desirable. Therefore, in our study, we regarded a difference of less than 1.5 mm as acceptable. However, the standard with which the results of image processing are compared should be reliable. Normative data for surface anthropometry have been obtained primarily by direct measurement. Systematic differences between anthropometric measurements derived from calipers, rulers, and photographs highlight the need for consistency in data collection methods when measurements are compared (Shaner et al., 1998; Wong et al., 2008). Farkas (1996) emphasized the importance of the choice of instruments, and technique in surface anthropometry may be translated to the choice of imaging system and image-processing algorithm for craniofacial landmark measurement based on photographs ES and cephalograms.

All other things being equal, one would predict facial surface measurements obtained via indirect means (2D or 3D) to be, on average, larger than those obtained through direct means (Douglas, 2004). This is because direct anthropometry, by its very nature, requires physical contact with the soft tissues of the face; whereas, indirect anthropometry does not. The results of the present study do not conform to this prediction, and studies in the literature have been inconsistent on this issue. Aung et al. (1995) for example, found that laser scanner–derived measurements were larger than analogous direct measurements in approximately 81% of the 83 facial variables they considered. Similar patterns have been reported in studies comparing facial 2D photogrammetric methods with traditional anthropometry (Shaner et al., 1998; Douglas, 2004). Farkas et al. (1980) on the other hand, found the reverse pattern:
Indirect 2D photogrammetry tended to produce shorter measurements than direct anthropometry the majority of the time.

5.5 Conclusion

Results indicate very high levels of accuracy and very good congruence with traditional anthropometry. Those results suggest that STSM generated from CBCT scans with the SimPlant® Ortho Pro (Materialise Dental) software performs at a level that can be compared with direct anthropometric measurements. Cone beam computed tomography demonstrates a number of advantages over direct anthropometry, including increased speed of data collection, less invasiveness, and the ability to obtain a

3D archive of the subject's facial morphology. Although more research is needed, this method is applicable in clinical practice.

5.6 Reference

Al-Omari I, Millett DT, Ayoub AF. Methods of assessment of cleft related facial deformity: a review. Cleft Palate Craniofac J. 2005;42: 145–156

Arridge SR, Moss JP, Linney AD, James DR. Three-dimensional digitization of the face and skull. J Maxillofac Surg. 1985;13:136–143

Aung SC, Ngim RCK, Lee ST. Evaluation of the laser surface scanner as a measuring tool and its accuracy compared with direct facial anthropometric measurements. Br J Plast Surg. 1995;48:551–558

Ayoub AF, Siebert P, Moos KF, Wray D, Urquhart C, Niblett TB. A vision based three-dimensional capture system for maxillofacial assessment and surgical planning. Br J Oral Maxillofac Surg. 1998; 36:353–357

Bacja DB, Deutsch CK, D'Agostino RB. Correspondence between direct anthropometry and structured light digital measurement. In: Farkas LG, ed. Anthropometry of the Head and Face. New York: Raven Press; 1994:235–238

Burke PH, Banks P, Beard LFH, Tee JE, Hughes C. Stereo-photography measurement of change in soft tissue following surgery. Br J Oral Surg. 1983;21:237–245. ET

Burke PH, Beard LFH. Stereo-photogrammetry of the face. Am J Orthod. 1967;53:769–782.

Bush K, Antonyshyn O. Three-dimensional facial anthropometry using a laser surface scanner: validation of the technique. Plast Reconstr Surg. 1996;98:226–235

Cavalcanti MG, Vannier MW. Quantitative analysis of spiral computed tomography for craniofacial clinical applications. Dentomaxillofac Radiol. 1998;27:344–350

Damstra J, Fourie Z, Huddleston Slater JJR, Ren Y. Accuracy of linear measurements from cone-beam computed tomography–derived surface models of different voxel sizes. Am J Orthod Dentofacial Orthop. 2010;137:16.e1–16.e6

Danforth RA, Dus I, Mah J. 3-D volume imaging for dentistry: a new dimension. J Calif Dent Assoc. 2003;31:817–823

Deutsch CK, Mulliken JB. Discussion of surface anatomy of the face in Down's syndrome: anthropometric indices in the craniofacial regions. J Craniofac Surg. 2008;12:525–526

Douglas TS. Image processing for craniofacial landmark identification and measurement: a review of photogrammetry and cephalometry. Comput Med Imaging Graph. 2004;28:401–409

Enomoto K, Nishimura H, Inohara H, Murata J, Horii A, Doi K. A rare case of a glass foreign body in the parapharyngeal space: pre-operative assessment by contrast-enhanced CT and three-dimensional CT images. Dentomaxillofac Radiol. 2009;38:112–115

Farkas LG. Accuracy of anthropometric measurements: past, present and future. Cleft Palate Craniofac J. 1996;33:10–18

Farkas LG. Anthropometry of the Head and Face. New York: Raven Press; 1994.

Farkas LG, Bryson W, Klotz J. Is photogrammetry of the face reliable? Plast Reconstr Surg. 1980;66:346–355

Forsyth DB, Davis DN. Assessment of an automated cephalometric analysis system. Eur J Orthod. 1996;18:471–478

Fourie Z, Damstra J, Gerrits PO, Ren Y. Accuracy and reliability of facial soft tissue depth measurements using cone beam computer tomography. Forensic Sci Int. 2010;199:9–14

Grayson B, Cutting C, Bookstein FL, Kim H, McCarthy JG. The three-dimensional cephalogram: theory, technique and clinical application. Am J Orthod Dentofacial Orthop. 1988;94:327–337

Hilgers ML, Scarfe WC, Scheetz JP, Farman AG. Accuracy of linear TMJ measurements with cone beam computed tomography and digital cephalometric radiography. Am J Orthod Dentofacial Orthop. 2005; 128:803–811

Jameson PL, Ward RE. Brief communication: measurement size, precision, and reliability in craniofacial anthropometry: bigger is better. Am J Phys Anthropol. 1993;90:495–500

Kawai T, Natsume N, Shibata H, Yamamoto T. Three-dimensional analysis of facial morphology using moire´ stripes. Part I. Method. Int J Oral Maxillofac Surg. 1990;19:356–358

Kawano Y. Three-dimensional analysis of the face in respect of zygomatic fractures and evaluation of the surgery with the aid of moire topography. J Craniomaxillofac Surg. 1987;15:68–74

Kobayashi K, Shimoda S, Nakagawa Y, Yamamoto A. Accuracy in measurement of distance using limited cone-beam computerized tomography. Int J Oral Maxillofac Implants. 2004;19:228–231.

Kobayashi T, Ueda K, Honma K, Sasakura H, Hanada K, Nakauima T. Three-dimensional analysis of facial morphology before and after orthognathic surgery. J Craniomaxillofac Surg. 1990;18:68–73

Lascala CA, Panella J, Marques MM. Analysis of the accuracy of linear measurements obtained by cone beam computed tomography (CBCTNewTom). Dentomaxillofac Radiol. 2004;33:291–294.

Ludlow JB, Davies-Ludlow LE, Brooks SL, Howerton WB. Dosimetry of 3 CBCT devices for oral and maxillofacial radiology: CB Mercuray, NewTom 3G and i-CAT. Dentomaxillofac Radiol. 2006;35:219–226

McCance AM, Moss JP, Wright WR, Linney AD, James DR. A three-dimensional soft tissue analysis of 16 skeletal class III patients following bimaxillary surgery. Br J Oral Maxillofac Surg. 1992;30:221–232

Meintjes EM, Douglas TS, Martinez F, Vaughan CL, Adams LP, Stekhoven A, Viljoen D. A stereo-photogrammetric method to measure the facial dysmorphology of children in the diagnosis of fetal alcohol syndrome. Med Eng Phys. 2002;24:683–689

Mischkowski RA, Pulsfort R, Ritter L, Neugebauer J, Brochhagen HG, Keeve E, Zo¨ ller JE. Geometric accuracy of a newly developed conebeam device for maxillofacial imaging. Oral Surg Oral Med Oral Pathol Oral Radiol Endod. 2007;104:551–559

Moss JP, Linney AD, Grindrod SR, Arridge SR, Clifton JS. Three-dimensional visualization of the face and skull using computerized tomography and laser scanning techniques. Eur J Orthod. 1987;9:247–253

Moss JP, Linney AD, Grindrod SR, Mosse CA. A laser scanning system for the measurement of facial surface morphology. Opt Lasers Eng. 1989;10:179–190

Motoyoshi M, Namura S, Arai HY. A three-dimensional measuring system for the human face using three-directional photography. Am J Orthod Dentofacial Orthop. 1992;101:431–440

Mulliken JB, Burvin R, Farkas LG. Repair of bilateral complete cleft lip: intraoperative nasolabial anthropometry. Plast Reconstr Surg. 2001; 107:307–314

Periago DR, Scarfe WC, Moshiric M, Scheetz JP, Silveira AM, Farman AG. Linear accuracy and reliability of cone beam CT derived 3- dimensional images constructed using an orthodontic volumetric rendering program. Angle Orthod. 2008;78:387–395

Posnick JC, Farkas LG. The application of anthropometric surface measurements in craniomaxillofacial surgery. In: Farkas LG, ed. Anthropometry of the Head and Face. New York: Raven Press; 1994: 125–138

Rakosi T. An Atlas of Cephalometric Radiography. London: Wolfe Medical Publications; 1982.

Richardson A. A comparison of traditional and computerized methods of cephalometric analysis. Eur J Orthod. 1981;3:15–20

Shaner DJ, Bamforth JS, Petersen AE, Beattie OB. Facial measurements in clinical genetics: how important are the instruments we use? Am J Med Genet. 1998;77:384–390

Stratemann SA, Huang JC, Maki K, Miller AJ, Hatcher DC. Comparison of cone beam computed tomography imaging with physical measures. Dentomaxillofac Radiol. 2008;37:80–93

Sukovic P. Cone beam computed tomography in craniofacial imaging. Orthod Craniofac Res. 2003;6:31–36

Ward RE, Jamison PL. Measurement precision and reliability in craniofacial anthropometry: implications and suggestions for clinical applications. J Craniofac Genet Dev Biol. 1991;11:156–164

Weinberg SM, Kolar JC. Three-dimensional surface imaging: limitations and considerations from the anthropometric perspective. J Craniofac Surg. 2005;16:847–851

Weinberg SM, Scott NM, Neiswanger K, Brandon CA, Marazita ML. Digital three-dimensional photogrammetry: evaluation of anthropometric precision and accuracy using a Genex 3D camera system. Cleft Palate Craniofac J. 2004;41:507–518

Wong JY, Oh AK, Ohta E, Hunt AT, Rogers GF, Mulliken JB, Deutsch CK. Validity and reliability of 3D craniofacial anthropometric measurements. Cleft Palate Craniofac J. 2008;45:232–239

Chapter 6

Evaluation of anthropometric accuracy and reliability using different three-dimensional scanning systems

This chapter is based on the following publication:
Fourie Z, Damstra J, Gerrits PO, Ren Y. Evaluation of anthropometric accuracy and reliability using different three-dimensional scanning systems. Forensic Sci Int 2010; doi: 10.1016/j.forsciint .2010.09.018

Abstract

The aim of this study was to evaluate the accuracy and reliability of standard anthropometric linear measurements made with three different three-dimensional scanning systems namely laser surface scanning (Minolta Vivid 900), cone beam computed tomography (CBCT), 3D stereo-photogrammetry (Di3D system) and to compare them to physical linear measurements. The study sample consisted of seven cadaver heads. The reliability and accuracy were assessed by means of a series of 21 standardized, linear facial measurements derived from 15 landmarks taken both directly on the face with a set of digital callipers and indirectly from three-dimensional (3D) soft tissue surface models derived from CBCT, laser surface scans and 3D photographs. Statistical analysis for the reliability was done by means of intraclass correlation coefficients (ICCs). Accuracy was determined by means of the absolute error (AE) and absolute percentage error (APE) by comparison of the 3D measurements to the physical anthropometrical measurements. All the 3D scanning systems were proved to be very reliable (ICC > 0.923–0.999) when compared to the physical measurements (ICC; 0.964–0.999). Only one CBCT measurement (t-g) and one Di3D measurement (t-sn left) had a mean AE of more than 1.5 mm. There are clear potential benefits of using 3D measurements appose to direct measurements in the assessment of facial deformities. Measurements recorded by the three 3D systems appeared to be both sufficiently accurate and reliable enough for research and clinical use.

6.1 Introduction

Craniofacial anthropometry is very suitable for identification and quantification of clinical features, treatment planning, monitoring of operative outcomes, and assessment of longitudinal change [1] and [2]. The problem of accurately measuring the size and shape of the human cranium is a subject of long-standing interest among both forensic and physical anthropologists [3]. Until recently, anthropometry had been limited to measurement using traditional instruments (e.g., sliding and spreading callipers) during an examination. These 'direct' measurements are reliable and inexpensive to make, and an extensive normative database exists for reference [4] and [5]. Nevertheless, there are several limitations to the use of direct anthropometry, including prerequisite training on live subjects (which can be painstaking) and the time-consuming nature of performing multiple direct measurements during an examination. In addition, patient compliance must be maintained, as well, requiring live subjects to patiently remain still [5].

Today, several competing methods are available for capturing and quantifying craniofacial surface morphology [6] and [7]. These include traditional methods, such as direct anthropometry and two-dimensional (2D) photogrammetry, and more recent three-dimensional (3D) methods, such as laser surface scanning and even more recently digital 3D photogrammetry. From an anthropometric perspective, non-contact 3D surface capture methods offer many advantages over direct measurements e.g. quantification of angles, surface areas, and volumes in addition to linear distances; potential for extracting x, y, and z coordinate data for a wide variety of statistical shape analyses; and quick captures resulting in a permanent archival record of a subject's face [8].

Three-dimensional (3D) laser scanners are increasingly being used by forensic scientists, physical anthropologists, and conservators to document, reconstruct, and analyze objects and human remains, including craniofacial features [9], [10], [11], [12] and [13]. Their work has served to illustrate the many advantages of laser scanners over other types of 3D imaging technology in terms of cost, speed, and portability [3]. Laser surface scanning is reliable and accurate for identifying craniofacial surface landmarks [14]. However, image capture can be slow and may result in motion artefact in live subjects.

3D stereo-photogrammetry, overcomes the limitations of laser scanning. With this technique, synchronized digital cameras obtain images from multiple angles and reconstruct a digital 3D image. The advantages of 3D stereo-photogrammetry are near-

instantaneous image capture (in the order of 1.5 ms) which minimizes motion artefact, provision of archived image for subsequent and repeated analyses, collection of data points in 3D coordinate format for subsequent morphometric studies, and high resolution colour representation. Furthermore, software tools are available that allow the user to manipulate the image to facilitate identification of landmarks and calculate anthropometric measurements and measuring volumes [15] and [16]. In recent years, a wide variety of commercially available digital 3D photogrammetric devices have become available, many of which differ considerably in terms of cost, capture method, imaging hardware and software [5], [8], [17], [18], [19] and [20].

A recently introduced 3D surface capture system, the Di3D system (Di3D, Dimensional Imaging, Hillington Park, Glasgow, UK), uses three-dimensional stereo-photogrammetry to produce fully textured 3D surface contour maps of the head and face (180° ear to ear view). The system captures two stereo pairs of images (4 cameras in total) and specialist software is used to create a 3D surface using triangulation [20]. By using commercially available professional high-resolution colour digital cameras (4000 pixels × 3500 pixels) it is possible to capture images that resolve local details of linear densities approaching 0.1 mm/pixel on human faces. At this resolution there is enough information about local texture to achieve reliable area-based stereo matching. Projection of texture is therefore no longer required to achieve a good three-dimensional reconstruction of the human face based on high-resolution stereo-pair images of the subject and the capture time is shortened to a fraction of a seconds. Although the Di3D system has been technically validated by Khambay et al. [20] and Winder et al. [21], there is a lack of data regarding the reliability and accuracy of linear measurements obtained from the Di3D imaging system. In addition, the 3D measurements derived from the Di3D techniques needs to be compared to other 3D measuring techniques, like laser surface scanner and cone beam computed tomography (CBCT) to detect possible differences.

Therefore, the purpose of this present study was to compare linear measurements obtained manually on cadaver heads to three 3D systems (CBCT, laser surface scanning and Di3D stereo-photogrammetry) and to examine the accuracy and repeatability of the methods.

Figure 1. *Soft tissue landmarks and landmark description. (A) Frontal and (B) lateral views*

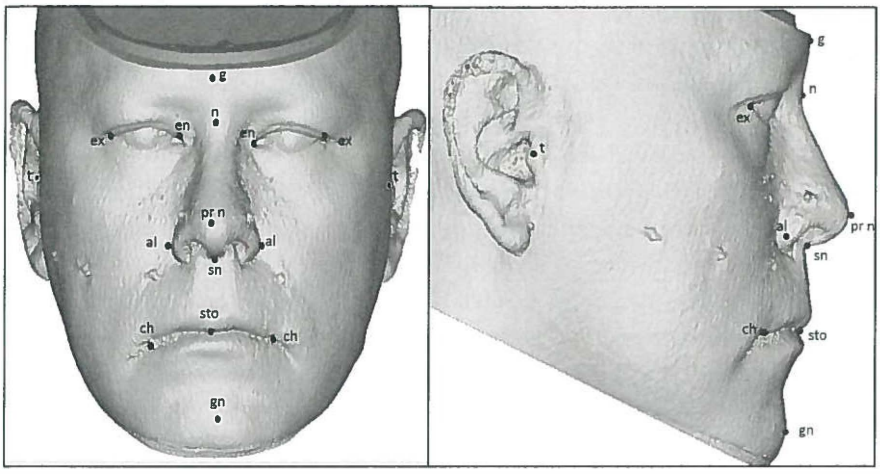

Landmark descriptions		
Abbreviation	Landmark	Description
g	glabella	Most prominent midpoint between eyebrows
n	soft tissue nasion	Midline depth
en	endocanthion	Inner commisure of palpebral fissure(left and right)
ex	exocanthion	Outer commisure of palpebral fissure(left and right)
prn	pronasale	Most prominent midpoint of nasal tip
sn	subnasale	Midpoint of columellar base at junction of upper lip
al	nasal alare	Most lateral point of alar contour (left and right)
ch	cheilion	Lateral extent of labial commisure (left and right)
sto	stomion	Midpoint of the labial fissure between gently closed lips
t	tragion	Positioned on the same level as the upper rim of the external meatus
gn	gnation	Most anterior inferior point on the soft tissue chin

6.2 Materials and methods

Our study sample consisted of seven fresh cadaver heads, supplied by the Department of Anatomy (University Medical Centre Groningen, Groningen, the Netherlands). Ethical approval was granted before we started with this project. We used a series of 11

landmarks (Fig. 1A and B) and 21 linear measurements (11 midline and 10 bilateral measurements) (Fig. 2A and B) in all 3 planes of space on each subject. They were based on 17 standard anthropometric landmarks and 19 standard linear measurements used by Weinberg et al. [19] and Wong et al. [5], and originally defined by Farkas [4]. Some standard facial landmarks were excluded because they could not be identified well enough on the 3D images made by the 3D techniques e.g. landmarks sa (supra auriculare) and sba (sub auriculare) which are used by Weinberg et al. [19] to determine the auricular length (length of the ear). The landmarks were marked on the subjects faces using a sharp black permanent marker by one operator (ZF). Thereafter, glass spheres with a diameter of 1.5 mm were glued to the black dot using super glue. The glass spheres produce no scattering when surface models are rendered from the CBCT technique [22]. The glass balls were painted black prior to placement to enhance the visibility of the markers on the stereo-photogrammetry image which was also recommended in other studies (Fig. 3) [5], [23] and [24]. The midpoint of the outer-most part of the sphere, was the reference mark. The distances between the reference marks were determined manually with an electronic digital calliper (GAC, Bohemia, NY). The physical measurements were made three times by consensus of two operators (ZF and JD). The mean of the measurements was designated as the reference value, or anatomical truth. During the physical measurements, care was taken not to distort the soft tissue while measuring the linear distances. The readouts were not visible to the observer during the actual measurements.

Laser surface scanning procedure

The laser surface scanning, 3D stereo-photogrammetry and CBCT scanning were performed directly after making the physical measurements. For the laser scanning procedure, the Minolta Vivid 900 (Osaka, Japan) laser-scanner was used. The head was positioned and fixated in a specially designed holder and scanned three times: once from directly in front, once from 45 from the right and 45 from the left. The acquired laser surface images were saved to an external hard disc (LACIE 120 MB hard disc) and then transferred to a personal laptop computer (Acer Aspire 5738ZG). The 3D image was then imported into SimPlant® Ortho Pro (Version 2.0 Materialize, Leuven, Belgium) for analysis.

Cone beam computed tomography (CBCT) procedure

For the CBCT scanning procedure the KaVo 3D exam (KaVo Dental GmbH, Bismarckring, Germany) scanner was used. The head was positioned and fixated in the scanner with the head facing forward and Frankfurt horizontal plane parallel to the floor. The specimen was handled carefully to prevent distortion of the soft tissues. The head was scanned with a 0.3 mm voxel size with a 17 mm field of view [25]. The acquired CBCT DICOM datasets were transferred to a personal laptop computer. The DICOM files were then imported into SimPlant® Ortho Pro software (version 2.0, Materialise Dental, Leuven, Belgium). The measuring procedure was the same for all three scanning systems and as follows: the reference points were identified on the spherical glass markers by using a cursor-driven pointer. After landmark identification, the pre-programmed analysis provided the distances to the nearest 0.01 mm of the 21 linear measurements as described in Fig. 2. The values were then exported and saved in Excel file format (Microsoft, Redmond, WA). This was repeated on 3 separate occasions by 1 observer (ZF). This was done for all three of the 3D techniques. Because markers (glass spheres) were used, landmark identification error was eliminated and only one observer was needed. The mean of the 3 measurements was regarded as the true value (Table 1).

3D stereo-photogrammetry procedure:

Photographs were taken directly after the laser surface scans with the Di3D camera system. The Di3D system uses four high resolution 8 megapixel Canon EOS 350D colour digital cameras with 50 mm lenses. All 3D surfaces were captured and reconstructed using the standard system settings as prescribed by the manufacturer for imaging the face (flash brightness – 1/4, camera shutter speed 1/200 s) [21]. The cadaver head was positioned facing the centre of the camera configuration, according to the manufacturer's instruction. The heads were still in the specially designed holder, the same as with the laser scanning procedure with the Frankfort horizontal plane parallel to the floor. After calibration, using the manufacturer's calibration target and calibrating software, the heads were photographed. The photographs were then imported into a software program DI3Dcapture™ 3D Capture Software (Dimensional Imaging, Hillington Park, Glasgow, UK).

All statistical analysis was performed with a standard statistical software package (SPSS version 16, Chicago, IL). Means and standard deviations were calculated for the four measuring techniques e.g. direct calliper, CBCT, laser surface scanning and 3D

Figure 2. *Linear soft tissue measurement and measurement description. (A) Frontal and (B) lateral views*

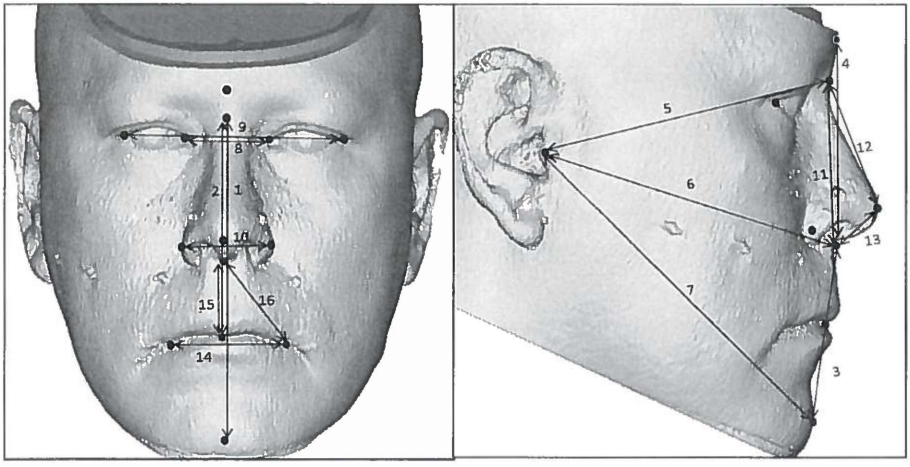

List of measurements			
No	Linear measurements	Region	Landmarks
1	Total facial height	face	n-gn
2	Upper facial height	face	n-sto
3	Lower facial height	face	sn-gn
4	Glabella-subnasale distance	face	g-sn
5	Upper facial depth (right)	face	t-n
6	Upper facial depth (left)	face	t-n
7	Midfacial depth right)	face	t-sn
8	Midfacial depth (left)	face	t-sn
9	Lower facial depth (right)	face	t-gn
10	Lower facial depth (left)	face	t-gn
11	Intercanthal width	eye	en-en
12	Biocular width	eye	ex-ex
13	Nasal width	nose	al-al
14	Nasal height	nose	n-sn
15	Nasal projection	nose	n-prn
16	Alar length (right)	nose	al-prn
17	Alar length (left)	nose	al-prn
18	Labial fissure width	mouth	ch-ch
19	Upper lip height	mouth	sn-sto
20	Upper lip length (right)	mouth	sn-ch
21	Upper lip length (left)	mouth	sn-ch

stereo-photogrammetry (Table 1). As a measure of reliability, the intraclass correlation coefficient (ICC) for absolute agreement based on a 2-way random effects analysis of variance (ANOVA) was calculated. ICCs of the repeated measurements tested the reliability of the four measuring techniques (Table 2). Intra-observer reliability of the CBCT measurements was determined by comparison of the repeated measurements. Because the direct calliper measurements were regarded as the reference; the reliability of the laser surface scanning, CBCT and 3D stereo-photogrammetry techniques were determined by comparison of these measurements to the direct calliper measurements (Table 2).

Figure 3. *An example of the rendered image of the nose to illustrate the glass spheres with minimal scattering on the rendered CBCT image*

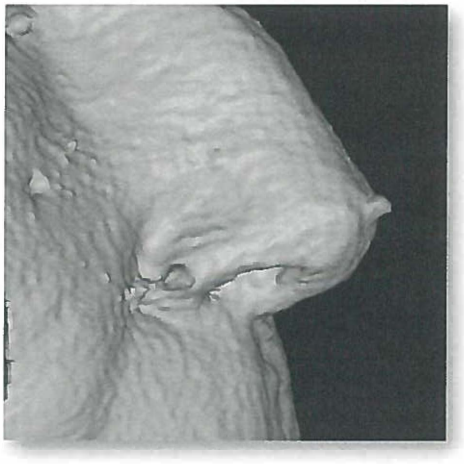

6.3 Results

The mean, standard deviation and reliability of the four measuring techniques are reported in [Table 1] and [Table 2]. Physical measurements with the digital calliper determined by consensus of the two observers were very reliable (ICC; 0.964–0.999). The CBCT, Laser surface scanner and Di3D measurements were found to be very reliable. The intra-observer reliability for the CBCT (ICC; 0.972–0.999), laser surface scanner (ICC; 0.968–0.998) and for the Di3D measurements (ICC; 0.965–0.998) was high.

Table 1	Mean and standard deviation (SD) of the four anthropometric measuring techniques in mm							
soft tissue	measuring techniques							
measurements	reference (calliper)		cone-beam CT		laser surface scan		3D stereo-photogrammetry	
	mean	SD (±)	mean	SD (±)	mean	SD (±)	mean	SD (±)
1.(n-gn)	114.99	6.10	115.48	6.04	115.06	6.04	115.01	6.06
2.(n-sto)	77.68	3.92	78.16	3.69	78.24	4.05	77.83	3.60
3.(sn-gn)	60.27	5.89	60.20	5.72	60.54	5.80	59.54	5.82
4.(g-sn)	70.02	5.96	70.16	5.90	70.72	5.51	70.31	5.48
5.(t-n) - right	125.72	6.61	125.53	7.39	126.65	6.74	126.55	5.68
6.(t-n) - left	126.14	6.30	125.77	6.61	126.15	6.40	126.49	6.86
7.(t-sn) - right	130.89	8.76	128.93	7.37	130.59	8.99	130.45	8.10
8.(t-sn) - left	131.14	2.24	131.59	2.78	128.31	6.68	129.50	6.63
9.(t-gn) - right	149.79	12.07	149.27	11.76	147.83	13.56	146.17	11.93
10.(t-gn) - left	148.24	9.05	149.63	7.61	146.72	11.02	147.98	9.36
11.(en-en)	33.62	4.03	33.92	3.66	34.04	4.02	33.48	3.71
12.(ex-ex)	89.81	6.22	88.86	5.95	89.75	5.46	89.43	6.28
13.(al-al)	37.70	4.66	36.99	3.84	37.30	4.81	36.99	4.92
14.(n-sn)	56.44	3.39	55.33	3.20	56.69	3.88	56.46	3.88
15.(n-prn)	53.52	3.20	50.09	5.26	51.46	4.44	51.87	4.75
16.(al-prn) - right	33.28	5.23	33.46	4.82	34.94	5.01	36.31	2.35
17.(al-prn) - left	33.03	3.52	32.02	4.60	34.29	4.02	31.49	4.30
18.(ch-ch)	55.04	10.10	57.77	8.79	58.03	9.30	56.87	8.67
19.(sn-sto)	23.90	3.66	22.92	3.50	21.68	2.60	21.72	3.11
20.(sn-ch) - right	43.76	3.97	43.24	3.89	41.38	5.04	43.27	4.30
21.(sn-ch) - left	43.20	1.97	43.10	2.21	41.98	3.44	42.95	2.39

Table 2	Intraclass correlation coefficients (ICC): Intraobserver reliability and the reliability of the measurements of the three techniques when compared to the reference values						
soft tissue measurements	observer reliability				reliability (vs. reference)		
	reference (calliper)	CBCT	laser surface scan	3D stereo-photogramm etry	CBCT	laser surface scan	3D stereo-photogramme try
1.(n-gn)	0.993	0.999	0.995	0.993	0.977	0.987	0.991
2.(n-sto)	0.981	0.999	0.990	0.990	0.982	0.989	0.964
3.(sn-gn)	0.988	0.998	0.980	0.995	0.976	0.992	0.984
4.(g-sn)	0.989	0.999	0.990	0.997	0.997	0.988	0.995
5.(t-n) - right	0.995	0.999	0.992	0.996	0.962	0.986	0.979
6.(t-n) - left	0.991	0.999	0.996	0.997	0.962	0.986	0.987
7.(t-sn) - right	0.998	0.999	0.998	0.995	0.976	0.994	0.991
8.(t-sn) - left	0.964	0.999	0.997	0.992	0.923	0.971	0.958
9.(t-gn) - right	0.999	0.999	0.998	0.998	0.989	0.994	0.999
10.(t-gn) - left	0.999	0.999	0.995	0.998	0.996	0.991	0.997
11.(en-en)	0.995	0.989	0.993	0.994	0.962	0.988	0.992
12.(ex-ex)	0.992	0.999	0.994	0.994	0.995	0.990	0.988
13.(al-al)	0.990	0.987	0.968	0.993	0.989	0.975	0.978
14.(n-sn)	0.975	0.996	0.985	0.992	0.974	0.968	0.992
15.(n-prn)	0.992	0.998	0.990	0.991	0.976	0.981	0.992
16.(al-prn) - right	0.991	0.988	0.978	0.965	0.996	0.988	0.985
17.(al-prn) - left	0.976	0.998	0.993	0.991	0.995	0.979	0.928
18.(ch-ch)	0.998	0.998	0.997	0.999	0.999	0.995	0.986
19.(sn-sto)	0.988	0.996	0.985	0.986	0.966	0.963	0.964
20.(sn-ch) - right	0.984	0.989	0.993	0.987	0.994	0.996	0.995
21.(sn-ch) - left	0.987	0.982	0.997	0.986	0.974	0.987	0.997

Table 3	Absolute error (AE) of the measuring techniques in mm											
soft tissue	cone-beam CT				laser surface scan				3D stereo-photogrammetry			
measurements	mean	SD	CI (95%)		mean	SD	CI (95%)		mean	SD	CI (95%)	
1.(n-gn)	0.76	0.73	0.22 -	1.30	0.87	0.59	0.44 -	1.31	0.73	0.45	0.40 -	1.07
2.(n-sto)	0.69	0.50	0.33 -	1.06	0.68	0.30	0.35 -	0.79	0.93	0.54	0.53 -	1.33
3.(sn-gn)	1.11	0.62	0.66 -	1.57	0.57	0.41	0.37 -	0.98	0.91	0.68	0.41 -	1.42
4.(g-sn)	0.40	0.20	0.25 -	0.55	0.72	0.63	0.25 -	1.18	0.46	0.44	0.13 -	0.79
5.(t-n)- right	1.52	1.21	0.62 -	2.42	1.06	0.48	0.70 -	1.41	1.11	0.64	0.63 -	1.58
6.(t-n)- left	1.20	1.05	0.42 -	1.98	1.07	0.39	0.79 -	1.36	0.93	0.66	0.44 -	1.42
7.(t-sn) - right	1.17	1.31	0.21 -	2.14	0.97	0.36	0.70 -	1.24	1.10	0.52	0.72 -	1.49
8.(t-sn) - left	1.10	0.55	0.69 -	1.51	1.48	1.22	0.58 -	2.38	1.84	1.35	0.83 -	2.84
9.(t-gn) - right	1.41	0.96	0.70 -	2.11	1.42	0.94	0.72 -	2.12	0.69	0.41	0.39 -	0.99
10.(t-gn) - left	0.58	0.45	0.25 -	0.91	1.22	1.01	0.47 -	1.97	0.74	0.67	0.24 -	1.24
11.(en-en)	0.94	0.54	0.54 -	1.34	0.51	0.44	0.18 -	0.84	0.44	0.29	0.23 -	0.66
12.(ex-ex)	0.50	0.43	0.18 -	0.82	0.71	0.53	0.32 -	1.10	0.83	0.66	0.34 -	1.32
13.(al-al)	0.64	0.28	0.43 -	0.85	0.93	0.87	0.29 -	1.57	0.96	0.72	0.43 -	1.50
14.(n-sn)	0.63	0.42	0.32 -	0.94	0.87	0.53	0.48 -	1.26	0.46	0.22	0.30 -	0.62
15.(n-prn)	0.57	0.36	0.30 -	0.84	0.75	0.57	0.32 -	1.17	0.56	0.29	0.34 -	0.77
16.(al-prn) - right	0.39	0.39	0.10 -	0.68	0.77	0.41	0.46 -	1.07	0.92	0.30	0.70 -	1.15
17.(al-prn) - left	0.41	0.27	0.21 -	0.60	0.87	0.29	0.65 -	1.08	1.27	0.81	0.67 -	1.87
18.(ch-ch)	0.27	0.27	0.08 -	0.47	0.87	0.36	0.61 -	1.14	1.28	0.94	0.58 -	1.97
19.(sn-sto)	0.68	0.86	0.04 -	1.32	0.77	0.30	0.55 -	0.99	0.78	0.41	0.48 -	1.08
20.(sn-ch) - right	0.50	0.32	0.26 -	0.73	0.64	0.44	0.32 -	0.97	0.66	0.68	0.16 -	1.17
21.(sn-ch) - left	0.41	0.28	0.21 -	0.61	0.87	0.70	0.35 -	1.38	0.46	0.29	0.25 -	0.68
Average	0.76	0.57	0.33 -	1.18	0.89	0.56	0.47 -	1.30	0.86	0.57	0.44 -	1.28

Table 4	Absolute percentage error (APE) of the measuring techniques								
soft tissue	cone beam CT			laser surface scan			3dMD		
measurements	mean	SD	CI (95%)	mean	SD	CI (95%)	mean	SD	CI (95%)
1.(n-gn)	0.78	0.92	0.09 - 1.46	0.77	0.53	0.38 - 1.17	1.26	0.83	0.65 - 1.88
2.(n-sto)	0.89	0.65	0.41 - 1.37	0.73	0.38	0.44 - 1.01	1.37	0.83	0.76 - 1.98
3.(sn-gn)	1.87	1.08	1.07 - 2.68	1.11	0.68	0.60 - 1.62	0.72	0.53	0.34 - 1.11
4.(g-sn)	0.56	0.27	0.36 - 0.77	1.07	0.95	0.37 - 1.77	0.37	0.35	0.10 - 0.63
5.(t-n)- right	1.21	0.95	0.50 - 1.91	0.84	0.37	0.57 - 1.11	0.86	0.50	0.49 - 1.23
6.(t-n)- left	0.94	0.82	0.33 - 1.55	0.85	0.29	0.63 - 1.06	0.71	0.49	0.34 - 1.07
7.(t-sn) - right	0.90	0.99	0.16 - 1.63	0.75	0.29	0.53 - 0.96	0.76	0.38	0.48 - 1.04
8.(t-sn) - left	0.83	0.41	0.52 - 1.13	1.17	1.00	0.43 - 1.91	1.27	1.06	0.49 - 2.05
9.(t-gn) - right	0.97	0.74	0.43 - 1.52	0.98	0.66	0.49 - 1.48	2.07	1.18	1.19 - 2.95
10.(t-gn) - left	0.34	0.37	0.06 - 0.61	0.78	0.60	0.33 - 1.23	0.83	0.77	0.26 - 1.39
11.(en-en)	2.97	2.00	1.49 - 4.45	1.54	1.35	0.54 - 2.54	1.20	0.76	0.64 - 1.76
12.(ex-ex)	0.57	0.50	0.20 - 0.94	0.77	0.51	0.39 - 1.15	1.47	1.20	0.58 - 2.35
13.(al-al)	1.72	0.73	1.18 - 2.25	2.77	2.86	0.65 - 4.88	1.90	1.43	0.84 - 2.96
14.(n-sn)	1.11	0.74	0.56 - 1.66	1.53	0.87	0.89 - 2.18	1.33	0.68	0.83 - 1.84
15.(n-prn)	1.07	0.66	0.58 - 1.56	1.39	1.02	0.63 - 2.15	1.67	0.94	0.98 - 2.37
16.(al-prn) - right	1.23	1.42	0.17 - 2.28	2.43	1.62	1.23 - 3.62	1.59	0.36	1.32 - 1.86
17.(al-prn) - left	1.27	0.89	0.61 - 1.93	2.58	0.88	1.93 - 3.23	5.65	3.40	3.13 - 8.17
18.(ch-ch)	0.91	0.76	0.34 - 1.47	1.55	0.70	1.04 - 2.07	3.15	2.16	1.55 - 4.75
19.(sn-sto)	3.20	3.86	0.34 - 6.06	3.51	1.29	2.55 - 4.47	2.07	1.19	1.19 - 2.95
20.(sn-ch) - right	1.10	0.64	0.63 - 1.58	1.68	1.16	0.82 - 2.54	3.12	3.05	0.86 - 5.38
21.(sn-ch) - left	0.96	0.67	0.46 - 1.46	2.22	1.70	0.95 - 3.48	1.15	0.60	0.70 - 1.60
Average	1.21	0.96	0.50 - 1.92	1.48	0.94	0.78 - 2.17	1.64	1.08	0.84 - 2.44

When comparing the 3D scanning systems to the physical measurements, the data proved to be very reliable with an ICC between 0.923 and 0.999 for the CBCT, 0.963 and 0.996 for the laser surface scanner and 0.965 and 0.997 for the Di3D system.

The mean, standard deviation and confidence intervals of the AE and APE were calculated and confirmed the accuracy of the measurements ([Table 3] and [Table 4]). The mean AE of all seven subjects was very small for the CBCT (0.76 ± 0.57 mm), for the laser surface scanner (0.89 ± 0.56 mm) and for the Di3D system (0.87 ± 0.56 mm). The APE was 1.21 ± 0.96% for the CBCT, 1.48 ± 0.94% for the laser surface scanner and 1.64 ± 1.08% for the Di3D system. For this study, we regarded the mean AE of more than 1.5 mm as clinically significant. Only one CBCT measurement (t-g) and one Di3D (t-sn left) had a mean AE of more than 1.5 mm.

6.4 Discussion

New advances in 3D surface imaging are having a dramatic impact on the field of craniofacial anthropometry. To be of any practical use, though, such imaging techniques must be capable of precisely and accurately quantifying facial surface topography as well as, if not better than, current existing alternatives. Determining precision is critical because high levels of intra- or inter-observer measurement error can generate misleading results, especially when comparing groups statistically [26].

Relatively few studies have directly compared anthropometric measurements obtained through alternative methods. Previous studies have focused mainly on the concordance between direct and indirect measurement techniques, comparing traditional calliper-based anthropometry with either standard 2D photogrammetry [27] and [28] or cephalometry [29] and [30]. Along these same lines, a few studies have also compared direct anthropometric measurements with those obtained by way of indirect 3D surface imaging methods, including traditional stereo-photogrammetry [8] and [31], surface laser scanning [14] and [32], and fully automated digital 3D photogrammetry [19] and [33]. It is difficult, however, to make any definitive statements regarding the results of previous studies comparing 3D surfaces. The extreme (sub-millimetre) accuracy observed in the present study is likely to be influenced by the fact that our sample comprised of inanimate cadaver heads as opposed to living subjects. In terms of intra-observer error, direct comparison of our results with those of previous studies is hindered once again by methodological inconsistencies, in particular, the fact that previous studies rarely reported comparable precision estimates. Nevertheless, the results of the present study generally agree with previous reports that suggest measurements obtained by indirect 3D surface imaging methods are capable of a very high degree of precision

[17], [31], [34] and [35]. For the few studies that have calculated precision for both direct anthropometry and indirect 3D surface imaging methods, the results suggest that 3D methods are capable of a greater overall precision [19], [31] and [36].

The choice to use an inanimate sample was based on estimates of precision and accuracy. With living subjects, a certain amount of measurement error is unavoidable when performing direct anthropometry, primarily because direct contact is made with the pliable tissues of the face. Non-contact 3D imaging obviously eliminates this source of error but may still be affected by motion artefacts. In terms of accuracy, when comparing mean measurement values between direct anthropometry and a 3D imaging system, results on living subjects, although still relatively accurate, often demonstrate substantially less concordance than results on non -animated heads. Wong et al. [5] found that some landmarks, e.g. al, sto and ch can change with facial movement during direct measurement on living subjects. The use of a non-animated subject is much more useful for a study like this. Kau and Richmond [37] indicated that soft tissue studies are inherently difficult and the tissue structures are inevitably affected by movement and distortions. Therefore imaging research involving soft issue requires a reproducible set-up in order be accurate and reliable.

In this present study the measurements are accurate because the landmark identification error was reduced by using opaque glass spheres as fiducial markers. The glass markers did not produce any scattering when the 3D soft tissue surface model was rendered and because they were painted black before placement, they were clearly visible with the stereo-photogrammetry [5], [23] and [24]. Weinberg et al. [19] compared cranio-facial measurements from 3D and direct anthropometry measurements, both with landmarks labelled. They found that 3D photographs had higher precision than direct measurements; they labelled the subjects prior to photographing them in order to improve accuracy. Differences of up to 2 mm were found, but these were not considered to be of clinical significance [19].

The mean AE of all seven subjects was very small for the CBCT (0.76 ± 0.57 mm), for the laser surface scanner (0.89 ± 0.56 mm) and for the Di3D system (0.87 ± 0.56 mm). These are consistent with previously reported mean errors of less than 1 mm [38]. Our results showed that linear measurements made on CBCT soft tissue are accurate and reliable and confirmed the accuracy of CBCT surface models reported in previous studies [6] and [20]. Although most of the other studies were made on dry sculls, our results justify the use of CBCT soft tissue surface models for anthropometric measurements. Ghoddousi et al. [39] compared three methods e.g. manual measurements, 3D stereo-photogrammetry and 2D photogrammetry. They found the stereo-photogrammetry measurements to compare well with the manual measurements; while the 2D measurements were less reliable [39]. Weinberg et al.

[19] compared the 3dMD and Genex imaging systems with each other and with direct measurements using mannequins. They found both imaging systems very reliable and comparable with the direct measurements [8]. The Di3D stereo-photogrammetry imaging system [20] and [21], used in the present study, displayed similar high precision results as the 3dMD [5] and [8] and Genex stereo-photogrammetry imaging system [8] and [19] used in previous studies. Importantly, these 3D imaging systems differ primarily in terms of capture method; the Genex system projects a structured light pattern into an object's surface to generate and extract 3D information, whereas the 3dMD system uses multiple cameras, three on each side (one colour and two infra-red) to get a photorealistic 3D image [8]. The Di3D system captures two stereo pairs of images (4 cameras in total) and specialist software are used to create a three-dimensional surface using triangulation [20].

The intra-observer reliability for the Di3D measurements (ICC; 0.965–0.998) was very high in the present study (Table 2). Weinberg et al. also reported very high reliability (0.98–1) of the Genex and the 3dMD measurements [5], [8] and [17]. Difference in study design, measurement protocols, and statistical analyses prevent comparison of our results to other studies using 3D digital photogrammetry systems [18], [39], [40] and [41]. Weinberg et al. [19] used a similar study design and landmarks to compare the Genex stereo-photogrammetry system to direct measurements. They compared direct calliper measurements 3D software measurements with and without markers and found the stereo-photogrammetry system to be sufficiently precise and accurate for the anthropometric needs of most medical and craniofacial research design [19]. The Di3D stereo-photogrammetry system has been technically validated in 2008 by Khambay et al. [20] An error within 0.2 mm was found and considered clinically acceptable. They stated that the system a major improvement in the use of stereo-photogrammetry for facial capture and analysis [20]. The result of this study confirms the accuracy and reliability of 3D anthropometric measurements using the Di3D stereo photogrammetry system.

Previous studies have identified laser scanning to be accurate to approximately 0.5 mm [34], whilst a comparison to laser scanning tomography with stereo-photogrammetry in 3D optic disc analysis found that very similar measurements were obtained in both techniques [42]. The accuracy and reliability of the Minolta Vivid 900 laser scanner was confirmed with this study. Sholts et al. [3] have shown that portable, low-cost 3D laser scanners are valuable tools for measuring human remains recovered from forensic and archaeological contexts. They used measurements of surface area and volume from human crania to illustrate the validity of this technology [3]. They stated that there are many advantages of laser scanners over other types of 3D imaging technology in terms of cost, speed, and portability [43].

Numerous studies done in the past found it to be very useful in orthodontics to analyze growth, soft-tissue changes, treatment simulation, appliance designs and treatment effects in three-dimensions [1], [37], [44], [45] and [47]. In addition, the spatial resolution of 3D models produced by laser scanners is equal to or greater than many 3D models produced under standard clinical conditions by CT and MRI machines [43]. Aung et al. [32] also compared laser surface scanning to direct anthropometry, but they used living subjects. The difference between each technique's mean score for all 83 variables was calculated. Results were highly variable, ranging from 0.36 to 7 mm. For the vast majority of head and face measurements, difference scores were well above the 2 mm mark [33]. The potential for inter- and intra-observer error is particularly high with 3D laser scanning, as subjective decisions made by the scanner operator can affect the resulting 3D model and its geometric properties, possibly obscuring or distorting meaningful aspects of morphological variation. These decisions include the positioning of the object to be scanned, the number of scans to be recorded, and especially how scans taken from different angles are merged. Such factors are potentially problematic for forensic anthropologists who may present findings based on 3D model measurements in expert witness testimony of their casework [46] and [47].

There were no clinical differences when comparing the accuracy and reliability of the 3D anthropometric measurements in the present study. The fact that the observer measurements were so similar across the 3D imaging methods suggests that antropometrical data obtained from the 3D systems used in this study (CBCT, laser surface scanner and stereo-photogrammetry) are capable of being combined or compared statistically. Thus, the potential for large, multicentre collaborative studies to investigate craniofacial surface morphology, despite the fact that the same 3D imaging technology may not be available at all sites, can be considered viable.

6.5 Conclusion

The results of the present study validate the use of the Di3D stereo-photogrammetry system for indirect anthropometric measurements. Linear measurements on 3D soft tissue surface model made with the Minolta Vivid 900 laser scanner, KaVo 3D exam CBCT scanner and Di3D stereo-photogrammetry system are accurate when compared with direct calliper measurements. Therefore, the measurements recorded by all three 3D systems appear to be extremely accurate and very reliable for research and clinical use. There were also no clinical differences between the 3D techniques suggesting that data obtained from these systems maybe combined for future research. By analyzing human remains via 3D models, forensic anthropologists can

construct biological profiles using precise and accurate metrical data to determine key aspects of identity.

6.6 Reference

1. Farkas LG, Deutsch CK. Anthropometric determination of craniofacial morphology. Am J Med Genet. 1996;65:1-4
2. Deutsch CK, Farkas LG. Quantitative methods of dysmorphology diagnosis. In: Farkas LG, ed. Anthropometry of the Head and Face. New York: Raven Press; 1994;151-158
3. Sholts SB, Wärmländer SKTS, Flores LM, Miller KWP, Walker PL. Variation in the measurements of cranial volume and surface area using 3D laser scanning technology. J Forensic Sci. 2010 Apr 8. [Epub ahead of print]
4. Farkas LG. Anthropometry of the Head and Face. New York: Raven Press, 1994
5. Wong JY, Oh AK, Ohta E, Hunt AT, Rogers GF, Mulliken JB, Deutsch CK. Validity and reliability of 3D craniofacial anthropometric measurements. Cleft Palate Craniofac J. 2008;45:232-239
6. Hajeer MY, Millett DT, Ayoub AF, et al. Applications of 3D imaging in orthodontics: Part 1. J Orthod 2004;31:62-70
7. Al-Omari I, Millett DT, Ayoub AF. Methods of assessment of cleft-related facial deformity: A review. Cleft Palate Craniofac J 2005;42:145-156
8. Weinberg SM, Naidoo S, Govier DP, Martin RA, Kane AA, Marazita ML. Anthropometric Precision and Accuracy of Digital Three-Dimensional Photogrammetry: Comparing the Genex and 3dMD Imaging Systems with One Another and with Direct Anthropometry. J Cranio fac surg. 17; 2006: 477-483
9. Karas BV, Beaubien HF. Three-dimensional laser scanning of cultural heritage: the deer stones of Mongolia. Scanning 2006;28(3):187-188
10. Park H-K, Chung J-W, Kho H-S. Use of hand-held laser scanning in the assessment of craniometry. Forensic Sci Int 2006;160:200-206
11. Friess M, Marcus LF, Reddy DP, Delson E. The use of 3D laser scanning techniques for the morphometric analysis of human facial shape variation. BAR Int Series 2002;1049:31-35
12. De Angelis D, Sala R, Cantatore A, Grandi M, Cattaneo C. A new computer-assisted technique to aid personal identification. Int J Legal Med. 2009:123:351-356
13. Yoshino M, Matsuda H, Kubota S, Imaizumi K, Miyasaka S. Computer-assisted facial image identification system using a 3-D physiognomic range finder. Forensic Sci Int. 2000;109:225-237
14. Baca DB, Deutsch CK, D'Agostino RB. Correspondence between direct anthropometry and structured light digital measurement. In: Farkas LG, ed. Anthopometry of the Jacobs RA. Plastic Surgery Educational Foundation DATA Committee. Threedimensional photography. Plast Reconstr Surg. 2000;107:276-277

15. Weinberg SM, Kolar JC. Three-dimensional surface imaging: limitations and considerations from the anthropometric perspective. J Craniofac Surg. 2005;16:847-851
16. Aldridge K, Boyadjiev SA, Capone GT, DeLeon VB, Richtsmeir JT. Precision and error of three-dimensional phenotypic measures acquired from 3dMD photogrammetric images. Am J Med Genet. 2005;138:247-253
17. Al-Omari I, Millett DT, Ayoub A, Bock M, Ray A, Dunaway D, Crampin L. An appraisal of three methods of rating facial deformity in patients with repaired complete unilateral cleft lip and palate. Cleft Palate Craniofac J.2003;40:530-537
18. Weinberg SM, Scott NM, Neiswanger K, Brandon CA, Marazita MA. Digital three-dimensional photogrammetry: evaluation of anthropometric precision and accuracy using a Genex 3D camera system. Cleft Palate Craniofac J. 2004;41:507-518
19. Head and Face. New York: Raven Press; 1994:235-238
20. Khambay B, Nairn N, Bell A, Miller J, Bowman A, Ayoub AF. Validation and reproducibility of a high-resolution tree-dimensional facial imaging system. Br J Oral Maxillofac Surg. 2008;46:27-32
21. Winder RJ, Darvann TA, McKnight W, Magee JDM, Ramsay-Baggs P. Technical validation of the Di3D stereo-photogrammetry surface imaging system. Br J Oral Maxillofac Surg.2008;46:33-37
22. Damstra J, Fourie Z, Huddleston Slater JJR, Ren Y. Accuracy of linear measurements from cone-beam computed tomography-derived surface models of different voxel sizes. AJO-DO 2010;137:16.e1-16.e6
23. Ward RE, Jamison PL. Measurement precision and reliability in craniofacial anthropometry: implications and suggestions for clinical applications. J Craniofac Genet Dev Biol. 1991;11:156-164
24. Jamison PL, Ward RE. Brief communication: measurement size, precision, and reliability in craniofacial anthropometry: bigger is better. Am J Phys Anthropol. 1993;90:495-500
25. Fourie Z, Damstra J, Gerrits PO, Ren Y. Accuracy and Reliability of Facial Soft Tissue Depth Measurement using Cone Beam Computed Tomography. For Sci Int. 2010; [epub before publication]
26. Bailey RC, Byrnes J. A new, old method for assessing measurement error in both univariate and multivariate morphometric studies. Syst Zool. 1990;39:124–130
27. Tanner JM, Weiner JS. The reliability of the photogrammetric method of anthropometry, with a description of a miniature camera technique. Am J Phys Anthropol.1949;7:145-186
28. Guyot L, Dubuc M, Richard O, et al. Comparison between direct clinical and digital photogrammetric measurements in patients with 22q11 microdeletion. Int J Oral Maxillofac Surg.2003;32:246-252
29. Farkas LG, Tompson BD, Phillips JH, et al. Comparison of anthropometric and cephalometric measurements of the adult face. J Craniofac Surg.1999;10:18-25

30. Budai M, Farkas LG, Tompson B, et al. Relation between anthropometric and cephalometric measurements and proportions of the face of healthy young white adult men and women. J Craniofac Surg.2003;14:154-161
31. Meintjes EM, Douglas TS, Martinez F, et al. A stereophotogrammetric method to measure the facial dysmorphology of children in the diagnosis of fetal alcohol syndrome. Med Eng Phys.2002;24:683-689
32. Aung SC, Ngim RC, Lee ST. Evaluation of the laser surface scanner as a measuring tool and its accuracy compared with direct facial anthropometric measurements. Br J Plast Surg.1995;48:551-558
33. Losken A, Seify H, Denson DD. Validating three-dimensional imaging of the breast. Ann Plast Surg 2005;54:471-476
34. Hajeer MY, Ayoub AF, Millett DT, et al. Three-dimensionalimaging in orthognathic surgery: The clinical application of a new method. Int J Adult Orthod Orthognath Surg. 2002;17:318-330
35. Foong KWC, Sandham A, Ong SH, et al. Surface laser scanning of the cleft palate deformity: Validation of the method. Ann Acad Med Singapore.1999;28:642-649
36. Brooke-Wavell K, Jones PR, West GM. Reliability and repeatability of 3-D body scanner (LASS) measurements compared to anthropometry. Ann Hum Biol 1994;21:571- 577
37. Kau CH, Richmond S. Three-dimensional analysis of facial morphology surface changes in untreated children from 12 to 14 years of age. Am J Orthod Dentofacial Orthop 2008; 134: 751-60
38. Hassan B, Van der Stelt P, Danderink G. Accuracy of three-dimensional measurements obtained from cone beam computed tomography surface-rendered image for cephalometric analysis: influence of patient scanning position. Eur J Orthod 2009;31:129-34
39. Ghoddousi H, Edler R, Haers P, Wertheim D, Greenhill D. Comparison of three methods of facial measurements. Int J Oral Maxillofac Surg. 2007;36:250-258.
40. Ayoub AF, Siebert P, Moos KF, Wray D, Urquhart C, Niblett TB. A vision based three-dimensional capture system for maxillofacial assessment and surgical planning. Br J Oral Maxillofac Surg. 1998;36:353-357
41. Ayoub A, Garrahy A, Hood C, White J, Bock M, Sibert JP, Spencer R, Ray A. Validation of a vision-based, three-dimensional facial imaging system. Cleft Palate Craniofac J. 2003;40:523-529
42. Burk RO, Rohrschneider K, Takamoto T, Volcker HE, Schwartz B. Laser scanning tomography and Sterio-photogrammetry in three-dimensional optic disc analysis. Graefes Arch Clin Exp Opthalmol.1993:231:193–198
43. Grieshaber BM, Osborne DL, Doubleday AF, Kaestle FA. A pilot study into the effects of X-ray and computed tomography exposure on the amplification of DNA from bone. J Archaeol Sci 2008;35(3):681–7
44. Kusnoto B, Evans CA. Riability of a 3D surface laser scanner for orthodontic applications. Am J Orthod Dentofac Orthop.2002; 122:342-8

45. Baik HS, Lee HJ, Lee KJ. A proposal for soft tissue landmarks for craniofacial analysis using 3-dimensional laser scan imaging. World J Orthod.2006;7:7-14
46. Christensen AM. The impact of Daubert: implications for testimony and research in forensic anthropology (and the use of frontal sinuses in personal identification). J Forensic Sci.2004;49(3):1–4
47. Rogers T, Allard TT. Expert testimony and positive identification of human remains through cranial suture patterns. J Forensic Sci.2004;49(2): 203–207

Chapter 7

Accuracy and Reliability of Facial Soft Tissue Depth Measurements using Cone Beam Computer Tomography

This chapter is based on the following publication:

Fourie Z, Damstra J, Gerrits PO, Ren Y. Accuracy and Reliability of Facial Soft Tissue Depth Measurements using Cone Beam Computer Tomography. Forensic Sci Int 2010; 199: 9–14

Abstract

It is important to have accurate and reliable measurements of soft tissue thickness for specific landmarks of the face and scalp when producing a facial reconstruction. In the past several methods have been created to measure facial soft tissue thickness (FSTT) in cadavers and in the living. The conventional spiral CT is mostly used to determine the FSTT but is associated with high radiation doses. The cone beam CT (CBCT) is a relatively new computer tomography system that focuses on head and neck regions and has much lower radiation doses. The aim of this study is to determine the accuracy and reliability of CBCT scans to measure the soft tissue thicknesses of the face. Seven cadaver heads were used. Eleven soft tissue landmarks were identified on each head and a punch hole was made on each landmark using a dermal biopsy punch. The seven cadaver heads were scanned in the CBCT with 0.3 and 0.4 mm resolution. The FSTT at the 11 different sites (soft tissue landmarks) were measured using SimPlant-ortho volumetric software. These measurements were compared to the physical measurements. Statistical analysis for the reliability was done by means of the interclass coefficient (ICC) and the accuracy by means of the absolute error (AE) and absolute percentage error (APE). The intra-observer (0.976–0.999) and inter-observer (0.982–0.997) correlations of the CBCT and physical measurements were very high. There was no clinical significant difference between the measurements made on the CBCT images and the physical measurements. Increasing the voxel size from 0.4 to 0.3 mm resulted in a slight increase of accuracy. Cone beam CT images of the face using routine scanning protocols are reliable for measuring soft tissue thickness in the facial region and give a good representation of the facial soft tissues. For more accurate data collection the 0.3 mm voxel size should be considered.

7.1 Introduction

The main purpose of any forensic facial approximation is to recreate the face of a deceased individual at the time of death based on his/her skull. The most extensive and detailed post-mortem data are useless without any link to the ante-mortem data. In these cases, forensic facial approximation can be considered as a last resort to identify the deceased [1]. Forensic facial reconstruction is a mixture of science and art in which the reconstruction of faces on skulls is attempted for the purpose of individual identification [2].

For correct facial reconstruction of the human face it is necessary to know the average facial soft tissue thickness of specific sites on the face. This requires establishing a database of soft tissue thickness related to age, sex, race and ethnicity. Since the first attempts in the late 19th century, manual or computer-aided reconstruction techniques have been developed [1], [3], [4], [5], [6] and [7]. There are two basic methods [8], [9] and [10] of modelling faces: a morphoscopic method using an anatomical approach of reconstructing the musculature, fat and skin [3], [8] and [9] and a morphometric method which rests heavily on the use of average facial soft tissue depth measurements that have been gathered by various researchers [2], [3], [8], [9] and [11]. Studies into the soft tissue depth for the main ethnic groups have been carried out. The most often quoted are Rhine and Moore [12] for Caucasians; Suzuki [13] for Mongoloids and Rhine and Campbell [14] for the Negroids. Various other databases for smaller ethnical groups also exist [9], [12], [15] and [16]. Gender also plays a significant role in facial reconstruction. El-Mehallowi and Soliman [17] found a notable sexual dimorphism in facial soft tissue thickness among Egyptians. In contrast with the studies form Rhine and Campbell [14] and Suzuki [13], there was a significantly greater soft tissue thickness in the female Egyptian facial soft tissues compared to the male. Starbuck and Ward [18] found that the variations in weight (obese, normal, and emaciated) of a deceased individual may be an important contributor to the ability to achieve correct recognition of a reconstructed face. It appears that variation in the size of a face may be more important than facial configuration in identifying individuals [18]. Due to secular trends like immigration and the fact that the world's population are becoming more homogenized, the soft tissue databases should be updated constantly to ensure a good outcome of the facial reconstruction. The sample sizes of most of these FSTT studies were not very big because they were done on cadavers and invasive techniques were used. The less invasive the technique, the more individuals can be included and the more accurate the FSTT database will become.

Several methods have been created to measure FSST in cadavers and in the living [15]. Traditionally facial soft tissue measurements were studied using the needle

depth probing method on cadavers, but this method has its limitations [19]. Several imaging-based methods for measuring living facial soft tissue thickness have been reported [8]. These include lateral cephalometric radiography [20], computed tomography (CT) [2] and [8], ultrasound [17] and magnetic resonance imaging (MRI) [21].

A new generation of compact CT scanners has been developed specifically for imaging the head and neck region [22]. These scanners use a cone beam geometry which allows for better efficiency in X-ray photon utilization [23]. The advantages of the cone beam CT (CBCT) when compared to multislice CT include lower radiation dose, lower cost and high spatial resolution [24]. Due to these advantages, CBCT 3D imaging techniques have become popular and are used routinely in dentistry. To our knowledge, there is no study yet of the accuracy and reliability of the CBCT technology for the use of measuring facial soft tissue thickness.

Therefore, the purpose of this study was to determine the reliability and accuracy of soft tissue thickness measurements using Cone Beam Computed Tomography and the effects of slice thickness on the precision.

7.2 Materials and methods

Seven cadaver heads, supplied by the Department of Anatomy (University Medical Centre Groningen, Groningen, The Netherlands) were available for this study. The method as described by Rhine and Campbell [14], were used in this study. The soft tissue thickness was measured at 90° to the underlying bone over three midlines and eight lateral facial areas (Fig. 1). We used a method described by Kim et al. to ensure minimal distortion of the soft tissue at the sites between the physical measurement and the imaging measurements [8].

We used 10 points in this study (2 midline and 8 bilateral) as described by Kim et al. [8]. We also added soft tissue Pogonion to get an overall impression of the soft tissue thickness of the face. Therefore a total of 11 soft tissue sites were created on each head. The locations of the points can be seen in Table 1. The measurement sites were prepared as follows: a sterile disposable dermal biopsy punch (Stiefel, Brüchensrasse, D-63607, Wächtersbach, Germany) with a diameter of 4.00 mm was used to make a cylindrical hole down to the bone, on each of the landmark sites.

The operator made sure that no soft tissue was left on the base of the punch hole, so that it will not interfere with the physical measurement. After the punches were made the tissue was left overnight to return to normal thickness.

Figure I. *Schematic illustration of the landmarks and list of abbreviations.*

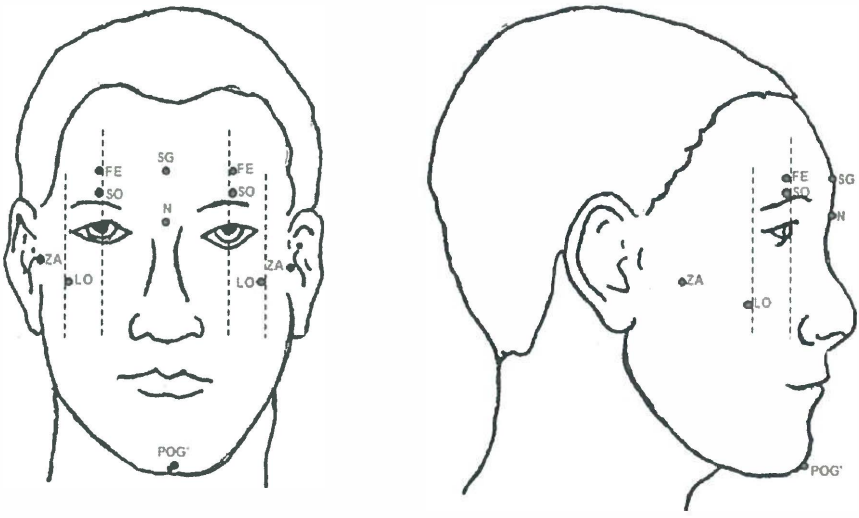

Abbreviation	Landmark	Definition
FE	Frontal eminence (left and right)	Centred on eye pupil, most anterior point of the forehead.
LO	Lateral orbit (left and right)	Lateral side of the eye, point on the zygomatic bone
N	Nasion	Midpoint of the fronto-nasal suture
SO	Supra-orbital (left and right)	Centred on eye pupil, just above the eyebrow
SG	Supra-glabella	Most anterior point on the midline
ZA	Zygomatic arch (left and right)	Maximum, most lateral curvature of the zygomatic bone

The physical measurements were made five times on each landmark by consensus of two operators (ZF and JD) with a digital calliper. This was regarded as the gold standard. The calliper had been previously modified by reducing the shaft diameter to permit insertion into the centre of the punch holes, and measure the depth of the punch holes. During the physical measurements, care has been taken not to distort the soft tissue while measuring the FSTT. The readouts were not visible to the observer during the actual measurements.

CBCT imaging was undertaken directly after making the physical measurements. For the scanning procedure the KaVo 3D exam (KaVo Dental GmbH, Bismabring,

Germany) CBCT scanner was used. The head was positioned and fixated in the scanner with the head facing forward and Frankfort horizontal parallel to the ground. The specimen was handled carefully to prevent distortion of the soft tissues. Importantly, the head was scanned with a 0.3 mm voxel size and 0.4 mm voxel size during the same session. For both voxel sizes a 17 mm field of view was used. The acquired CBCT DICOM (Digital Image and Communication in Medicine) images were saved to an external hard disc (LACIE 120MB hard disc) and then transferred to a personal laptop computer (Acer Aspire 5738ZG).

The DICOM images were then imported into SimPlant-ortho (Materialise Dental, Leuven, Belgium) and the reconstructed CT image of the cadavers were created. The landmarks (punch holes) were located on the axial slices (Fig. 2a) and measured by two operators (ZF, JD) separately during three sessions, each session a week apart. The measuring procedure was as following: a special analysis was created on SimPlant-ortho where a point was placed at the highest point on both sides of the punch hole and one on the bone surface in the middle of the punch hole. The computer then constructed a line between the two points on the skin surface, and measured the distance between the middle point of the line and the point on the bone surface (Fig. 2b). This measurement was then confirmed on the sagittal slice.

Statistical analysis

Means and standard deviations were calculated for the direct calliper and CBCT measurements. As a measure of reliability, the intraclass correlation coefficient (ICC) for absolute agreement based on a 2-way random effects analysis of variance (ANOVA) was calculated. ICC's of the repeated measurements tested the reliability of the direct calliper measurements. Intra-observer reliability of the CBCT measurements was determined by comparison of the repeated measurements of each examiner. Inter-observer reliability of the CBCT measurements was determined by comparison of the mean of the measurements between the two observers. The reliability of the CBCT measurements was determined by comparison CBCT and direct calliper measurements.

The accuracy of the CBCT measurements was expressed by means of the absolute error (AE) and absolute percentage error (APE). Absolute measuring error was defined as the CBCT measurement value subtracted by the reference value. The reference values were calculated as the mean of the direct calliper measurements while the CBCT values were determined by the mean of the CBCT measurements made by the two examiners. Absolute percentage error was calculated by means of the following equation: APE = 100 × (AME/reference value). All statistical analysis was performed with a standard statistical software package (SPSS version 16, Chicago, IL).

Figure 2 *Axial (a) and corresponding view of the punch hole on the supra orbital left (SO) that was used to measure the FSTT on the SimPlant-ortho volumetric software. Enlarged in (b): the punch hole with the highest points on both sides of the punch hole (A and B) and one on the bone surface (D) in the middle of the punch hole. The computer then constructed a line (AB) between the two points on the skin surface, and measured the distance between the middle point (C) of the line and the point on the bone surface (D).*

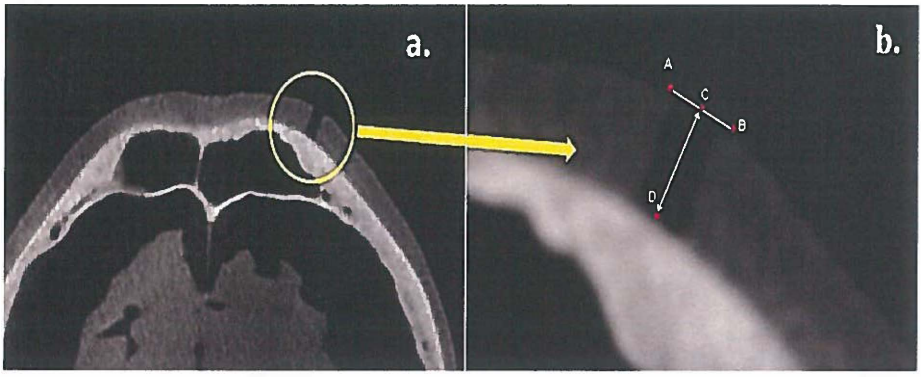

7.3 Results

Physical measurements with the digital caliper determined by consensus of the two observers were very reliable (0.975–0.997). The CBCT measurements were found to be very reliable. The intra-observer reliability for the 0.3 voxel size (0.972–0.999) and for the 0.4 voxel size (0.980–0.998) was high. The inter-observer (0.980–0.998) and inter-observer (0.982–0.997) reliability for both groups was also very high. The CBCT measurements, the 0.3 voxel size (0.985–0.996) as well as the 0.4 voxel size (0.967–0.998) also were found to be very reliable when compared to the physical measurements.

Accuracy of the measurements was determined by the AE (absolute error) and APE (absolute percentage error) ([Table 2] and [Table 3]). The mean, standard deviation and confidence intervals of the AE and APE were calculated and confirmed the accuracy of the measurements (Table 4). The mean AE of all seven subjects was very small for the 0.3 voxel size (0.25 ± 0.17 mm) and for the 0.4 voxel size (0.29 ± 0.24 mm). The APE was 3.66 ± 2.53% for the 0.3 voxel size and 4.19 ± 3.26% for the 0.4 voxel size.

Table I Reliability (ICC) of the direct calliper measurements, the 0.3 voxel and the 0.4 voxel CBCT measurements and the direct calliper measurements compared to the CBCT measurements.

subject number	direct caliper measurement (reference)	CBCT measurements							
		0.3 voxel Size				0.4 voxel Size			
		intra-observer		inter-observer	reference vs. CBCT	intra-observer		inter-observer	reference vs. CBCT
		observer 1	observer 2	1 vs. 2		observer 1	observer 2	1 vs. 2	
1	0.995	0.997	0.992	0.990	0.990	0.995	0.988	0.982	0.992
2	0.987	0.998	0.996	0.998	0.996	0.994	0.995	0.993	0.998
3	0.980	0.993	0.994	0.995	0.987	0.992	0.991	0.997	0.990
4	0.993	0.997	0.993	0.996	0.995	0.994	0.984	0.989	0.991
5	0.975	0.990	0.976	0.989	0.985	0.994	0.980	0.985	0.967
6	0.997	0.997	0.999	0.997	0.996	0.997	0.997	0.996	0.995
7	0.976	0.972	0.987	0.980	0.989	0.998	0.990	0.989	0.992

Table II Absolute error (mm) of the 0.3 and 0.4 voxel groups.

voxel size	measurement	subject Number							mean	SD
		1	2	3	4	5	6	7		
0.3	1.(SG)	0.00	0.01	0.21	0.23	0.26	0.08	0.16	0.16	0.10
	2.(FE-R)	0.11	0.18	0.12	0.03	0.22	0.42	0.22	0.19	0.12
	3.(FE-L)	0.07	0.02	0.20	0.00	0.32	0.29	0.22	0.16	0.13
	4.(SO-R)	0.41	0.18	0.44	0.61	0.37	0.17	0.18	0.34	0.17
	5.(SO-L)	0.49	0.15	0.11	0.16	0.11	0.15	0.36	0.22	0.15
	6.(N)	0.26	0.39	0.16	0.02	0.44	0.31	0.21	0.26	0.14
	7.(ZA-R)	0.13	0.33	0.54	0.19	0.27	0.03	0.44	0.28	0.18
	8.(ZA-L)	0.29	0.26	0.43	0.60	0.06	0.02	0.00	0.24	0.23
	9.(LO-R)	0.58	0.15	0.24	0.45	0.32	0.17	0.40	0.33	0.16
	10.(LO-L)	0.76	0.24	0.15	0.22	0.12	0.24	0.08	0.26	0.23
	11.(POG')	0.19	0.18	0.64	0.05	0.11	0.82	0.45	0.35	0.29
0.4	1.(SG)	0.07	0.09	0.31	0.04	0.21	0.07	0.27	0.15	0.11
	2.(FE-R)	0.19	0.27	0.03	0.14	0.23	0.32	0.12	0.19	0.10
	3.(FE-L)	0.02	0.00	0.20	0.13	0.71	0.36	0.32	0.25	0.25
	4.(SO-R)	1.06	0.05	0.33	0.92	0.35	0.12	0.11	0.42	0.41
	5.(SO-L)	0.61	0.20	0.12	0.30	0.18	0.04	0.16	0.23	0.19
	6.(N)	0.25	0.45	0.01	0.19	0.40	0.50	0.28	0.30	0.17
	7.(ZA-R)	0.64	0.19	0.49	0.95	0.60	0.03	0.48	0.48	0.30
	8.(ZA-L)	0.23	0.26	0.23	0.08	0.00	0.23	0.05	0.15	0.11
	9.(LO-R)	0.79	0.46	0.10	0.44	0.24	0.48	0.27	0.40	0.22
	10.(LO-L)	0.61	0.11	0.03	0.19	0.54	0.05	0.37	0.27	0.24
	11.(POG')	0.13	0.14	0.6	0.21	0.14	0.85	0.40	0.35	0.28

Table III Absolute percentage error (%) of the 0.3 and 0.4 voxel groups

voxel size	measurement	subject number							mean	SD
		1	2	3	4	5	6	7		
0.3	1.(SG)	0.00	0.27	4.73	4.43	4.28	1.74	2.91	2.62	1.99
	2.(FE-R)	1.88	5.08	2.55	0.67	3.72	9.79	6.20	4.27	3.08
	3.(FE-L)	1.15	0.51	4.10	0.00	6.08	6.47	5.98	3.47	2.85
	4.(SO-R)	4.66	2.68	7.99	9.52	6.53	3.26	3.24	5.41	2.65
	5.(SO-L)	5.80	2.23	1.93	3.51	1.81	2.28	7.71	3.61	2.29
	6.(N)	3.48	8.70	4.25	0.34	6.64	6.18	5.30	4.98	2.66
	7.(ZA-R)	1.32	5.28	7.36	2.16	2.94	0.25	6.70	3.72	2.75
	8.(ZA-L)	2.33	3.87	6.65	8.19	0.73	0.16	0.00	3.13	3.25
	9.(LO-R)	4.64	1.46	2.83	3.73	3.07	1.39	5.71	3.26	1.59
	10.(LO-L)	6.83	2.46	1.58	1.92	1.92	1.97	1.03	2.53	1.95
	11.(POG')	1.48	1.69	6.34	0.71	1.39	5.47	5.62	3.24	2.43
0.4	1.(SG)	1.02	2.36	6.98	0.77	3.46	1.52	4.91	3.00	2.28
	2.(FE-R)	3.25	7.08	0.64	3.11	3.89	7.46	3.38	4.11	2.39
	3.(FE-L)	0.33	0.00	4.10	2.95	13.49	8.03	8.70	5.37	4.93
	4.(SO-R)	12.05	0.75	6.00	14.36	6.17	2.30	1.98	6.23	5.22
	5.(SO-L)	7.22	2.89	2.11	6.58	2.96	0.61	3.22	3.66	2.39
	6.(N)	3.35	9.12	0.27	3.20	6.04	9.96	8.00	5.70	3.57
	7.(ZA-R)	6.52	2.95	6.68	10.80	6.52	0.25	7.31	5.86	3.37
	8.(ZA-L)	1.85	4.03	3.56	1.09	0.00	1.87	0.75	1.88	1.46
	9.(LO-R)	6.31	4.68	1.18	3.65	2.30	3.93	3.65	3.67	1.64
	10.(LO-L)	5.48	1.14	0.32	1.66	8.64	0.41	4.75	3.20	3.16
	11.(POG')	1.01	1.29	5.94	2.99	1.77	5.67	4.99	3.38	2.13

Table IV	Summary of the absolute error (mm) and absolute percentage error (%) of the 0.3 and 0.4 voxel groups. (CI = 95% confidence interval)			
error measurement	**voxel Size**	**mean**	**SD**	**CI**
AE (mm)	0.3	0.25	0.17	0.21 – 0.29
	0.4	0.29	0.24	0.24 – 0.34
APE (%)	0.3	3.66	2.53	1.94 – 3.06
	0.4	4.19	3.26	3.94 – 4.44

7.4 Discussion

Facial soft tissue reconstruction from skulls is of great importance in anthropological and forensic sciences. For correct facial reconstruction of the human skull it is necessary to know the average facial soft tissue thickness of specific sites of the face. This requires establishing a database of soft tissue thickness related to age, sex, race, ethnicity [8] and weight [18]. In the past this required direct physical soft tissue thickness measurements on cadavers [12]. Kim et al. states that this approach has been limited due to the large number of cadavers and the labour involved [8]. He also mentions that the results of the measurements have been questionable, because of the difficulty to measuring perpendicular to the skin surface. In this present study we experienced the same difficulty with puncturing and measuring perpendicular to the skin surface. This was made difficult because of the uneven nature of the underlying bone. Therefore the measurements were repeated five times by two observers to minimize the measuring error. Kim et al. had an additional problem in the hardness of the skin that prevented the manual manipulation of the skin during measurement [8]. This was not the case in the present study as we used fresh cadavers that made it easier to manipulate the areas that could interfere with the calliper while taking the measurement. In contrast a fixed cadaver was used in the study by Kim and co-workers. Care was taken not to distort the measuring site itself as it could influence the measurement. Kim et al. [8] selected a series of 6 anatomic sites out of a list of anatomical sites advocated by Rhine and Campbell [14]. They rejected most of the sites because in some areas with thick fatty tissues it was not possible to lace a puncture perpendicular to the skin surface or to reproducibly place the callipers for physical measurements [8]. In this present study we used same anatomical sites as recommended by Kim et al. [8]. We also added soft tissue Pogonion to get an overall impression of the soft tissue thickness of the face. The extra

landmark (soft tissue Pogonion) added in this study proved to be very reliable with a very low AE for both scans.

To avoid the limitations of the direct soft tissue measurement, various imaging modalities have been used [1], [4], [8] and [9]. In earlier studies the lateral cephalogramic radiographs to collect data on soft tissue depths in the living [19]. But because of the ill effects of the X-rays and superimposition of various anatomic structures in the film it was not often used [15]. New CBCT scanners, used specifically for imaging the head and neck region [25], have become increasingly popular and have opened new possibilities. The dose of CBCT is relatively low. It can be as little as 100 times less than the dose received from comparable medical CT images [26].

CBCT images of the face using routine scanning protocols are a reliable method of measuring the soft tissue thickness in the facial region and give a good representation of the facial soft tissues. Farman et al. reported that the soft tissue definition with CBCT is sufficient to determine air/soft boundaries, including the patient's lateral profile, greater clarity of soft tissue definition could improve the assessment of bulk and insertion patterns of the maxillofacial musculature [27]. Moerenhout et al. used phantom heads to determine the 3D surface accuracy of soft tissue acquired form a CBCT scan of a mannequin head and using two commercial 3D image processing software programs [28]. They found that 3D surface of the facial soft tissues segmented and reformatted form a CBCT scan proved to be accurate [28]. Heyland et al. stated that integration of flat panel detectors in mole CBCT systems results in an improved visualization of soft tissues in cadavers [29]. CBCT visualizes high-contrast in sufficient quality with a remarkable low level of metal artefacts. However, they stated that the image quality of corresponding CT and MRI proved to be superior in most of the evaluated criteria [29].

The results of this study suggest that CBCT images can be used to derive accurate measurements that can form the basis for establishing a soft tissue thickness database for any population. Kim et al. found the same with the MRI in 2005 [8]. The absolute error (AE) and absolute percentage error (APE) in the 0.4 voxel size group (0.29 ± 0.24 mm and 4.19 ± 3.26%) were slightly higher when compared to the 0.3 voxel size group (0.25 ± 0.17 mm and 3.66 ± 2.53%). This can be explained by the differences in voxel size that influence the resolution of the image as the effect of this resolution on subsequent analysis might influence the reproducibility and accuracy of measurements in CBCT [27]. Hassan et al. found the same with their study done on 25 patients. They stated that the very small voxel sizes (0.2, 0.3) resulted in a very large surface mesh

model, which made it difficult to process and make an accurate 3D surface model. With the bigger voxel sizes (0.6, 0.9, 1.2), they experienced a loss of relevant detail [30]. This suggests that, for more fine and accurate data collection of the facial soft tissue thickness form the CBCT, the 0.3 voxel size scan should be considered. In this study we investigated the 0.3 and 0.4 voxel sizes because the KaVo 3D exam CBCT scanner can only scan 0.3 and 0.4 voxel sizes on the 17 cm field of view, although other scanners might be able to scan the full face at a smaller voxel size. It might be kept in mind that the radiation exposure might be significantly higher when a scan is made with a view smaller voxel size in a 17 cm field of view.

This study confirms the accuracy and reliability of soft tissue measurements are possible with CBCT, therefore it permits the use of existing images made of patients that were scanned, e.g. dentistry. This will prevent the need for large numbers of cadavers and facilities to carry out the measurements. Most imaging centres now store their images on servers or a picture archiving and communications system (PACS). With proper and secure access, this CBCT data can be readily accessed from inside or outside the institution in real time, permitting use of a large file of images from which to create a database of soft tissue thickness from any population [8].

7.5 Conclusions

An image obtained of the face using routine scanning protocols with the CBCT is a reliable method of measuring the soft tissue thickness in the facial region. It also gives a good representation of the facial soft tissues. The data confirmed that CBCT soft tissue measurements can be used to create a database of soft tissue thickness.

The 0.3 mm slice thickness gives an accurate data collection of the soft tissue. There is a slight but definite difference in the facial soft tissue thickness measurements. For more fine and accurate data collection of the facial soft tissue thickness form the CBCT, the 0.3 voxel size scan is recommended.

7.6 References

1. S. De Greef, P. Cleas, D. Vandermeulen, W. Mollemans, P. Suetens, G. Willems. Large-scale in-vitro Caucasian facial soft tissue thickness database for craniofacial reconstruction. Forensic Sci Int. 159S (2006) S136-S146

2. V.M. Phillips, N.A. Smuts, Facial reconstruction: utilization of computerized tomography to measure facial tissue thickness in a mixed racial population, Forensic Sci. Int. 83 (1996) 51–59
3. M. Gerasimov, The Face Finder, J.B. Lippencott Co., Philadelphia, PA,1971.
4. W.A. Aulsebrook, M.Y. Iscan, J.H. Slabbert, P. Becker, Superimposition and reconstruction in forensic facial identification: a survey, Forensic Sci. Int. 75 (1995) 101–120
5. J. Prag, R. Neave, Making Faces, British Museum Press, London, 1997.
6. K.T. Taylor, Forensic Art and Illustration, CRC Press, Boca Raton, 2001.
7. C. Wilkinson, Forensic Facial Reconstruction, Cambridge University Press, Cambridge, 2004
8. D.K. Kim; A. Ruprecht, G. Wang, J.B. Lee, D.V. Dawson, M.W. Vannier. Accuracy of facial sort tissue thickness measurements in personal computer-based multiplanar reconstructed computed tomography images. Forensic Sci Int.155(2005)28-34.
9. W.A. Aulsebrook, P.J. Becker, M Y. Iscan. Facial soft-tissue thicknesses in the adult male Zulu. Forensic Sci Int. 79 (1996) 83-101
10. W.A. Aulsebrook, J.H.J van Rensburg. An evaluation of two techniques used for facial reconstruction in forensic anthropology. Paper presented at the 16th annual congress of the Anatomical Society of South Africa. S. Afr. J. Sci., 82 (1986) 448 (abstract).
11. W.M. Krogman, M.Y. I'scan, The Human Skeleton in Forensic Medicine, Charles C. Thomas, Springfield, IL, 1986
12. J.S. Rhine, C.E. Moore, Facial reproduction tables of facial tissue thicknesses of American Caucasoids in forensic anthropology. Maxwell Museum Techn. Ser. No.1, Albuquerque. NM 1982
13. K. Suzuki, On the thickness of the sot parts of the Japanese face. J. Anthropol. Soc. Nappon, 60 1948 7/11
14. J.S. Rhine, H.R. Campbell. Thickness of facial tissue in American Blacks. J Forensic Sci 24(1980) 847-858
15. D. Sahni, Sanjeev, G. Singh, I. Jit, P. Singh. Facial soft tissue thickness in Northwest Indian adults. Forensic Sci Int.176(2008)137-146
16. R. Helmer, Scha¨delidentifizierung durch elektronische bildmischung, Kriminalistik Verlag GmbH, Heidelberg, 1984
17. I.H. El-Mehallawi, E.M. Soliman, Ultrasonic assessment of facial soft tissue thicknesses in adult Egyptians, Forensic Sci.Int. 117 (2001) 99–107
18. J.M. Starbuck, R.E. Ward. The affect of tissue depth variation on craniofacial reconstructions. Forensic Sci. Int. 172(2007)130-136

19. S. De Greef, P. Claes, W. Mollemans, M. Loubele, D. Vandermeulen, P. Suetens, G. Willems, Semi-automated ultrasound facial soft tissue depth registration: method and validation, J. Forensic Sci. 50 (2005)
20. R.M. George, The lateral craniographic method of facial reconstruction, J. Forensic Sci. 32 (1987) 1305–1330
21. E.W. Lam, A.G. Hannam, W.W. Wood, J.S. Fache, W. Watanabe, Imaging orofacial tissues by magnetic resonance, Oral Surg. Oral Pathol. 68 (1989) 2–8
22. P. Sakovic. Cone beam computed tomography in craniofacial imaging. Orthod Draciofac Res. 6 (2003) 179-182
23. V. Kumar, J.B. Ludlow, A. Mol, L. Cevidanes. Comparison of conventional and cone beam CT synthesized cephalograms. Dentomaxillofac Radiol. 36 (2007) 263-269
24. V. Kumar, J. Ludlow, L.H.S. Cevidanes, A. Mol. In Vivo comparison of conventional and Cone Beam CT Synthesized Cephalograms. Angle. 78 (2005) 873-878
25. P. Sukovic. Cone beam computed tomography in craniofacial imaging. Orthod. Craniofac Res. 6(2003) 179-182
26. J.B. Ludlow, L.E. Davies – Ludlow, S.L. Brooks. Dosimetry of two extraoral direct digital imaging devices: NewTom cone beam CT and Orthophos Plus DS panoramic unit. Dentomoxillofac Radiol 32(2003) 229-234
27. A.G. Farman, W.C. Scarfe. Development of imaging selection criteria and procedures should precede cepalometric assessment with cone-beam computed tomography. AJO-DO.130 (2006) 257-265
28. B.A.M.M.L. Moerenhout, F. Gelaude, G.R.J. Swennen, J.W. Casselman, J. van der Sloten. Accuracy and repeatability of cone beam computed tomography (CBCT) measurements used in the determination of facial indices in the laboratory setup. J Craniomaxillofac Surg.37 (2009) 18-23
29. M. Heyland, P. Pohlenz, M. Blessmann, C.R.Habermann, L. Oesterhelweg, P.C. Bergemann, C. Schmidgunst, F.A.S. Blake, K. Puschel, R. Schmelzle, D. Schulze. Cervical soft tissue imaging using a mobile CBCT scanner with a flat panel detector in comparison with corresponding C and MRI data sets. Oral Surg Oral Med Oral Pathol Oral Radiol Endod. 104(2007)814-820
30. B. Hassan, P. C. Souza, R. Jacobs, S. De Azambuja Berti, P. Van der Stelt. Influence of scanning and reconstruction parameters on quality of three-dimensional surface models of the dental arches form cone beam computed tomography. Clin Oral Invest. 2009 (Epub ahead of print)

Chapter 8

General discussion

8.1 Introduction

The use of 3D records in facial imaging has increased significantly over the past decade.[1-4] Traditional 2D records have been gradually replaced by 3D images. In treatment planning more emphasis has been placed on the 3D virtual image [4,5] and soft-tissue aesthetics.[6] This paradigm shift in treatment philosophies also means that many clinicians plan their treatment objectives from the facial profile, placing importance on the soft tissues of the face to determine the limitations of orthodontic treatment. From the perspective of function, stability and aesthetics the orthodontist must plan the treatment within the limits of the soft tissue adaptations and contours.[7] 3D facial images can give the clinician information on soft tissues with a more accurate representation of the facial morphologies [8-10] and can be used to better understand, compare,[3,11] and predict treatment outcomes before and after orthodontic treatment.[12-14] Among all the different 3D methods, CBCT has become increasingly popular. It has been developed specifically for the maxillofacial region as a result of dramatic advances in computer and electronic technology.

The results of this thesis have implications for several different disciplines including anthropometry, plastic and reconstructive surgery, neurosurgery, maxillofacial surgery, orthodontics and forensic science in which 3D facial images are important. In the following discussion, the general aims and specific research aims described in Chapter 1 will be addressed in relation to the main results. In addition, the clinical relevance of the findings and future perspectives regarding CBCT imaging and its application in different fields will be explored.

8.2 Segmentation process

The introduction of maxillofacial CBCT equipment provides clinicians with an opportunity to generate 3D volumetric renderings, using relatively inexpensive third-party personal computer-based software.[15] The importance of having a segmentation engine in the software package is twofold. First, it allows the user to export anatomic models in a non-proprietary format. This information can be used in research and will always be accessible regardless of constantly changing software applications.[16] The second advantage is the option of loading anatomic modes in a non-proprietary format into the imaging software interface, which allows combining different modalities with the CBCT images.[16]

At present, 3D volumetric representation of a structure depends on accurate segmentation (Figure 1). Our results suggest that probably one of the most significant

factors determining the accuracy of the 3D model generated from a CBCT is likely to be the differences between the threshold dependant methods of segmentation. Although, the software has standard pre-set thresholds values for bone, soft tissue and teeth, the value can be adjusted by the operator to enhance the quality of a certain region of interest. This makes the method subjective. The threshold value in the mandible was less than in the maxilla. The bone thickness vary a lot in the maxilla, especially in the palate and tuberosity regions where significant bone dehiscence and fenestration artefacts in the 3D model might be created.[17] Therefore, during segmentation, even choosing a single threshold value for a single jaw is almost impossible.

In this thesis we compared the segmentation performed by the commercial company and that by a clinician (Table 1). Firstly, the 3D models derived from these segmentation protocols were superimposed over the laser surface model using an automated surface matching algorithm based method. The differences were determined between the models by the computer. Secondly, standard linear and angular measurements made on these models were compared. In both methods, the biggest deviation was found at the condylar area and the lingual part of the mandible. The inaccuracies of condylar segmentations might be due to the lower density of the bone in the condylar area compared to the rest of the mandible, a lot of overlapping bony structures and the difficulty to separate the condyle with the discus articulare during segmentation. The inaccuracies of the lingual area might be a result of the scattering of the beam and artifacts caused when the beam passes through the buccal cortical bone during the acquisition.

The image artefacts associated with the CBCT affect the segmentation accuracy which directly influences the landmark identification and the resulting measurements.[25] This artifact might have a clinical implication for 3D planning of surgical drilling guides for implant placement, where minimal transfer error from preoperative planning can result in significant errors to the surgical field.[18] These factors can be controlled by using the same CBCT scanner and scanning parameters as proposed in this thesis. With all these in mind the additional cost of CS models seems to be justified to produce a more accurate surface model, if needed for high precision.

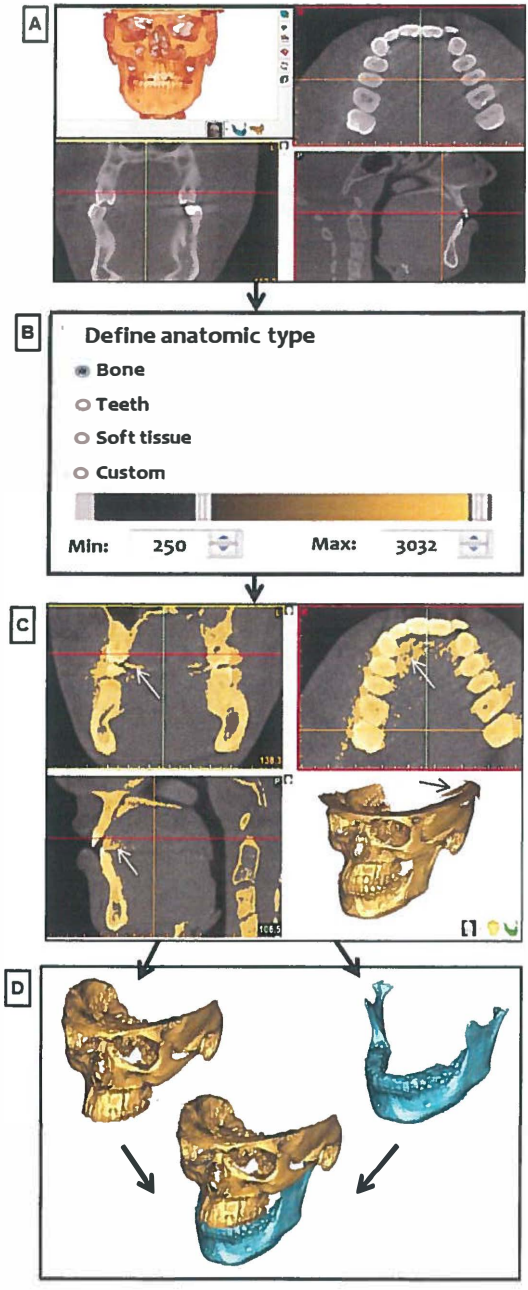

Figure 1: *Schematic illustration of the threshold based segmentation using SimPlant® Ortho software program.*

(A) Volume rendering,

(B) Threshold value selection (operator can manually adjust the threshold),

(C) Scattering and non-relevant structures removed (indicated by arrows),

(D) After maxilla is segmented, the process is repeated for mandible. A complete 3D surface model is ready for surgical planning.

Table 1	Advantages, disadvantages and possible applications	
	Commercial segmentation	**Segmentation done by the clinician**
Advantages	- Accuracy of the segmentation. - Time-saving for the clinician - Done by professionally trained technicians. - Smoother surface characteristics, thus more presentable towards the patients.	- Less costly - Clinician will gain more knowledge of the anatomy by doing this himself
Disadvantages	- Costly - Technicians do not have the knowledge of the anatomy and might remove anatomical structures unnecessarily.	- Clinician needs extra schooling/ training - Time consuming - Less accurate - Expensive specialist software needed.
Suggested applications	- Diagnosis of cleft palate patients - Pre-surgical planning for complex orthognatic surgery. - Fabricating a drilling guide for implant placement. - Pre-surgical dental implant placement, especially near the mandibular nerve. - Fabricating/rapid prototyping of a surgical splint - Examination of the TMJ - Producing models on which facial prostheses are being made.	- Localized assessment of impacted canines or other impacted teeth. - Determination of possible root resorption especially due to impacted canines. - Localizing facial asymmetries. - Assessment of post-surgical results

8.3 Accuracy of measurements and confidence intervals

Because CBCT images are often used for pre-surgical planning, the accuracy is of utmost importance. Sufficiently accurate CBCT information will prevent surgical inaccuracies.[19] Unfortunately, an accurate CBCT image does not always guarantee accurate measurements. In this thesis the smallest detectable difference (SDD) was used to look at the measurement error in 3D cephalometry. Each 3D landmark has its own unique configuration and envelope of error which contributes to measurement error.[19] In this thesis 95% confidence interval (CI) was used instead of the *P* values to determine clinical differences. In most previous studies, where comparisons are made between groups, some form of statistical analysis is performed and a test or a number of tests of significance are reported with corresponding *P* values. However, *P* values do not always give an indication regarding the clinical importance of the observed results.[20] A more appropriate presentation of the results should focus on the size of the difference between the treatment groups and its range, i.e. the 95% CI.[21] The CI's provide a range

of values within which the true difference of the study groups is believed to exist, thus giving the reader the opportunity to interpret the results in relation to clinical practice.[20]

8.4 Anthropometric measurements

The results from this thesis (Chapter 3) showed that 3D anthropometric surface measurements made on the computer generated surface model from a CBCT were very reliable and accurate compared with direct anthropometry. This has significant impact on the clinical practice as CBCT scans are a standard diagnostic and pre-surgical procedure for patients with extensive craniofacial deformities. Surgical planning requires visualization and quantification of dimorphic features and the ability to synchronize the expected changes. For the objective assessment of facial morphology and facial changes following orthodontic and/or surgical interventions, different methods and analyses have been proposed. [22-24] Surface descriptions of not only bone but also skin structures can be extracted from CBCT data.[25] Our results showed that this is possible to get as much information as needed from one CBCT scan and that no extra records like 2D photographs are needed for additional surface measurements.

One of the disadvantages of the CBCT is the lack of texture information of the soft tissue surface model. Although we did not experience it as a problem during our studies, we realized that it might be a problem when accurate anthropometric measurements and more texture information are needed. Multiple 2D photographs or one 3D image derived from stereo-photogrammetry or laser surface scan can be mapped or laid over CBCT soft tissue image to improve the texture information, which may make the 3D image more realistic.[26]

We also compared the accuracy of anthropometric measurements performed on 3D models derived from stereo-photogrammetry and laser surface scanning with the CBCT measurements and direct measurements. The results confirmed that there were no clinical differences in the accuracy and reliability of the 3D anthropometric measurements obtained from these 3D systems. All these systems have their own advantages and disadvantages, thus the decision on which system to use has to be made according to the type of patient, cooperation of the patient, accuracy required, the available funding and the surface details needed.

8.5 Facial soft tissue thickness

CBCT images are mostly used for hard tissue diagnostic purposes, like locating an impacted canine or pre-surgical planning. Although it has a lack of textured information and detail in muscle information, the quality of the soft tissue images derived from the CBCT are very often underestimated. The results from this thesis shows that CBCT imaging of the face using routine scanning protocols is a reliable method of measuring the facial soft tissue thickness and therefore give a good representation of the facial soft tissues. CBCT visualizes high-contrast in sufficient quality with a remarkable low level of metal artefacts. This improves the accuracy of facial reconstruction and can be applied in craniofacial surgery to make an accurate soft tissue prediction after orthognathic surgery.

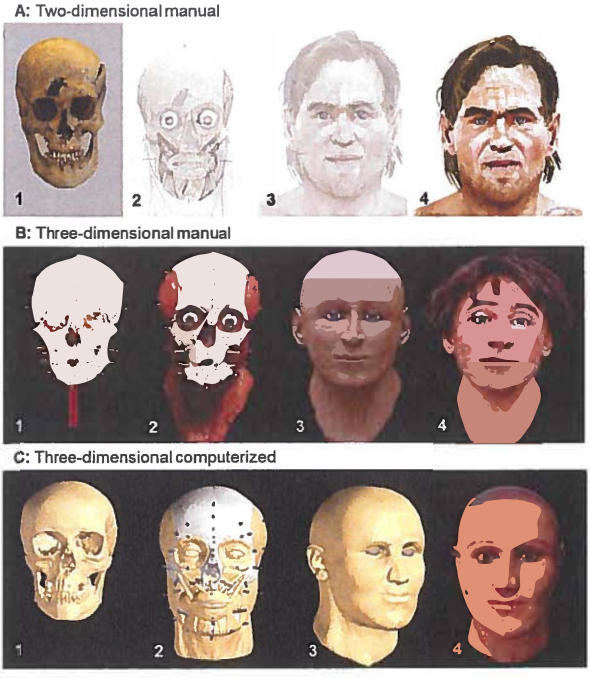

***Figure 2**: Facial reconstruction methods: (A) 2D manual (B) 3D manual (C) 3D computerized.*

(1) Skeletal remains,

(2) FSTT markers in place with the deeper muscle layers,

(3) build up to the right facial thickness and with the skin surface in place,

(4) the final reconstructed face with surface detail.

(Modified from Wilkinson et al.[27])

Facial soft tissue reconstruction from skulls is of great importance in anthropological and forensic sciences to identify human remains. For correct facial reconstruction of the human skull it is necessary to know the average facial soft tissue thickness of specific sites of the face. This requires establishing a database of soft tissue thickness related to age, sex, race, ethnicity [28] and weight.[29] Lateral cephalometric radiography[30], computed tomography (CT) [28,31], ultrasound[29] and magnetic resonance imaging (MRI) [32] are some of the imaging-based methods for measuring living facial soft tissue thickness that have been reported in the literature.[28] (Table 2)

Table 2 Indirect methods of measuring facial soft tissue thickness

Method	Advantages	Disadvantages
Conventional cephalogram	Commonly available in orthodontics Low radiation exposure	Not accurate because of its 2D nature. Needs lateral and anterior posterior cephalogram
Ultrasound	No radiation exposure	Distortion of soft tissue during measuring
Multislice CT	Very accurate	Expensive High radiation exposure
MRI	Very accurate soft tissue representation. No radiation exposure	No big database available Expensive
CBCT	Large amounts of CBCT's are available for a database Lower radiation than conventional CT	Radiation exposure still higher than conventional cephalograms

Several manual methods for facial reconstruction are currently used in practice. These reconstructions consist of physically modeling a face on a skull replica (the target skull) with clay or plasticine. Manual reconstruction methods, however, require a high degree of anatomical and artistic modeling expertise and the result remain difficult and subjective (Figure 2). Furthermore, these reconstructions are time consuming, and are therefore often limited to a single reconstruction.[33] The progress in computer science and the improvement of medical imaging technologies during recent years has led to the development of alternative computer-based craniofacial remodeling methods, which is more consistent and objective. Given all the modeling assumptions and the same input data, a computer always generates the same output data. As a result, the craniofacial remodeling process is much more accurate and becomes accessible to a wide range of people without the need for extensive expertise.[33]

8.6 The uniqueness and limitations of this thesis

We had the unique opportunity to first use fresh cadaver heads and then the skulls after maceration. With this method, all data from the same head could be compared and no artificial media was needed to mimic soft tissues. Moreover, if only the mandible is scanned, the missing cervical vertebra and skull base could influence the results. In this thesis the full fresh cadaver heads with cervical vertebrae were used for the CBCT scans. This is a set-up that is clinically sound and very close to the reality.

For the direct anthropometric measurements described in this thesis, the choice to use an inanimate sample was based on estimates of precision and accuracy. With living subjects, a certain amount of measurement error is unavoidable when performing direct anthropometry, primarily because direct contact is made with the pliable tissues of the face. With the use of a manikin for direct measurements, though distortion of the soft tissue is minimized it is far from the reality. Therefore, with the use of an unanimated cadaver head one can have a reproducible set-up that is close to the reality. According to our knowledge this is the first report on the application of CBCT for determining the facial soft tissue thickness and facial anthropometric measurements.

The relatively small sample size used in most of the studies described in this thesis might be seen as a limitation. However, we used 95% CI to overcome the small sample size and to get reliable results.

8.7. Future perspectives

More attempts are being made to integrate all these new 3D records. Eventually it will lead to a virtual head of the patient, which can be used for case analysis and treatment planning in the virtual image of the patient. Yet, it is important to remember that we are still treating patients and that communication with the patient and colleagues play the most important role in treatment. With the introduction of digital dental models at the end of the 20th century, 3D digital data sets, combining the bone, soft tissues, and the dentition, have gained increasing interest.[34] Instead of discussing treatment objectives and options using X-ray viewers, 2D photographs or composite tracings, life-like 3D models provide a very clear tool for showing areas of deformities, levels of asymmetry and relative relationships between different components of the face, all of which are in an interactive manneron-screen in front of the patient. Patient care is aided by the ability to share patients' 3D records over distance between colleagues. 'Tele-

orthodontics' is one of the promising applications especially in cases where inter-disciplinary treatment is required.[35]

The results in this thesis confirm the accuracy and reliability of soft tissue measurements on surface models derived from CBCT. This means that the existing CBCT images can be used to derive accurate measurements for establishing a soft tissue thickness database.-Most imaging centers now store their images on servers or a picture archiving and communications system (PACS). With proper and secure access, this CBCT data can be readily accessed from inside or outside the institution in real time, permitting use of a large file of images from which to create a database of soft tissue thickness of different populations can be created.[28]

8.8. General conclusions

The results of our specific aims confirm that:

1. The segmentation process influence the quality and the linear and angular measurements the 3D surface models from CBCT datasets using threshold based methods.
2. The measurement error of 3D measurements on CBCT images can be considered clinically relevant especially when considering the high level of accuracy required for pre-surgical planning and treatment outcome evaluation.
3. Indirect anthropometric measurements made on 3D soft tissue surface models derived from different 3D scanning systems are accurate and reliable for research and clinical use.
4. The soft tissue images of the face derived from a CBCT scan is an accurate representation of the human face.

References

1. Mah J, Sachdeva R. Computer-assisted orthodontic treatment: the SureSmile process. Am J Orthod Dentofacial Orthop 2001;120:85-87
2. Kau CH, Hunter LM, Hingston EJ. A different look: 3-dimensionalfacial imaging of a child with Binder syndrome. Am J Orthod Dentofacial Orthop 2007;132:704-9
3. Palomo JM, Hunt DW Jr, Hans MG, Broadbent BH Jr. A longitudinal3-dimensional size and shape comparison of untreated Class I and Class II subjects. Am J Orthod Dentofacial Orthop 2005;127:584-91

4. Xia J, Samman N, Yeung RW, Shen SG, Wang D, Ip HH, et al. Three-dimensional virtual reality surgical planning and simulation workbench for orthognathic surgery. Int J Adult Orthod Orthognath Surg 2000;15:265-82
5. Kau CH, Richmond S, Savio C, Mallorie C. Measuring adult facial morphology in three dimensions. Angle Orthod 2006;76:771-776
6. Sarver DM, Proffit WR, Ackerman JL. Diagnosis and treatment planning in orthodontics. In: Graber TM, Vanarsdall RL, editors. Orthodontics: current principles and techniques. 3rd ed. St Louis: Mosby; 2000
7. Ackerman JL, Proffit WR, Sarver DM. The emerging soft tissue paradigm in orthodontic diagnosis and treatment planning. ClinOrthod Res 1999;2:49-52
8. Kau CH, Cronin AJ, Richmond S. A three-dimensional evaluation of postoperative swelling following orthognathic surgery at 6 months. Plast Reconstr Surg 2007;119:2192-2199
9. McCance AM, Moss JP, Wright WR, Linney AD, James DR. A three-dimensional soft tissue analysis of 16 skeletal Class III patients following bimaxillary surgery. Br J Oral MaxillofacSurg 1992;30:221-232
10. Moss JP, Ismail SF, Hennessy RJ. Three-dimensional assessment of treatment outcomes on the face. OrthodCraniofac Res 2003;6:126-131
11. Hajeer MY, Ayoub AF, Millett DT. Three-dimensional assessment of facial soft-tissue asymmetry before and after orthognathic surgery. Br J Oral Maxillofac Surg 2004;42:396-404
12. Kau CH, Richmond S, Incrapera A, English J, Xia JJ. Threedimensional surface acquisition systems for the study of facial morphology and their application to maxillofacial surgery. Int J Med Robot 2007;3:97-110
13. Mah J, RittoAK. Imaging in othodontics: present and future. J ClinOrthod 2002;36:619-25
14. Marmulla R, Hassfeld S, Luth T, Mende U, Muhling J. Soft tissue scanning for patient registration in image-guided surgery. Comput Aided Surg 2003;8:70-81
15. Besimo CE, Lambrecht JT, Guindy JS. Accuracy of implant treatment planning utilizing template guided reformation computed tomography. Dentomaxillofacial Radiology 2000;29:46-51
16. Grauer D, LSH Cevidanes, Profitt WR. Working with DICOM craniofacial images. Am J OrthodDentofacialOrthop 2009; 136: 460-470
17. Liang X, Lambrichts I, Sun Y, Denis K, Hassan B, Li L, Pauwels R, Jacobs R. A comparative evaluation of Cone Beam Computed Tomography (CBCT) and Multi-Slice CT (MSCT). Part II: On 3D model accuracy. Eur J Radiol;2010: 270–274
18. Hofrath H. Bedeutung der Röntgenfern und Abstands Aufnahme für die Diagnostik der Kieferanomalien. FortschrOrthod 1931;1:231–258

19. Lou L, LagravereMO, Compton S, Major PW, Flores-Mir C. Accuracy of measurements and reliability of landmark identification with computed tomography (CT) techniques in the maxillofacial area: a systematic review. Oral Surg Oral Med Oral Pathol Oral RadiolEndod 2007; 104: 402-411
20. Cohen AM. Uncertainty in cephalometrics. Br J Orthod 1984;11:44-48
21. Polychronopoulou A, Pandis N, Eliades T. Appropriateness of reporting statistical results in orthodontics: the dominance of P values over confidence intervals. European Journal of Orthodontics 2011;33:22–25
22. Kobayashi T, Ueda K, Honma K, Sasakura H, HanadaK, Nakajima T. Three-dimensional analysis of facialmorphology before and after orthognathic surgery. JCraniomaxillofacSurg1990; 18: 68–73
23. McCance AM, Moss JP, Wright WR, Linney AD, JamesDR. A three-dimensional soft tissue analysis of 16 skeletal class III patients following bimaxillary surgery.Br J OralMaxillofacSurg1992; 30: 221–32
24. Moss JP, McCance AM, Fright WR, Linney AD, James DR. A three-dimensional soft tissue analysis of fifteen patients with Class II, Division 1 malocclusions afterbimaxillarysurgery.Am J Orthod DentofacOrthop1994;105: 430–437
25. Halazonetis DJ. From 2-dimensional cephalograms to 3-dimensional computed tomography scans. Am J Orthod Dentofacial Orthop 2005;127:627-637
26. Maal TJJ, Plooij JM, Rangel FA, Mollemans W, Schutyser FAC, Berge SJ. The accuracy of matching three-dimensional photographs with skin surfaces derived from cone-beam computed tomography. Int. J. Oral Maxillofac. Surg. 2008;37: 641–646
27. Wilkinson C. Facial reconstruction – anatomical art or artistic anatomy? J. Anat. 2010;216:235–250
28. Kim DK, Ruprecht A, Wang G, Lee JB, Dawson DV, Vannier MV. Accuracy of facial sort tissue thickness measurements in personal computer-based multiplanar reconstructed computed tomography images. Forensic SciInt.2005;155:28-34
29. Starbuck JM, Ward RE. The affect of tissue depth variation on craniofacial reconstructions. Forensic Sci. Int. 172(2007)130-136
30. George RM, The lateral craniographic method of facial reconstruction, J. Forensic Sci. 32 (1987) 1305–1330
31. Phillips VM, Smuts NA, Facial reconstruction: utilization of computerized tomography to measure facial tissue thickness in a mixed racial population, Forensic Sci. Int. 83 (1996) 51–59
32. Lam EW, Hannam AG, Wood WW, Fache JS, Watanabe W. Imaging orofacial tissues by magnetic resonance, Oral Surg. Oral Pathol. 68 (1989) 2–8

33. De Greef S, Cleas P, Vandermeulen D, Mollemans W, Suetens P, Willems G. Large-scale in-vitro Caucasian facial soft tissue thickness database for craniofacial reconstruction. Forensic Sci Int. 159S (2006) S136-S146
34. Rangel FA, Maal TJJ, Bergé SJ, van Vlijmen OJC, Plooij JM, Schutyser F, Kuijpers-Jagtman AM. Integration of digital dental casts in 3-dimensional facial photographs Am J Orthod Dentofacial Orthop 2008;134:820-826
35. Hajeer MY, Millett DT, Ayoub AF, Siebert JP. Current products and practices: Applications of 3D imaging in orthodontics: Part I. J Orthod 2004;31:62-70

Chapter 9

Summaries

9.1 Summary (English)

In **Chapter 1** the influence of facial imaging on the study of facial morphology and its developmental changes over time are discussed. This is important to diagnose malformations, to study normal and abnormal growth and to differentiate between the results of treatment and growth. The two main methods to study and record facial imaging are cephalometry and anthropometry. Cephalometrics is the scientific study of the measurements of the head's size and proportion while facial anthropometrics is the physical measurement of the human face and its parts.

Several competing methods are available for capturing and quantifying craniofacial morphology. These include traditional methods, such as direct anthropometry, 2D photogrammetry and 2D cephalometry. There are several limitations to these direct and 2D imaging methods. 3D imaging on the other hand is an innovative approach in the field of facial imaging that in a very short time has found a considerable number of applications throughout the medical, dental and forensic sciences.

3D reconstructed images can provide precise and detailed information for the diagnosis of craniofacial structural problems, enhancing the specialist's perception and facilitating a more efficient treatment planning, thus making them preferable to the conventional 2D modalities. Because of the accuracy, CBCT images are powerful tools for evaluation of craniofacial morphology. CBCT can be used in clinical practice and craniofacial research in many ways. The factors influencing the quality and accuracy of a 3D model derived from a CBCT model can be divided into 3 main categories. The first are the limitation in CBCT system itself or scanner related factors such as different CBCT scanners, Field of View (FoV), artifacts and voxel size. The second are patient or subject related factors like patient position or natural head position and metal artifacts. The third are operator related factors, including segmentation process and the operator self.

In **Chapter 2** the geometric accuracy of 3D surface models from two segmentation protocols were assessed. We had the unique opportunity in this study of first using fresh cadaver heads and then the same skulls after maceration and no artificial media was therefore needed to simulate soft tissue. There was a clear difference between the accuracy of the commercial segmentation (CS) and doctor's segmentation (DC) models if compared to the laser surface scans (LSS) as the gold standard. Overall, the CS models resembled more closely the LSS models than the DS models. This was especially true for the measurement involving the condylar landmarks and those on the lingual side of the

mandible. A general trend was found that the models from CS and DS groups were larger than the LSS. These findings are important for clinical procedures requiring high accuracy i.e. 3D planning of surgical drilling guides for implant placement in which minimal transfer error from preoperative planning can result in significant errors to the surgical field. Producing 3D surface models from CBCT datasets is still less accurate than the reality when using threshold based methods. If 3D models are needed for high precision, the additional cost of CS models seems to be justified to produce a more accurate surface model.

In **Chapter 3** the effect of two different CBCT segmentation protocols on the accuracy of linear and angular measurements was determined. Standard linear and angular measurements were made between different anatomic and cephalometric landmarks. The measurements from the CS and DS were in general bigger than the LLS. Moreover, the results from the DS models were larger than the CS. This was especially seen in the condylar region. These results confirm that it is very difficult to do an accurate segmentation of the condylar region without good software and sufficient training in this process. Possible reasons why this is such a difficult area to segment are: the lower density of the bone in the condylar area compared to the rest of the mandible, a lot of overlapping bony structures and the difficulty to separate the condyle with the discus articulare during segmentation could explain the inaccuracies of condylar area. Therefore, the segmentation process can be an essential cause of measurement error. The authors suggest that segmentation should be done by a commercial company if accurate measurements are required.

In **Chapter 4** the reliability and measurement error of 3D cephalometric measurements on CBCT images were determined by means of the smallest detectable difference (SDD). As a powerful tool for evaluation of craniofacial morphology, pre-surgical planning and treatment outcome, the accuracy of measurements on CBCT surface models is very important. Inaccurate measurements can cause inaccuracies in the pre-surgical planning and lead to undesirable post treatment effects. Our results showed that the intra-observer agreement of all measurements was good among 25 variables, the ANB angle was the only one with a measuring error of one or less than one measuring unit. Variation of landmark identification increases the measurement error because the errors in location are cumulative. The third dimension in 3D cephalometry, introduces an additional source of error in the transversal direction. Because a high level of accuracy required in pre-surgical planning and outcome evaluation, the measurement

error of 3D cephalometric measurements (except for the ANB angle) can be considered clinically relevant and therefore question the use of linear and angular 3D measurements to detect true treatment effect.

In **Chapter 5** the accuracy and reliability of standard anthropometric measurements made on the 3D soft tissue models derived from CBCT were investigated. Many craniofacial anomalies are characterized by complex deviations in the shape and configuration of facial soft tissue structures. For affected individuals, extensive surgical interventions are often required to correct malformed or malpositioned facial structures, thereby normalizing their craniofacial appearance. Nowadays, CBCT scans have become a standard tool for patients with significant craniofacial deformities for diagnosis and pre-surgical planning. Surgical planning requires visualization and quantification of dimorphic features and the ability to simulate the changes that surgery is expected to bring about. The CBCT measurements were very accurate when compared to the physical measurements. Except for one measurement, between point tragion (t) and nasion (n) (mean 1.52 mm), all the measurements had a mean error of less than 1.5 mm. These results shows that the 3D measurements on a computer generated surface model created from a CBCT datasets was accurate and the reproducibility was excellent when compared with direct anthropometry. This means that no additional anthropometric records like photographs or direct measurements are needed for surface information required for diagnosis and surgical planning.

In **Chapter 6** the accuracy and reliability of standard anthropometric linear measurements made on 3D surface models derived from 3 different scanning systems (laser surface scanning, 3D stereo-photogrammetry and CBCT) were investigated. All three 3D scanning systems proved to be very reliable when compared to the physical measurements. The mean absolute error as well as the absolute percentage error was very small. This means that the measurements recorded by all three systems appear to be extremely accurate and very reliable. There were also no clinical differences between the 3D techniques. In future research, the data obtained from these systems could be combined for i.e. inter-center comparisons. Each system has its own advantages and disadvantages. They differ in acquisition time, surface texture information, ability to visualize bony structures and radiation exposure. The choice of system will depend on the information required and the type of patient. This can be applied by forensic anthropologists to construct biological profiles using precise and accurate metrical data to determine key aspects of human identification.

In **Chapter 7** the aim was to determine the reliability and accuracy of facial soft tissue thickness (FSTT) measurements using CBCT and the effects of slice thickness on the precision of these measurements. Physical FSTT measurements were compared to the same measurements done indirectly on the soft tissue images derived from CBCT using 0.3 and 0.4 voxel sizes. The intra-observer and inter-observer correlations of the CBCT and physical measurements were very high. There was no significant difference between the measurements made on the CBCT images and the physical measurements. Decreasing the voxel size from 0.3 mm to 0.4 mm resulted in a slight increase of accuracy. The result showed that CBCT images of the face using routine scanning protocols are reliable for measuring soft tissue thickness in the facial region and give a good representation of the facial soft tissues. For a correct facial reconstruction of the human face it is necessary to know the average facial soft tissue thickness of specific sites. This will enable forensic scientist to make a correct identification from human remains. For this purpose, establishing a database of soft tissue thickness related to age, sex, race and ethnicity will be required.

In **Chapter 8** the general aims of this thesis are discussed in relation to the main results. In addition, the clinical relevance of the findings and future perspectives regarding CBCT imaging and its application in different fields has been addressed.
The results from this thesis confirm that:

1. The segmentation process does significantly influence the quality and accuracy of the 3D surface models derived from CBCT datasets using threshold based methods. In addition it also influence the accuracy of linear and angular measurements made on the 3D surface models.
2. The measurement error of 3D measurements can be considered clinically relevant. The linear and angular 3D measurements do not always detect the true 3D treatment effect.
3. The indirect anthropometric measurements made on 3D soft tissue surface models derived from different 3D scanning systems are very accurate and reliable. These 3D scanning systems can be used for research and in clinical practice and gives a true representation of the reality.
4. CBCT soft tissue images are an accurate representation of the human face. This is a very accurate method to measure the facial soft tissue thickness.

The results of this thesis have shown that 3D surface models derived from CBCT scan offer sufficient quality for anthropometric measurements and no additional

photographs or direct measurements are needed. These results implicate new future applications for CBCT data, especially the soft tissue database in forensic science. When CBCT scans are made for other purposes, the data can be stored and used for additional applications. Firstly, these data can be used to create a large database of FSTT from any population. This will in the long run improve the accuracy of facial reconstructions. Secondly, the same CBCT data can add values to the existing 2D normative anthropometric measurements databases for age prediction in identification of missing children. Eventually a 3D normative database may be set-up -when sufficient CBCT data have been collected.

9.2 Samenvatting (Dutch)

In **hoofdstuk 1** wordt de invloed besproken die de wijze van beeldvorming van het gelaat heeft op het onderzoek naar gelaatsopbouw. Daarnaast worden de ontwikkelingen die op dit gebied hebben plaatsgevonden genoemd. Deze beeldvorming is belangrijk om de normale en abnormale ontwikkeling van het gezicht te kunnen bestuderen, om afwijkingen te kunnen benoemen en om onderscheid te kunnen maken tussen de resultaten van behandeling en van groei. Cefalometrie en antropometrie zijn de twee belangrijkste methoden om de verhoudingen van het gelaat vast te leggen en te bestuderen. Cefalometrie doet dit voor het hoofd als geheel, antropometrie voor het menselijk gezicht. Er zijn verschillende methoden om craniofaciale morfologie te beschrijven. Bijvoorbeeld traditionele methoden als directe metingen, tweedimensionale fotogrammetrie en tweedimensionale cefalometrie. Deze methodes hebben duidelijk hun beperkingen. Driedimensionale beeldvorming is een nieuwe vorm van beeldvorming, die in korte tijd een groot aantal toepassingen heeft gevonden in de medische, tandheelkundige en forensische wetenschappen.

Driedimensionaal geconstrueerde beelden leveren nauwkeurige en gedetailleerde informatie om craniofaciale structuren te kunnen beschrijven, verhogen het inzicht van de specialist in de problematiek en maken een efficiëntere planning van de behandeling mogelijk. Om deze reden genieten zij de voorkeur boven tweedimensionale beelden. Zowel voor craniofaciaal onderzoek als in de klinische praktijk kan de "cone beam computerised tomography" (CBCT) op vele manieren worden gebruikt. Er zijn drie groepen factoren die de kwaliteit en nauwkeurigheid van de driedimensionale beelden verkregen vanuit een CBCT opname beïnvloeden. De eerste is de beperking van het CBCT systeem zelf, of factoren verbonden aan de scanner, zoals het type scanner, "field of view"(FoV), artefacten en voxel grootte. De tweede zijn factoren gerelateerd aan het onderwerp, zoals de positie van het hoofd ten opzichte van de scanner ("natural head position") en artefacten ten gevolge van metaal in het onderzochte gebied. De derde zijn factoren gerelateerd aan degene die de opname maakt, zoals de vaardigheid van de operateur en de keuze van het segmentatieproces.

In **hoofdstuk 2** wordt de geometrische betrouwbaarheid van driedimensionale oppervlaktemodellen van twee verschillende segmentatieprotocollen beoordeeld. De unieke mogelijkheid deed zich voor om gesegmenteerde oppervlaktemodellen van driedimensionale scans van "verse" kadaverhoofden te vergelijken met laser oppervlakte scans van dezelfde hoofden na verwijdering van de weke delen. Door het

gebruik van deze "verse" kadaverhoofden, was het gebruik van een kunstmatig medium om de weke delen te simuleren niet nodig. De resultaten geven aan dat er een duidelijk verschil in nauwkeurigheid bestaat tussen commercieel gesegmenteerde modellen (CS), modellen gesegmenteerd door een behandelaar (DS) en de laser oppervlakte scans (LSS), die diende als de gouden standard. De CS modellen komen over het algemeen beter overeen met de LSS, dan DS modellen. Dit was specifiek het geval voor de meetpunten ter plaatse van de condylus en die aan de linguale zijde van de mandibula. De modellen verkregen door middel van CS en DS waren gemiddeld groter dan de LSS. Deze bevindingen zijn belangrijk voor klinische procedures die een grote mate van nauwkeurigheid vereisen. Bijvoorbeeld bij de driedimensionale planning voor een chirurgische boorsjabloon voor het plaatsen van een implantaat, waarbij een minimale fout in de preoperatieve planning kan leiden tot een aanzienlijke fout in de boorsjabloon en dus bij het uitvoeren van de chirurgie. De driedimensionale modellen verkregen uit een CBCT scan komen helaas niet voor de volle 100% overeen met de werkelijkheid. Als een driedimensionaal model met een hoge nauwkeurigheid nodig is, kan het beste gebruik gemaakt worden van het meer nauwkeurige commercieel gesegmenteerde model. De hogere accuraatheid van deze modellen rechtvaardigt de hogere kosten.

In **hoofdstuk 3** wordt het effect van twee verschillende segmentatieprotocollen op de betrouwbaarheid van lineaire- en hoekmetingen onderzocht. Standaard lineaire- en hoekmetingen zijn gemaakt tussen verschillende anatomische en cephalometrische meetpunten. De metingen op de DS en CS modellen zijn over het algemeen groter dan de metingen op LLS modellen. Bovendien, zijn de metingen op de DS modellen groter dan de metingen op de CS modellen. Dit is vooral zichtbaar bij de metingen in het condylaire gebied. Deze resultaten bevestigen dat accurate segmentatie zonder een goed softwareprogramma en zonder voldoende scholing zeer moeilijk is. Mogelijke redenen wat de segmentatie in deze regio zo moeilijk maakt zijn: de verlaagde botdichtheid in het condylaire gebied vergeleken met de rest van de mandibula, veelvuldige overlappende botstructuren in dit gebied en de moeilijkheidsgraad van het onderscheiden van de condylus en de discus articularis gedurende het segmentatieproces. Ergo, het segmentatieproces kan de hoofdoorzaak zijn van de meetfout. Indien nauwkeurige metingen noodzakelijk zijn, adviseert de auteur de segmentatie uit te laten voeren door een commercieel bedrijf.

In **Hoofdstuk 4** worden de betrouwbaarheid en de meetfout van de driedimensionale cefalometrische metingen op CBCT beelden met behulp van de "smallest detectable difference" (SDD) bepaald. CBCT beelden kunnen zinvol zijn bij de evaluatie van de craniofaciale morfologie, bij het maken van een prechirurgische planning en het beoordelen van behandelresultaten. De nauwkeurigheid van de metingen op CBCT beelden is belangrijk. Onnauwkeurigheden in deze metingen kunnen onnauwkeurigheden in de prechirurgische planning veroorzaken en daarmee uiteindelijk leiden tot een ongewenst behandelresultaat. Uit de resultaten van deze studie blijkt dat de overeenkomst tussen de beoordelaars goed was voor 25 variabelen. De hoek ANB was de enige tussen deze variabelen met een meetfout gelijk of kleiner dan één meeteenheid. De meetfouten zijn cumulatief als gevolg van de variaties bij het bepalen van de cefalometrische punten. De toevoeging van een extra dimensie in de driedimensionale cefalometrie ten opzichte van de tweedimensionale cefalometrie zorgt voor een additionele bron van fouten in transversale richting. De prechirurgische planning en de evaluatie van het behandelresultaat vereisen een hoge mate van nauwkeurigheid. De meetfout van de driedimensionale cefalometrische metingen, met uitzondering van hoek ANB, is klinisch relevant. Om deze reden moeten er vraagtekens gezet worden bij het gebruik van deze metingen voor het bepalen van effecten van een behandeling.

In **hoofdstuk 5** worden de betrouwbaarheid en nauwkeurigheid van standaard antropometrische metingen op driedimensionale weke delen modellen afkomstig van CBCT scans bepaald. Veel craniofaciale anomalieën worden gekarakteriseerd door complexe afwijkingen in vorm en configuratie van de weke delen van het gelaat. Uitgebreide chirurgische interventies zijn vaak noodzakelijk voor correctie van misvormde gelaatsstructuren. Voor het stellen van een juiste diagnose en het maken van een prechirurgische planning bij patiënten met een significante craniofaciale afwijking worden tegenwoordig vaak als standaard CBCT scans gemaakt. Visualisatie en kwantificering van dysmorfische kenmerken is noodzakelijk voor het maken van een juiste chirurgische planning en bieden de mogelijkheid om de te verwachte resultaten van de chirurgische ingreep te simuleren. De resultaten van dit onderzoeken geven aan dat driedimensionale metingen op een computer gegenereerd oppervlaktemodel, gecreëerd uit een CBCT dataset, nauwkeurig zijn indien deze vergeleken worden met de fysische metingen. Met uitzondering van de meting tussen punt tragion (t) en punt nasion (n) (gemiddeld 1.52 mm), hadden al de metingen gemiddeld een meetfout van minder dan 1.5 mm. De reproduceerbaarheid in vergelijking met directe antropometrie

is uitstekend. Dit betekent dat aanvullende antropometrische gegevens (foto's en fysische metingen) niet noodzakelijk zijn voor het stellen van een diagnose en het maken van een chirurgische behandelplanning.

In **hoofdstuk 6** worden de nauwkeurigheid en betrouwbaarheid van standaard lineaire antropometrische metingen op driedimensionale oppervlaktemodellen, afkomstig van 3 verschillende scansystemen, onderzocht. De driedimensionale scansystemen die onderzocht worden zijn "laser surface scanning", driedimensionale stereo-fotogrammetrie (Di3Dface™ system) en CBCT. De resultaten geven aan dat alle driedimensionale systemen erg betrouwbaar zijn ten opzichte van de fysische metingen. Zowel de gemiddelde absolute fout als de absolute procentuele fout is erg klein. Dit betekent dat de metingen van alle driedimensionale systemen extreem nauwkeurige en betrouwbaar lijken te zijn. Ook waren er geen klinische verschillen zichtbaar tussen deze drie systemen. Dit betekent dat de data verkregen uit deze drie scansystemen gecombineerd kunnen worden voor toekomstig onderzoek, bijvoorbeeld voor de vergelijking tussen verschillende behandelcentra. De drie scansystemen zijn totaal verschillend van elkaar en hebben alle drie hun eigen plus- en minpunten. De systemen verschillen van elkaar in opnametijd, informatie over de oppervlaktestructuur, mogelijkheid tot visualiseren van botstructuren en radiatie dosis. De keuze van het systeem hangt af van de informatie die nodig is. Forensische antropologen kunnen gebruik maken van de nauwkeurige metrische data om de kernaspecten voor de identificatie van mensen te bepalen.

Het doel van **hoofdstuk 7** is het bepalen van de betrouwbaarheid en nauwkeurigheid van "facial soft tissue thickness" (FSTT) metingen op CBCT beelden. Daarnaast wordt het effect van de dikte van de sneden op de precisie van de metingen bepaald. Fysische metingen worden vergeleken met dezelfde metingen op CBCT beelden met een voxel grootte van 0.3 mm en 0.4 mm. De intra- en interbeoordelaarsbetrouwbaarheid van de fysische metingen en de metingen op CBCT beelden is hoog. Er was geen significante verschil tussen metingen op een CBCT beeld en de fysische metingen. Het verkleinen van de voxel grootte heeft een lichte toename in nauwkeurigheid tot gevolg. CBCT beelden die met voxel grootte 0,4 mm gemaakt worden zijn voldoende nauwkeurig voor het meten van de dikte van de weke delen. Indien een meer accurate beeldvorming wenselijk is, kan de voxel grootte aangepast worden naar 0,3 mm. Voor een correcte reconstructie van het menselijke gezicht is het noodzakelijk een database te hebben

met gemiddelde diktes van de weke delen op specifieke plaatsen in het gezicht. Deze gemiddelde diktes moeten gerelateerd zijn aan leeftijd, geslacht, ras en etniciteit.

In **hoofdstuk 8** worden de uitkomsten in relatie tot het algemene doel van dit proefschrift besproken. Daarnaast worden de klinische relevantie van de bevindingen en het toekomstperspectief van beeldvorming met behulp van CBCT en de toepassingen ervan in de verschillende werkvelden beschreven.
De uitkomsten van dit proefschrift bevestigen dat:

1. Het segmentatieproces is van doorslaggevende invloed op de kwaliteit en betrouwbaarheid van driedimensionale oppervlaktemodellen afkomstig van CBCT datasets. Daarnaast beïnvloedt het segmentatieproces de nauwkeurigheid van lineaire- en hoekmetingen op deze modellen.
2. De meetfout van driedimensionale metingen kan als klinisch relevant beschouwd worden. De lineaire- en hoek driedimensionale metingen geven niet altijd het juiste driedimensionale behandeleffect weer.
3. De indirecte antropometrische metingen op driedimensionale weke delen oppervlaktemodellen, afkomstig van verschillende driedimensionale scansystemen, zijn een nauwkeurig en betrouwbaar. Zij kunnen gebruikt worden voor onderzoek, zijn klinisch toepasbaar en geven een juiste representatie van de werkelijkheid weer.
4. CBCT beelden geven een accuraat beeld van het menselijke gelaat. Het is een zeer betrouwbare methode om de dikte van de weke delen van het gelaat te meten.

De resultaten van dit proefschrift geven aan dat antropometrische metingen op driedimensionale oppervlaktemodellen afkomstig van CBCT scans voldoende betrouwbaar en nauwkeurig zijn, zodat het maken van aanvullende foto's en directe antropometrische metingen niet noodzakelijk zijn.

De resultaten van dit proefschrift laten tevens zien dat de data afkomstig van CBCT scans die voor andere doeleinden gemaakt zijn, in de toekomst mogelijk gebruikt kunnen worden voor bijkomende toepassingen. Ten eerste kan het gebruikt worden om de bestaande database met informatie over de dikte van weke delen van verschillende populaties te vergroten. Ten tweede kan de bestaande database met normatieve tweedimensionale antropometrische waarden worden aangevuld. Deze database wordt gebruikt voor leeftijd voorspelling tijdens de identificatie van vermiste kinderen. Uiteindelijk kan met de gecombineerde data een database opgezet worden die normatieve driedimensionale antropometrische waarden bevat.

9.3 Opsomming (Afrikaans)

In **Hoofstuk 1** word die invloed van gelaats-beeldvormingstegnieke op die studie van gesigsmorfologie en die verandering daarvan, met verloop van tyd, ondersoek. Dit is baie belangrik vir die diagnose van wanformasie, vir die bestudering van normale en abnormale groei en om tussen die resultate van groei en die effekte van die behandeling, te kan onderskei. Die twee hoofmetodes om gelaats-beeldvorming te bestudeer en vas te lê is Kefalometrie en Antropometrie. Kefalometrie is die wetenskaplike bestudering van die metinge van die groote en proporsie van die pasiënt se kop terwyl antropometrie die fisiese meting van die pasiënt se kop en die komponente daarvan is.

Verskillende mededingende metodes bestaan tans om kraniofasiale morfologie vas te lê en te kwantifiseer. Hierdie metodes sluit in tradisionele metodes, soos byvoorbeeld direkte antropometrie, 2-D fotogrammetrie en 2-D kefalometrie. Daar is verskeie beperkinge t.o.v. hierdie 2-D beeldvormende tegnieke. 3-D beelvormende tegnieke aan die ander kant, is 'n innoverende benadering op die gebied van gelaats- beeldvormende tegnieke. Dit het in 'n kort tydperk 'n aansienlike aantal toepassings in die mediese, tandheelkundige en forensiese wetenskappe gekry.

3-D ge-rekonstrueerde beelde kan presiese en gedetaileerde informasie t.o.v. die diagnose van kraniofasiale strukturele probleme verskaf. Dit vergroot die spesialis se persepsie en fasiliteer 'n meer doeltreffende behandelingsplan. Hierdie metode word bo die konvensionele 2-D modaliteite verkies. As gevolg van die akkuraatheid van Konusbundel rekenaar tomografie (KBRT) beelde veroorsaak dit dat dit 'n baie kragtige instrument vir die evaluering van kraniofasiale morfologie is. Daar is verskeie toepassings vir KBRT in die kliniese praktyk en ook vir kraniofasiale navorsing. Die faktore wat die kwaliteit en akkuraatheid van die 3-D modelle (afgelei van 'n KBRT model) beïnvloed, kan in 3 hoofgroepe verdeel word. Die eerste is die beperkinge van die KBRT sisteem self, of skandeer-verwante faktore byvoorbeeld verskillende KBRT apparate, "Field of View" (FoV), beeldartifakte en Voxel resolusie. Die tweede is pasiënt- of onderwerp verwante faktore byvoorbeeld posisie van die pasiënt, die natuurlike kop-posisie (NHP) en metaalartifakte. Die derde groep is operateur afhanklike faktore, insluitend die segmentasieproses asook die operateur self.

In **Hoofstuk 2** word die geometriese akkuraatheid van 3-D modelle (afkomstig van twee segmentasie protokolle) bestudeer. Die outeur het die unieke geleentheid gehad om te

werk met vars kadawerkoppe en daarna die skelet van dieselfde kop (nadat die sagteweefsel verwyder is). Geen kunsmatige medium was nodig om die sagteweefsel te simuleer nie. Daar was 'n duidelike verskil tussen die kommersiële segmentasie (KS) en die klinikus- of dokter segmentasie (DS) modelle wanneer dit vergelyk is met die laser oppervlaks-opname (LOO) wat beskou word as die goue standaard. Oor die algemeen het die KS modelle veel beter ooreengekom met die LOO as die DS modelle. Dit was veral sigbaar by die metinge van die kondules landmerke en dié aan die linguale kant van die mandibula. Oor die algemeen was die modelle afkomstig van die KS en DS groepe groter as dié in die LOO groep. Hierdie bevindinge is klinies relevant vir prosedures wat hoë akkuraatheid vereis, byvoorbeeld 3-D beplanning van chirurgiese boor gids-groewe wat gebruik word vir implantaat plasing in gevalle waar minimale oordragsfoute (afkomstig van die pre-operatiewe beplanning) ernstige foute t.o.v. die chirurgie tot gevolg kan hê. Die 3-D oppervlaksmodel afkomstig van 'n KBRT opname is steeds minder akkuraat as die realiteit wanneer "threshold" gebaseerde metodes van segmentasie gebruik word. Indien 'n 3-D model met hoë presisie benodig word, regverdig dit die ekstra koste wat met 'n KS model gepaard gaan.

In **Hoofstuk 3** word die uitwerking wat twee verskillende KBRT segmentasie protokolle het op die akkuraatheid van liniêre- en hoekmetinge, bepaal. Standaard liniêre- en hoekmetinge is gemaak tussen verskillende anatomiese en kefalometriese landmerke. Die metinge van die KS en DS groepe was oor die algemeen groter as die metinge in die LOO groep. Verder was die resultate van die DS groep groter as die KS groep. Dit was veral sigbaar by metinge wat die kondulêre landmerke bevat het. Hierdie resultate bevestig dat dit ontsettend moeilik is om 'n akkurate segmentasie te doen van die kondulêre gebied te doen sonder 'n goeie segmentasie sagteware program asook die nodige opleiding in die segmentasieproses. Moonlike redes waarom die area so moeilik is om te segmenteer is: die laer digtheid van die been in die kondlus in vergelyking met die ander dele van die mandibula, oorvleueling van verskeie beenstrukture en die moeilikheidsgraad van die proses om die kondule van die diskus artikularis gedurende die segmentasieproses te skei. Dus, die segmentasieproses kan 'n groot oorsaak van metingsfoute wees. Die outeur stel voor dat segmentasie deur 'n kommersiële maatskapy gedoen moet word wanneer akkurate metings verlang word.

In **Hoofstuk 4** word die betroubaarheid en die metingsfout van die 3-D kefalometriese metings op KBRT beelde met behulp van de Kleinste Waarneembare Verskil (KWV) bepaal. Omdat dit 'n kragtige instrument is tydens die evaluasie van kraniofasiale

morfologie, pre-chirurgiese beplanning en behandelsuitkomste, speel die hoë akkuraatheid van die metings op 3-D modelle (afkomstig van KBRT) 'n belangrike rol. Onakkurate metings kan onakkuraathede in die pre-chirurgiese beplanning veroorsaak en ongewensde resultate in die uitkoms van 'n behandeling tot gevolg hê. Uit die resultate van hierdie navorsing blyk dit dat die ooreenkoms tussen verskeie evalueerders tussen 25 veranderlikes goed was (goeie Intra-evalueerder akkuraatheid). Die ANB hoek was die enigste veranderlike met 'n metingsfout kleiner, of gelyk aan, één meeteenheid. Die metingsfout is as gevolg van variasies t.o.v. die identifikasie van die landmerke. Die derde dimensie in 3-D kefalometrie voeg 'n moontlike addisionele metingsfout in die transversale rigting by. A.g.v. die hoë mate van akkuraatheid wat by pre-chirurgiese beplanning en beoordeling van die uitkoms van 'n behandeling vereis word, kan die metingsfout van kefalometriese metings (behalwe hoek ANB) 'n aansienlike klinies-betekenisvolle invloed hê. Die resultate bevraagteken dus die vermoë van Kefalometriese liniêre- en hoekmetings om die ware effekte van die behandeling op te spoor.

In **Hoofstuk 5** word die akkuraatheid en betroubaarheid van standaard antropometriese metings wat gemaak is op 3-D sagteweefsel modelle (verkry deur KBRT beelde) te ondersoek. Verskeie kraniofasiale afwykinge word gekarakteriseer deur ingewikkelde afwykings in die vorm en konfigurasie van die sagteweefsel strukture van die gelaat. Uitgebreide chirurgiese intervensie is dikwels nodig om die misvormde of wangeposisioneerde gelaatstrukture te korrigeer. KBRT opnames is 'n belangrike hulpmiddel en maak deesdae deel uit van standaard opnames wat nodig is by pasiënte met 'n beduidende kraniofasiale afwyking ten einde die diagnose en pre-chirurgie van sodanige pasiënte te vergemaklik. Visualisasie en kwantifisering van dismorfiese kenmerke is noodsaaklik om die regte pre-chirurgiese beplanning te maak en bied 'n moontlikheid om die verwagte resultaat van die chirurgie na te boots. Die resultate van hierdie navorsingsprojek wys dat 3-D metings, op 'n rekenaar-gegenereerde oppervlaktemodel, afkomstig van 'n KBRT opname baie akkuraat is as dit vergelyk word met fisiese metings. Met uitsondering van die meting tussen tragion (r) en nasion (n) (gemiddeld 1.52 mm), het al die metings 'n metingsfout van kleiner as 1.5mm. Die reproduseerbaarheid van hierdie metings, in vergelyking met die fisiese metings is baie hoog. Dit beteken dat daar geen aanvullende antropometriese opnames (byvoorbeeld foto's of direkte metings) nodig is om 'n goeie diagnose en pre-chirurgiese beplanning te kan maak nie.

In **Hoofstuk 6** is die akkuraatheid en betroubaarheid van standaard antropometriese liniêre metings (gemaak op 3-D oppervlaks-modelle afkomstig van drie verskillende skandeer apparate nl. laser oppervlaksopname, 3-D stereo-fotogrammetrie en KBRT), getoets. Al drie die skandeer apparate blyk baie betroubaar te wees wanneer dit met fisiese metings vergelyk is. Die gemiddelde absolute fout, sowel as die absolute persentasiefout, was baie klein. Dit beteken dat die metings wat gemaak is op al drie skandeertegnieke uiters akkuraat en baie betroubaar blyk te wees. Daar was ook geen klinies waarneembare verskille tussen die verskillende 3-D tegnieke nie. Dit beteken dat die data afkomstig van hierdie drie 3-D skandeertegnieke gekombineer kan word vir toekomstige navorsingsprojekte, byvoorbeeld vir vergelyking tussen verskillende behandelingsentrums. Die drie skandeertegnieke is almal verskillend van mekaar en het hulle eie voor- en nadele. Hulle verskil van mekaar wat betref opnametyd, informasie oor die oppervlakstruktuur, moontlikheid om skeletale strukture te skandeer en die radiasieblootstelling. Die keuse van welke sisteem gebruik moet word hang af van die informasie wat benodig word. Dit kan onder andere ook gebruik word deur forensiese antropoloë om akkurate en betoubare metriese data te verkry ten einde biologiese profielle te kan maak wat kan help om die sleutelaspekte van menslike identifikasie te bepaal.

In **Hoofstuk 7** was die doel om die akkuraatheid en betroubaarheid van gelaats-sagteweefsel dikte metings te bepaal deur gebruik te maak van KBRT en om die effek van Voxel resolusie op die presiesie van hierdie metings te bepaal. Fisiese metings is vergelyk met dieselfde metings wat indirek gedoen is op die sagteweefsel beelde wat verkry is vanaf die KBRT opnames met gebruikmaking van 0.3 en 0.4 Voxel groottes. Die inter- en intra waarnemer korrelasie van die KBRT en die fisiese metings was baie hoog. Daar was geen betekenisvolle verskille tussen die metings wat op de KBRT en die fisiese metings gemaak is nie. Daar was 'n geringe verhoging in die akkuraatheid wanneer die Voxel groote verlaag is van 0.4 mm na 0.3 mm. Die resultate van hierdie navorsing het getoon dat die KBRT opnames heel betroubaar is vir bepaling van die dikte van sagteweefsel van die gesig en dit gee ook 'n realistiese weergawe van die sagteweefsel van die gelaat. Dit is noodsaaklik om presies te weet wat die gemiddelde sagteweefsel diktes op spesifieke landmerke op die gesig is, sodat die forensiese antropoloë in staat kan wees om 'n akkurate gesigsrekonstruksie te maak. Dit sal hulle in staat stel om 'n korrekte identifikasie van menslike oorskot te kan maak. Vir die rede is dit noodsaaklik

om 'n databank saam te stel van die gemiddelde sagteweefsel-diktes m.b.t. verskillende ouderdomme, geslag, ras en etniese groepe.

In **Hoofstuk 8** word die algemene doelwitte van hierdie proefskrif in verhouding tot die belangrikste resultate bespreek. Verder word die kliniese relevansie van die bevindinge en die toekomsperspektiewe met betrekking tot KBRT beeldvorming, en die toepassing daarvan in verskillende velde, volledig bespreek.

Die resultate van hierdie proefskrif bevestig dat:

1. Die segmentasieproses 'n beduidende invloed kan hê op die kwaliteit en die akkuraatheid van die 3-D oppervlaksmodelle afkomstig van KBRT data waar daar gebruik gemaak word van standaard "threshold" gebaseerde metodes. Daarbenewens het dit ook 'n invloed op die liniêre- en hoekmetings wat gemaak word op die 3-D oppervlaksmodelle.

2. Die metingsfout van 3-D metings kan as klinies relevant bestempel word. Die 3-D liniêre- en hoekmetings gee nie altyd die ware 3-D behandelingseffek weer nie.

3. Die indirekte metings wat gemaak is op 3-D sagteweefsel oppervlaksmodelle (afkomstig van 3-D skandeersisteme) is baie akkuraat en betroubaar. Hierdie 3-D modelle kan gebruik word vir navorsing asook vir kliniese doeleindes, en is 'n ware weergawe van die realiteit.

4. KBRT sagteweefselbeelde verskaf 'n akkurate weergawe van die menslike gesig. Dit is ook 'n akkurate metode om die sagteweefsel-diktes te bepaal.

Die resultate van hierdie proefskrif het gewys dat antropometriese metings op 3-D oppervlaksmodelle (afkomstig van KBRT) voldoende betroubaar en akkuraat is. Dit beteken dat geen aanvullende opnames soos foto's of direkte metings noodsaaklik is nie.
Die resultate van hierdie proefskrif dui ook aan dat die KBRT data, wat verkry is vir watter rede ookal, moontlik in die toekoms vir ander toepassings gebruik kan word. In die eerste plek kan dit gebruik word om bestaande databanke t.o.v. die diktes van sagteweefsel van die gesig van verskillende bevolkingsgroepe uit te brei. Dit sal op die langduur die akkuraatheid van gesigsrekonstruksies verbeter. In die tweede plek kan die bestaande databanke met normatiewe 2-D antropometriese waardes aangevul word. Hierdie databanke kan word gebruik vir die voorspelling van die

ouderdom en dus identifikasie van vermiste kinders. Uiteindelik kan daar 'n gekombineerde databank saamgestel word, wat normatiewe 3-D antropometriese waardes sowel as 2-D en KBRT metinge bevat.

Appendices

I. List of publications

1. **Fourie Z**, Ozcan M, Sandham A. Effect of dental arch convexity and type of archwire on frictional forces. Am J Orthod Dentofacial Orthop 2009;13614.e1-7; discussion 14-5
2. **Fourie Z**, Damstra J, Gerrits PO, Ren Y. Accuracy and reliability of facial soft tissue thickness measurements of cone beam CT scans. Forensic Sci Int 2010; 199: 9-14
3. Damstra J, Huddleston Slater JJR, **Fourie Z**, Ren Y. Reliability and the smallest detectable difference of lateral cephalometric measurements. Am J Orthod Dentofacial Orthop 2010; 138: 546.e1-e8
4. **Fourie Z**, Damstra J, Gerrits PO, Ren Y. Linear accuracy and repeatability of anthropometric facial measurements using cone-beam computed tomography. Cleft-Palate Craniofac J 2010; doi: 10.1597/10-076
5. **Fourie Z**, Damstra J, Gerrits PO, Ren Y. Evaluation of anthropometric accuracy and reliability using different three-dimensional scanning systems. Forensic Sci Int 2010; doi: 10.1016/j.forsciint .2010.09.018
6. Damstra J*, **Fourie Z***, Huddleston Slater JJR, Ren Y. Reliability and the smallest detectable difference of three-dimensional cephalometric measurements. Am J Orthod Dentofacial Orthop 2011, Accepted (*Shared first authorship)
7. Damstra J, **Fourie Z**, Ren Y. Simple technique to achieve natural head position for cone beam CT scans. Br J Oral Maxillofac Surg 2010; 48: 236-238
8. Damstra J, **Fourie Z**, Huddleston-Slater JJR, Ren Y. Accuracy of linear measurements of cone beam CT derived surface models of different voxel sizes. Am J Orthod Dentofacial Orthop 2010; 137: 16.w1-16.e6
9. Damstra J, **Fourie Z**, Ren Y. A comparison between two-dimensional and midsagittal three-dimensional cephalometric measurements of dry human skulls. Br J Oral Maxillofacial Surg 2010, doi: 10.1016/j.boms.2010.06.006
10. **Fourie Z**, Damstra J, Schepers R, Gerrits PO, Ren Y. Segmentation significantly influences the accuracy of 3D models derived from cone beam computed tomography. Eur J Radiol 2011, Jul 4. [Epub ahead of print]
11. **Fourie Z**, Engelbrecht WP, Damstra J, Gerrits PO, Ren Y. The Influence of the Segmentation Process on 3D Measurements from Cone Beam Computed Tomography-derived Surface Models. Clin Oral Investig, 2011; Accepted.

12. Damstra J, **Fourie Z**, Ren Y. Evaluation and comparison of postero-anterior cephalograms and cone-beam computed tomography images for the detection of mandibular asymmetry. Eur J Orthod 2011; Accepted
13. Damstra J, **Fourie Z**, De Wit MF, Ren Y. A three-dimensional comparison of a morphometric midsagittal plane to cephalometric midsagittal planes for craniofacial asymmetry. Clin Oral Investig 2011; doi:10.1007/s00784-011-0512-4
14. Damstra J, **Fourie Z**, Ren Y. Practical limitations of cone-beam computed tomography in 3D cephalometry. Shanghai J Stomatol 2011; Accepted
15. **Fourie Z**, Damstra J, Ren Y. Application of cone beam computed tomography in facial imaging science. Shanghai J Stomatol 2011; Accepted

II. Acknowledgements

With this thesis I end a very pleasant time of research. I would like to extend my thanks to several individuals without whose guidance and help in one way or another contributed to this manuscript.

Firstly I would like to thank my Lord Jesus Christ for giving me the talent and opportunity to live out my dreams and for making the following scripture reality during this project. "Not by power or by might but by the spirit says the Lord of hosts" Zech 4:6.

To **Prof. dr. Yijin Ren**, my promoter. Your experience as researcher, motivation, wisdom, patience and steadfast encouragement have really been necessary in the completion of this research work.

Janalt Damstra, you have been like a brother to me the past few years. It was really an honour to work alongside you. I have got great memories of the time that we worked together and the fun we had during this project.

Prof. dr. Andrew Sandham, for believing in me and giving me the opportunity to work part-time at the Department of Orthodontics and kick-start my orthodontic career.

Prof.dr. Mutlu Özcan for your guidance as my first research mentor. I learned a lot from you and really enjoyed working with you. Your passion for research is really admirable. I realized while working with you that doing research can be very rewarding and enjoyable.

I greatly appreciate and wish to thank the members of the reading committee: **Prof. dr. R.R.M. Bos, Prof. dr. P.E. Rossouw and Prof.dr. A.M. Kuijpers-Jagtman** for taking the time and making the effort reviewing this thesis.

I am extremely grateful for being part of a very close knit group of post-graduate students who all became dear friends of mine, **Janalt Damstra, Katrina Finnema, Floris Pelser and Alianne Renkema**. I had an unbelievable 4 years and will never forget you guys.

I would like to extend my thanks to **Alianne Renkema and Katrina Finnema**, for being my two paranymphs and a special thanks to Alianne who helped translate the summary to Dutch.

Mrs. Gea van der Bijl for her excellent support in the administration and organization for the PhD defense.

The **Department of Anatomy (UMCG) and Dr. Peter Gerrits**. For providing the subjects we used for most of the studies done in this thesis. Dr. Gerrits, thank you for always being so enthusiastic, positive and helpful. You are an inspiring researcher and academic.

Henk Rouwé for an excellent Dutch translation of the summary and for the brilliant clinical teacher and mentor you have been to me. Your adventurous spirit and life experiences are really admirable.

Prof. Dr. FA de Wet - for your outstanding help with the translation of the summary into Afrikaans.

Drs. Joerd van der Meer and Marnix de Wit for all the technical support and advice you have given me during this project.

The company **Lamoral and Nico Snijders** for providing the di3D camera system and for his help in setting it up at the Department of Anatomy.

CNC consultants for supplying the laser surface scanner and for making the very high quality laser scans used in this thesis.

Materialise Dental for the use of their software program (SimPlant Ortho®). The program was used for all the studies in this thesis. **Hans Meeus** for the training and technical support that he has given to us regarding the software program.

Department of Orthodontics UMCG for being the platform for making all this possible.

Department of Orthodontics at the University of Pretoria - for introducing me to the wonderful world of orthodontics.

All my dear friends here in Groningen. Thank you for all the love and support that you have given to me the last few years. You guys have been our family away from home.

A special thanks to **Petrie Engelbrecht** who is also a college and dear friend that has assisted me with some of the studies in this thesis.

To my three **brothers, Kobus, Carl and Lehann and my sister Sunette**. For all the moral support, you all have been an inspiration to me. I am really proud to be part of this dynamic family.

My parents **Callie and Freda Fourie**. Thank you for EVERYTHING! There are no words to describe my love and thanks for all you have done for me and my family.

My big boy, **Leo**. You are the best thing that I have ever done! I love you very much and am extremely proud to be your dad.

To my pretty and lovely wife **Heidi**. Thank you for being all that I could hope or dream for in a life partner. Thank you for being an amazing wife to me and wonderful mother to Leo. You are the most amazing thing that has happened to me. I cannot wait to start the rest of our lives together.

III. Curriculum Vitae

The author was born on July the 12th, 1976 in Heidelberg, South Africa. He finished secondary school in 1994 at the "Hoër Volkskool Heidelberg" in Heidelberg, South Africa. The following year he started his dental education at the University of Pretoria, Pretoria, South Africa. He graduated as a dentist in June 2001. Whilst working at the South African Military he started a part-time Postgraduate Diploma in Orthodontics from the University of Pretoria which he completed in 2002. In 2003 he started working in a private practice in the Netherlands. The author started part-time lecturing at the Department of Dentistry at the University Medical Center Groningen (UMCG) in 2005. He also worked part-time as a researcher at the Department of Orthodontics in orthodontic materials. In 2007 he started the full-time orthodontic training program at the Department of Orthodontics at the University Medical Center Groningen (UMCG). He combined his post graduate training in orthodontics with the research in this thesis. He is expected to finish his post graduate training in August, 2011. He is married to Heidi Fourie-Dormehl and they have a son named Leo (2009) and they are expecting a little girl in September 2011.